Cell surface mobility of $GABA_B$ receptors

Saad Bin Hannan

September 2011

A thesis submitted in fulfilment of the requirements for the degree of Doctor of Philosophy of the University College London

Department of Neuroscience, Physiology, and Pharmacology
University College London
Gower Street
London WC1E 6BT
UK

‘I, Saad Hannan confirm that the work presented in this thesis is my own. Where information has been derived from other sources, I confirm that this has been indicated in the thesis.'

_____

Saad Hannan

September 2011

To

Ammu,

Abbu,

Polu

Abstract

Type-B γ-aminobutyric acid receptors ($GABA_BRs$) are important for mediating slow inhibition in the central nervous system and the kinetics of their internalisation and lateral mobility will be a major determinant of their signalling efficacy.

Functional $GABA_BRs$ require R1 and R2 subunit co-assembly, but how heterodimerisation affects the trafficking kinetics of $GABA_BRs$ is unknown. Here, an α-bungarotoxin binding site (BBS) was inserted into the N-terminus of R2 to monitor receptor mobility in live cells. $GABA_BRs$ are internalised via clathrin- and dynamin-dependent pathways and recruited to endosomes. By mutating the BBS, a new technique was developed to differentially track R1a and R2 simultaneously, revealing the subunits internalise as heteromers and that R2 dominantly-affects constitutive internalisation of $GABA_BRs$. Notably, the internalisation profile of R1aR2 heteromers, but not R1a homomers devoid of their ER retention motif ($R1^{ASA}$), is similar to R2 homomers in heterologous systems. The internalisation of $R1a^{ASA}$ was slowed to that of R2 by mutating a di-leucine motif in the R1 C-terminus, indicating a new role for heterodimerisation, whereby R2 subunits slow the internalization of surface $GABA_BRs$.

R1a and R1b are the predominant $GABA_BR1$ isoforms in the brain, differing by the two Sushi Domains (SDs) in R1a. Introduction of a BBS into the N-terminus of R1b and comparison with R1a revealed that R1bR2 internalises faster than R1aR2. Introduction of the SDs into the BBS-tagged metabotropic glutamate receptor-2 also conferred a decrease in internalisation.

Finally, the lateral surface mobility of $GABA_BRs$ was studied by extending the BBS-tagging method to single-particle tracking using quantum dots. R1aR2 and R1bR2 exhibited different mobility profiles on hippocampal neurons and differentially responded to baclofen.

In conclusion, this study provides new and important insight into the mobility of cell surface $GABA_BRs$ and the underlying mechanisms that ensure they provide efficacious slow synaptic inhibition.

Acknowledgements

During the course of this work I have worked with an amazing group of people who form the core of the Smart lab. Needless to say, this work would not have been possible without the careful supervision, support, and encouragement of Professor Trevor Smart. I would like to thank Dr. Phil Thomas, Dr. Lorena Carcamo, Dr. Paul Miller, Mr. Mike Lumb, Ms. Helena da Silva, and all the other members of the lab who have extended their expertise on many of the techniques included in this work; Dr. Martin Mortensen and Dr. Marc Gielen, and for their kind and helpful discussions on science and matters outside. Thanks to Dr. Stuart Lansdell for his help with radioligand binding experiments; Dr. Chris Trastavalou and Dr. Daniel Ciantar, from the UCL centre for imaging, for extending their expertise on imaging. Thanks also to Dr. M. Wilkins for performing the electrophysiology experiments.

Thanks to Professor Antoine Triller, Dr. Kim Gerrow, and Dr. Marianne Renner for teaching us Quantum Dot technology in Paris and for their continued collaboration on the project.

Finally, I would like to thank my parents and my brother for their endless support. Without their assistance and encouragement this would not have been possible.

Saad Hannan

Contents

List of figures

List of tables

List of abbreviations

7-TM	Seven transmembrane domain
β_2AR	β_2-adrenergic receptor
AChR	Acetylcholine receptor
AF488	Alexa fluor 488
AF555	Alexa fluor 555
AMPA	2-amino-3-(5-methyl-3-oxo-1,2- oxazol-4-yl)propanoic acid
AMPK	5' adenosine monophosphate-activated protein kinase
ANOVA	Analysis of variance
AP	Alkaline phosphate
AP2	Adapter protein complex 2
ARF	ADP-ribosylation factor
ATF4	Activating transcription factor 4
Baclofen	(*RS*)-4-amino-3-(4-chlorophenyl)butanoic acid
BBS	α-bungarotoxin binding site
BRET	Bioluminescence resonant energy transfer
BSA	Bovine serum albumin
BTX	α-bungarotoxin
BTX-B	α-bungarotoxin-biotin
CaMKII	Ca^{2+}/ Calmodulin-dependent kinases II
CB1	Cannabinoid receptor type 1
CHOP	Transcription factor CCAAT/enhancer-binding protein (C/EBP) homologous protein
CNS	Central nervous system
COPI	Coat protein complex I
D	Diffusion coefficient
D1	Dopamine receptor type 1
D2	Dopamine receptor type 2
DAMGO	[D-Ala^2, N-MePhe^4, Gly-ol]-enkephalin
DIC	Differential interference contrast
DIV	Days *in vitro*
DMEM	Dubecco's modified Eagle medium
DPDPE	[d-Pen^2, d-Pen^5]-enkephalin
DRG	Dorsal root ganglion
d-TC	d-tubocurarine
DTT	Dithiothreitol

EC_{50}	Concentration eliciting 50% of total activation
ECD	Extracellular domain
eGFP	Enhanced green fluorescent protein
EMCCD	Electron-multiplying charge coupled device
EPSP	Excitatory postsynaptic potential
ER	Endoplasmic reticulum
FCS	Fetal calf serum
FRAP	Fluorescence recovery after photobleaching
FRET	Förster resonance energy transfer
GABA	γ-aminobutyric acid
$GABA_A$	γ-aminobutyric acid receptor type A
$GABA_B$	γ-aminobutyric acid receptor type B
GDP	guanosine diphosphate
GEF	Guanine-nucleotide exchange factor
GHB	γ-hydroxybutyric acid
GISP	GPCR interacting scaffolding protein
GIRK	G-protein-coupled inwardly rectifying potassium channel
GluR2	AMPA receptor subunit 2
GPCR	G-protein coupled receptor
GPI	Glycosylphosphatidylinositol
GRK	G-protein coupled receptor kinase
GST	Glutathione S-transferase
GTP	Guanosine triphosphate
HEK-293	Human embryonic kidney 293 cells
IC_{50}	Concentration eliciting 50% of total inhibition
IP	Inositol monophosphate
IPSP	Inhibitory postsynaptic potential
LB	Lysogeny broth
LT	Low temperature
LTD	Long-term depression
LTP	Long-term potentiation
Marlin 1	Multiple alpha helices and RNA-linker protein 1
MC4	Melanocortin 4 receptor
MEM	Minimum essential media
mGluR	Metabotropic glutamate receptor
mGluR1	Metabotropic glutamate receptor, type – 1
mGluR2	Metabotropic glutamate receptor, type – 2

MSD	Mean square displacement
MTSES	Sodium-(2-Sulphonatoethyl)-methanethiosulfonate
MW	Mann-Whitney test
NEM	N-ethyl-maleimide
NMDA	*N*-methyl-D-aspartic acid
NMR	Nuclear magnetic resonance
NS	Not significant
NSF	NEM sensitive fusion protein
PAR1	Protease activated receptor 1
PBS	Phosphate buffered saline
PCR	Polymerase chain reaction
PDB	Protein data bank
PFA	Paraformaldehyde
PKA	Protein kinase A (c-AMP-dependent protein kinase)
PLC	Phospholipase C
PP2A	Protein phosphatase 2A
PT	Near-physiological temperature
QD	Quantum Dot
QD655	Quantum Dot streptavidin conjugate
R1a	γ-aminobutyric acid receptor type B, Subunit 1, Isoform a
R1b	γ-aminobutyric acid receptor type B, Subunit 1, Isoform b
R2	γ-aminobutyric acid receptor type B, Subunit 2
Rab	Ras-related protein
RGS	Regulators of G-protein signalling
ROI	Region of interest
RT	Room temperature
SD	Sushi Domain
SEM	Standard error of mean
SPT	Single particle tracking
TR-FRET	Time-resolved Förster resonance energy transfer
VFTD	Venus fly-trap domain
VGCC	Voltage-gated calcium channels

Chapter I

Introduction

Living organisms are composed of cells, which form the basic unit of life. In multicellular organisms, cells assemble to form higher order structures, with increasing levels of complexity, in the form of tissues, organs, and organ systems that work in concert to ensure the sustainability of life. Robert Hooke was the first person to observe and document the existence of cells in 1665 (Hooke, 1965) and the “cell theory” was postulated in 1838 by Theodor Schwann (Schwann, 1839) laying the foundation for cellular biology. With advancements in the field of microscopy, the study of cellular physiology has now become a major area of biological research.

Of all the organ systems, the nervous system is perhaps the most intriguing given the important roles played by this system in physiology and disease. The nervous system is made up of glial cells and electrically excitable cells, or neurons. A typical neuron contains a soma or the cell body, an axon that arises at the axon hillock and dendrites that can form a complex branching morphology. Signals are usually sent from the axon of one neuron to the dendrites of others although there exceptions to this rule. The central nervous system (CNS) is formed of the brain and the spinal cord both of which contain a complex array of local and region specific networks of neurons. The neurons within a local network communicate with each other and in addition, there is signalling

between networks that originate in different regions of the brain. Such communication is achieved mostly via chemical release at synapses, which are the closest points of contact between two neurons (Sherrington, 1906). It is via these synapses that the nervous system enables sensory perception, motor co-ordination, control over other organ systems, information processing, judgement, intelligence, and memory. Neurotransmitters are the chemicals that are released at synapses by neurons and for rapid transmission, there are two major types of neurotransmitters: excitatory which increase the excitability of neurons and inhibitory that reduce excitability. Excitatory neurotransmitters

1.1 GABA

The small molecule γ-aminobutyric acid (GABA; Fig. 1.1A) is the main inhibitory neurotransmitter in the mammalian central nervous system (CNS) (Burt and Kamatchi, 1991; McCormick, 1989; Olsen, 2002) and it has been estimated that around 30-40% of inhibitory neurotransmission in the adult brain is mediated by this neurotransmitter (Beleboni et al., 2004; Hendry et al., 1987; Roberts, 1986). The presence of GABA (Fig. 1.1) in the CNS was discovered in 1950 using paper chromatography (Awapara et al., 1950; Roberts and Frankel, 1950) and in 1956, the first demonstration of the inhibitory action of GABA on electrical activity in the nervous system was reported (Hayashi, 1956). At inhibitory synapses, GABA-mediated post-synaptic potentials consist of an early (fast) and a late (slow) component and the fast component of the synaptic inhibition imparted by GABA is mediated by the ionotropic $GABA_{A/C}$ receptors whereas the slow and prolonged component is mediated by the metabotropic $GABA_B$ receptors (Bowery and Smart, 2006).

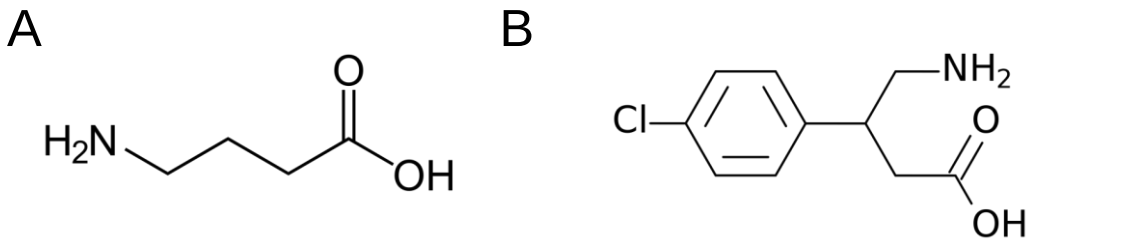

γ -aminobutyric acid (*RS*)-4-amino-3-(4-chlorophenyl)butanoic acid

Figure 1.1 – Structure of GABA and Baclofen
Molecular structure of γ-aminobutyric acid (GABA; *A*) and the $GABA_B$ receptor specific agonist (*RS*)-4-amino-3-(4-chlorophenyl)butanoic acid (baclofen; *B*)

1.2 $GABA_B$ receptors

$GABA_B$ receptors were first identified in the peripheral nervous system in 1979 (Bowery and Hudson, 1979) and later in the CNS in 1980 (Bowery et al., 1980) as a bicuculline-, isoguvacine- and picotoxin-insensitive receptor that reduced the evoked release of radiolabelled noradrenaline in response to GABA. Baclofen ((*RS*)-4-amino-3-(4-chlorophenyl)butanoic acid) (Fig. 1.1B) was identified as a selective agonist of this 'new' receptor and the receptor was defined as $GABA_B$ soon afterwards (Bowery et al., 1981). Since its discovery, several functional and signalling properties were assigned to $GABA_B$ receptors, but in the absence of a cloned receptor the molecular basis of the receptor's function remained unclear. Cloning of the $GABA_B$ R1 subunit in 1997 (Kaupmann et al., 1997) using a high affinity $GABA_B$ receptor antagonist, [^{125}I]CGP64213, identified two isoforms: R1a and R1b. $GABA_B$ R2 was later identified in a homology-based screen of sequence databases where R1 was used as a probe (Kaupmann et al., 1998; White et al., 1998). The sequence of the cloned receptor revealed, as expected, that the $GABA_B$ receptor is a G-protein coupled receptor (GPCR).

1.3 G-protein coupled receptors

GPCRs make up the largest known family of receptors in mammals and nearly 4% of the entire protein coding part of the genome encodes for over 800 predicted and cloned GPCRs (Mirzadegan et al., 2003; Takeda et al., 2002; Fredriksson and Schioth, 2005). The importance of GPCRs is highlighted by more than 40% of clinically-used drugs exerting their effects on cellular physiology through these receptors (Overington et al., 2006). GPCRs share a common structural architecture with seven α helices spanning the cell membrane giving rise to three extracellular and three intracellular loops of variable sizes and an extracellular N-terminal and an intracellular C-terminal domain. They form receptors for a diverse range of ligands including photons, ions, hormones and neurotransmitters and activate numerous downstream signalling pathways by coupling through heterotrimeric G-proteins (McCudden et al., 2005; Tuteja, 2009).

GPCRs have been divided into three classes: A, B, and C based on sequence homologies (Foord et al., 2005). Class A GPCRs are characterised by their homology to the rhodopsin receptor (Palczewski, 2006) and form the largest and probably best characterised group with the crystal structure of several receptors, including the β_2 adrenergic receptor (β_2AR) (Cherezov et al., 2007) and the rhodopsin receptor (Palczewski et al., 2000), resolved. The class B GPCRs are composed of the secretin family of receptors. Some members of this family bind to peptides hormones. The class C group contains the metabotropic GPCRs and includes $GABA_B$ receptors, metabotropic glutamate receptors (mGluRs), calcium sensing receptors, pheromone receptors, sweet and amino acid taste receptors, and some orphan receptors (Pin et al., 2003). All

class C GPCRs (Fig. 1.2), with the exception of the orphan receptors, are composed of a large extracellular domain that contains a venus flytrap domain (VFTD) and the characteristic GPCR seven transmembrane (7-TM) region (Fig. 1.2). An extracellular cysteine-rich region separates the VFTD from the 7-TM region in all class C GPCRs except for $GABA_B$ receptors (Pin et al., 2004). The consequences of the absence of the cysteine-rich domain in $GABA_B$ receptor function has not been studied thus far.

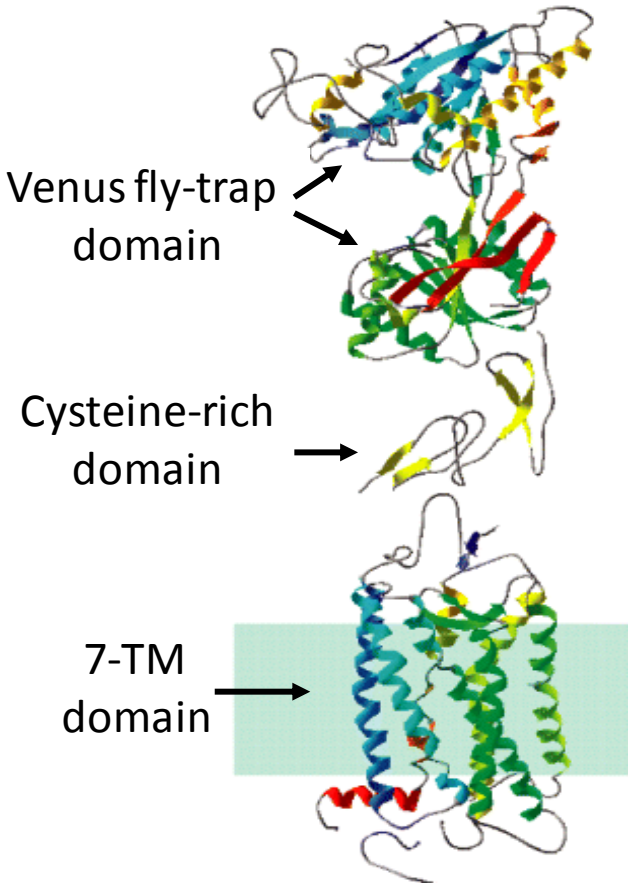

Figure 1.2 – Structure of class-C GPCRs.

Class C GPCRs are composed of three main structural domains, the Venus fly-trap domain where agonists bind, the cysteine-rich domain and the 7-TM domain. Figure adapted from Pin et al., 2005

1.4 $GABA_B$ receptor structure

$GABA_B$ receptors in the CNS are composed of two subunits, R1 and R2, forming a heterodimer (Fig. 1.3). The two subunits share a common architecture and 35% amino acid conservation. Like other class C GPCRs, the N-terminus VFTD of $GABA_B$ receptors is

similar in structure to the bacterial periplasmic substrate-binding proteins (PBPs) (Felder et al., 1999). PBP containing receptors mediate chemotaxis and solute uptake in Gram-negative bacteria and similar VFTDs are present in ionotropic glutamate receptors: GluR2 and NMDAR. A crystal structure of the $GABA_B$ receptor N-terminus is currently unavailable. However, crystal structures of the VFTDs of mGluR1 (Kunishima et al., 2000) are available and is likely to be similar to the structure of the $GABA_B$ VFTD. Based on this assumption, the structure of the VFTD of mGluR1 (Fig. 1.2) has been used as a template to develop a homology based model of the $GABA_B$ R1 and R2 VFTDs that suggests that the $GABA_B$ VFTDs are made up of two lobes (Rondard et al., 2008). The R1 VFTD contains the GABA binding site (Galvez et al., 2000; Galvez et al., 1999; Kniazeff et al., 2002; Nomura et al., 2008). To date a naturally occurring ligand that binds to the R2 and activates the $GABA_B$ receptor has not been identified although several allosteric modulators have been identified that bind to R2 subunits and enhance the efficacy of signalling by the $GABA_B$ receptor as discussed below. The presence of R2 VFTD *in vitro* has been reported to increase the affinity of GABA for binding to the R1 VFTD and a mechanism for the increase of affinity has been proposed in which the closed state of the R1 VFTD is stabilized in the presence of R2 VFTD (Galvez et al., 2001; Liu et al., 2004).

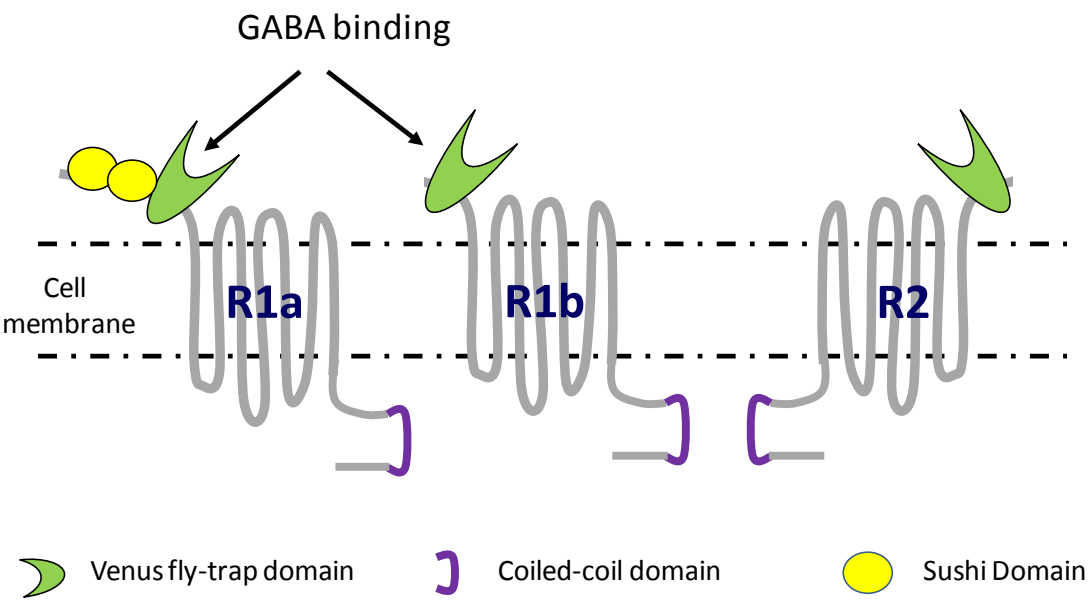

Figure 1.3 – $GABA_B$ receptor structure.
Schematic diagram showing the overall structure of the $GABA_B$ receptor. The receptor is composed of two subunits (R1 and R2) which form a heterodimer. The venus fly trap domains in R1 forms the agonist binding domain. The intracellular loops in R2, form the G-protein coupling domain. The coiled-coil domain of R1 contains an endoplasmic reticulum (ER) retention motif (-RSR-).

The extracellular domains (ECDs) of the R1 and R2 interact with each other as revealed by time-resolved Förster resonance energy transfer (TR-FRET) approaches. FRET can be used to reveal protein-protein interactions and a signal is achieved when a donor molecule, upon excitation, transfers energy to an acceptor molecule when the two are in close proximity (Fig. 1.4). In TR-FRET, donor molecules with long emission durations are used in order to reduce the levels of background fluorescence. The R1 ECD, anchored on the cell membrane by glycosylphosphatidylinositol (GPI), was found to interact with R2 subunits truncated in the first intracellular loop, after the first transmembrane domain, on the cell surface of COS-7 cells using TR-FRET (Fig. 1.4) (Liu et al., 2004). An HA-tag containing R1 ECD was cloned in the N-terminus of a synthetic gene fragment encoding the GPI anchor signal peptide of mouse cellular prion protein.

After translation, the GPI anchor signal peptide is cleaved and a GPI modification is added to the R1 ECD in the ER. This allowed R1 ECD to express on the cell surface anchored by GPI. R1 ECD was detected by an anti-HA monoclonal antibody coupled to europium cryptate-pyridine bipyridine which serves as the donor for TR-FRET and Myc-tagged R2 subunits were detected by an anti-c-Myc monoclonal antibody coupled to Alexa Fluor 647 (Fig. 1.4). The excitation of europium cryptate-pyridine bipyridine at 337 nm resulted in the detection of a FRET signal at 665 nm which corresponds to the emission wavelength of Alexa Fluor 647. Although this sheds light on the interactions between R1 and R2, the full scale of the implications of this interaction is unclear in the absence of the 7-TM regions. Other techniques such as co-immunoprecipitation and sucrose density gradient centrifugation has also been used to demonstrate the interactions between R1 and R2 ECDs (Nomura et al., 2008). This interaction between the two ECDs is important for signalling via the $GABA_B$ receptor and disrupting the interaction interface, by the introduction of bulky N-glycan moieties, abolishes the receptor's functional activity assessed by inositol monophosphate (IP) accumulation assays (Rondard et al., 2008). R1a and R1b form the two major isoforms of the R1 subunit in the CNS and differ due to the presence of two Sushi domains (SDs) present only in R1a.

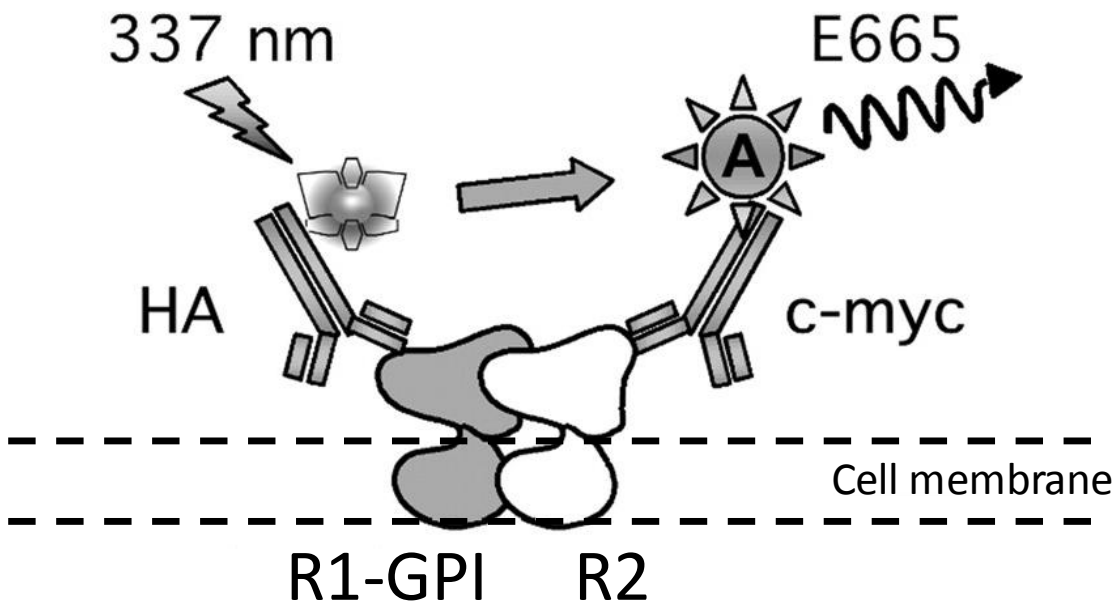

Figure 1.4 – Time-resolved FRET reveals interaction of R1 and R2 extracellular domains

R1 extracellular domain (dark gray) anchored on the cell surface of COS-7 cells were tagged with anti-HA antibodies coupled to a donor molecule (europium cryptate-pyridine bipyridine) and R2 was tagged with anti-c-Myc antibodies coupled to an acceptor molecule (Alexa Fluor 647). The FRET signal between the two antibodies was measured at 665 nm (*E665*) after excitation at 337 nm. Adapted from Liu et al., 2004

The 7-TM region of R1 and R2 are similar in structure and it is through the loops of R2 $GABA_B$ receptors couple to G-proteins. Exchange of the intracellular loops of R1 with equivalent loops of R2 does not alter the signalling properties of the heteromeric receptor but exchange of any of the three intracellular loops of R2 with equivalent loops of R1 abolishes receptor signalling (Margeta-Mitrovic et al., 2001a). Point mutations in the second and the third intracellular loops can also disrupt or abolish the receptor signalling (Duthey et al., 2002; Havlickova et al., 2002). Recently, the two 7-TM domains of R1 and R2 have been hypothesised to interact using TR-FRET assays suggesting that upon agonist binding, the R1 7-TM domain activates the R2 7-TM domain leading to G-protein coupling (Monnier et al., 2011). Another study has used a series of constructs with insertions of fluorescent proteins in the intracellular loops of

R1a and R2 (Matsushita et al., 2010) and has demonstrated that upon agonist treatment in HEK cells FRET signals decrease between loop 2 of R1 and loops 1 and 2 of R2 compared to controls providing evidence that the intracellular loops dissociate upon receptor activation. Together these results suggest that conformational changes in the 7-TM domain of R1 in response to agonist binding can initiate signalling via R2 subunits. This has been proposed for the class A GPCRs in which a large movement of the TM6 upon agonist binding leads to G-protein signalling (Gether et al., 2002; Schwartz et al., 2006; Nygaard et al., 2009).

$GABA_B$ R1 and R2 have intracellular C-terminal tails that are over a hundred amino acids long and are likely to play important roles in trafficking of the receptor. The tails contain a coiled-coil domain. Coiled-coil domains are structural motifs in which 2-7 alpha helices, distinguished by heptad repeats, form a coil-like structure (Liu et al., 2006). The coiled-coil domains of R1 and R2 are known to interact (Kuner et al., 1999) and have been described to form heterodimeric parallel coiled-coils at physiological temperatures (Kammerer et al., 1999). The R1 subunits contain an RSR-type endoplasmic reticulum (ER) retention signal that prevents it from being targeted to the cell surface alone. R2 subunits mask this ER retention motif via an interaction through the coiled-coil domain allowing R1 to reach the cell surface. Several studies have looked at the importance of the C-terminal tails of R1 and R2 in G-protein coupling. Deletion of both tails in R1 and R2 have no effect in G-protein coupling of $GABA_B$ receptors assessed using intracellular Ca^{2+} mobilisation assay in response to GABA stimulation (Calver et al., 2001).

The C-terminal tails provide an important interface for interaction with receptor-associated proteins that modulate function and trafficking. 14-3-3η and 14-3-3ζ were identified in yeast two hybrid assays to interact with R1 and 14-3-3ζ was pulled down from adult rat brain lysates using glutathione *S*-transferase R1 (GST-R1) and co-immunoprecipitated with R1 in transfected COS-7 cells (Couve et al., 2001). The area of interaction overlaps with the coiled-coil domain and 14-3-3 allowed the dimerisation of the receptors by scavenging R1 subunits. 14-3-3 proteins bind to diverse proteins and offer a scaffold to kinases, phosphatases and other receptors. They have also been described to mediate the correct assembly of proteins and release of multimeric complexes from the ER (Yuan et al., 2003). In addition, the coat protein I (COPI) complex can also interact with the RSR sequence of R1 (Brock et al., 2005). COPI takes part in retrograde trafficking of proteins form the *cis*-Golgi back to the ER. The presence of unassembled R1 in the *cis*-Golgi supports the notion that R1 subunits exit the ER and are shuttled back by COPI from the *cis*-Golgi preventing their expression in the absence of R2.

Another protein that interacts with the coiled-coil domain of R1 regulating the expression of these receptors is msec7-1 (Restituito et al., 2005). msec7-1 is a guanine-nucleotide exchange factor (GEF) (Casanova, 2007) of ADP ribosylation factor 6 (Arf6) (Ashery et al., 1999) and interacts specifically with a di-leucine motif on the coiled-coil domain of R1. Di-leucine motifs are involved in the regulation of endocytosis, exocytosis and the targeting of proteins to specific subcellular compartments (Marchese et al., 2008; Pandey, 2009). In addition, expression of msec7-1 with an ER retention motif mutated R1 in COS-7 cells increases the surface expression levels of the mutant R1 subunit compared to cells expressing only the mutant R1 (Restituito et

al., 2005). Mutating the di-leucine motif in R1 abolished this effect of msec7-1 suggesting the interaction of the di-leucine motif with msec7-1 is important for cell surface expression of R1.

Recently, a novel protein, GPCR interacting scaffolding protein (GISP), has been identified that interacts with the coiled-coil domain of R1 (Kantamneni et al., 2007). GISP was also able to pull-down $GABA_B$ R1 from rat brain lysates, co-immunoprecipitate with R1 and R2 and co-localise with $GABA_B$ receptors as probed with immunolabelling. Interestingly, GISP interacts with the heterodimeric complex and the co-expression of GISP with R1 and R2 in human embryonic kidney 293 (HEK-293) cells enhances the expression of $GABA_B$ receptors and decreases the rundown of baclofen-evoked currents in HEK-293 cells containing a stable transformation with potassium channels, Kir3.1 and Kir3.2 (GIRK cells) as assessed by whole-cell patch clamp electrophysiology. These results suggest that GISP is also important in the trafficking and functioning of the $GABA_B$ receptor.

The activating transcription factor 4 (ATF4) (Vernon et al., 2001;White et al., 2000;Nehring et al., 2000) has been reported by several studies to interact with the $GABA_B$ R1 coiled-coil domain. This interaction was only observed in the absence of R2 (Vernon et al., 2001) and suggests that ATF4 takes part in the assembly of $GABA_B$ receptor heterodimers.

The transcription factor CCAAT/enhancer-binding protein (C/EBP) homologous protein (CHOP) interacts with the coiled-coil domain of $GABA_B$ R2 and the N-terminus of R1a but not R1b receptors (Sauter et al., 2005). More importantly, CHOP interacts with $GABA_B$ heterodimers and co-immunoprecipitates with $GABA_B$ receptors from rat brain

extracts and co-localises with primary hippocampal neurons suggesting that this protein can interact with heterodimeric $GABA_B$ receptors. In addition, co-expression of CHOP with $GABA_B$ receptor subunits in HEK-293 cells reduces the cell surface expression of R1aR2 receptors in a subtype-selective manner but has no effect in the expression of R1bR2 receptors.

The $GABA_A$ subunit γ2S has been reported to achieve cell surface expression of $GABA_B$ R1 subunits in HEK-293 cells in the absence of R2 subunits (Balasubramanian et al., 2004) . In addition, $GABA_B$ heterodimers and γ2S have been co-immunoprecipitated from rat brain lysates demonstrating the existence of such interactions in native tissues. Multiple interactions between R1 and γ2S have been hypothesised and at least one of these lies in close proximity of the ER retention motif of R1 suggesting a masking of this motif by γ2S for cell surface expression.

The C-terminal tail of R2 also contains some important motifs that interact with unidentified protein(s) that regulate the cell surface trafficking of $GABA_B$ receptors. The region of amino acids 841-862 is important as their deletion reduces the cell surface expression levels of $GABA_B$ receptors (Pooler et al., 2009). The potassium channel tetramerisation domain-containing (KCTD) proteins 8, 12, 12b and 16 that share conserved domains in their amino termini T1 domain with voltage-gated K^+ channels, interact with the $GABA_B$ R2 C-terminus and increase the targeting of $GABA_B$ receptors on the axonal plasma membrane, increase agonist potency, and alter G-protein coupling by accelerating onset and promoting desensitization of the receptors (Schwenk et al., 2010; Bartoi et al., 2010). Table 1.1 lists a summary of the $GABA_B$ interaction proteins discussed.

Table 1.1 – Protein-protein interactions of the $GABA_B$ receptor.

Interacting Protein	$GABA_B$ Subunit	Region	Function	References
14-3-3	$GABA_B$ R1	Coiled-coil domain	Assembly and trafficking	Couve et al., 2001
COPI	$GABA_B$ R1	Coiled-coil domain	Assembly and trafficking	Brock et al., 2005
msec7-1	$GABA_B$ R1	Coiled-coil domain; Leu 889 and 890 in R1a	Assembly and trafficking	Restituito et al., 2005
GISP	$GABA_B$ R1	Coiled-coil domain	Cell surface expression and signalling	Kantamneni et al., 2007
ATF4	$GABA_B$ R1	Coiled-coil domain	Assembly	Vernon et al., 2001; White et al., 2000; Nehring et al., 2000
CHOP	$GABA_B$ R2 $GABA_B$ R1a	Coiled-coil domains; N-terminus	Cell surface expression	Sauter et al., 2005
$GABA_A$ γ2S	$GABA_B$ R1	Amino acids 934 - 960 on R1a and other areas	Cell surface expression	Balasubramanian et al., 2004
KCTD 8, 12, 12a and 16	$GABA_B$ R2	C-terminus	Cell surface expression, desensitisation and signalling	Schwenk et al., 2010; Bartoi et al., 2010

1.5 $GABA_B$ agonists and antagonists

The most widely used specific $GABA_B$ receptor agonist is baclofen (Fig. 1.1B). This was synthesized in an attempt to increase the lipophilicity of GABA (Cates et al., 1984) to achieve greater penetration of the blood brain barrier. The main use of baclofen is as a muscle relaxant to treat spasticity for patients with multiple sclerosis (Brar et al., 1991; Smith et al., 1991), post-stroke (O'Brien et al., 1996), cerebral palsy (Krach, 2009), stiffman syndrome (Stayer et al., 1997), and other forms of paralysis (Penn and Kroin, 1985; Penn and Kroin, 1984; Becker et al., 1997; Muller et al., 1987). Baclofen has also been used successfully for pain relief in trigeminal neuralgia (Fromm, 1994; Baker et al., 1985), in cluster headache (Hering-Hanit and Gadoth, 2000) and in migraine

(Hering-Hanit, 1999). More recently, baclofen has been used in the treatment of cravings during withdrawal from alcohol (Addolorato et al., 2002a; Addolorato et al., 2002b), cocaine (Haney et al., 2006; Ling et al., 1998; Shoptaw et al., 2003), and nicotine (Franklin et al., 2009).

There are two enantiomers of baclofen: (*R*)-(-)-baclofen and (*S*)-(+)-baclofen. (*R*)-(-)-baclofen is more potent than (S)-(+)-baclofen and a racemic mixture is also more potent than (*S*)-(+)-baclofen (Froestl et al., 1995a). In addition to baclofen, several other $GABA_B$ receptor agonists have been reported, these include a carbamate derivative of (*R*)-(-)-baclofen, Arbaclofen placarbil (XP19986) (Lal et al., 2009), and a des-chloro analogue of baclofen, Phenibut (Ong et al., 1993). In addition, several phosphonic acid analogues of GABA are potent agonists of the $GABA_B$ receptor (Froestl et al., 1995a; Froestl et al., 1995b). γ-hydroxybutyric acid (GHB), commonly referred to as the "date rape drug" is a weak agonist of the $GABA_B$ receptor (Xie and Smart, 1992b; Xie and Smart, 1992a).

Several $GABA_B$ receptor antagonists have been developed over the last few years. Phaclofen was the first selective antagonist (Kerr et al., 1987) and could block the slow inhibitory postsynaptic potential (Dutar and NIcoll, 1988; NIcoll, 2004), soon followed by the more potent 2-hydroxy-saclofen (Kerr et al., 1988).

Several potent and selective $GABA_B$ receptor antagonists can bind to the receptor with nanomolar affinities and one of these, CGP55845A has been tested in several *in vitro* and *in vivo* conditions and has an IC_{50} of 6 nM in antagonising binding of a radiolabelled agonist to rat cerebral cortex membranes (Bowery et al., 2002). In addition, CGP55845A inhibits $GABA_B$ receptor activation in the CA1 region of the rat

hippocampus (Pozza et al., 1999) and has been described to reverse age-related learning impairment (Lasarge et al., 2009), and improve learning in rats (Getova and Bowery, 1998).

In addition to agonists and antagonists, several positive allosteric modulators have been identified for $GABA_B$ receptors (Pin et al., 2001; Urwyler, 2011). Positive allosteric modulators bind to a site away from the ligand binding site and positively modulate the functional efficacy of the receptor in response to agonists. For the $GABA_B$ receptor all binding sites identified to date for the positive allosteric modulators are on the R2 subunit with CGP7930 and GS39783 being two of the most potent (Urwyler et al., 2001; Urwyler et al., 2003) . These positive allosteric modulators enhance endogenous $GABA_B$ receptors signalling both in terms of potency and efficacy and have therefore been the focus of several studies (Pin et al., 2001; Pin and Prezeau, 2007). Of note, GS39783 has been described to have strong anxiolytic activity in both rats and human (Cryan and Kaupmann, 2005) and both GS39783 and CGP7930 have been described to reduce cocaine self-administration in rats (Smith et al., 2004) indicative of the potential therapeutic significance of these compounds.

1.6 $GABA_B$ receptor signalling

GPCRs predominantly signal in a guanosine triphosphate (GTP)-dependent manner through G-proteins, which are trimeric proteins made up of three subunits: Gα**,** Gβ, and Gγ. The G-protein trimer in its inactive state contains guanosine diphosphate (GDP) bound to the Gα subunit. Activation of a GPCR induces a conformation change

enabling the receptor to act as a GEF. This leads to the exchange of GDP for a GTP molecule on the Gα subunit, thereby activating the G-protein trimeric complex. Upon activation, Gα dissociates from the trimeric complex and activates downstream signalling cascades. In addition, $G_{\beta\gamma}$ can also activate downstream signalling. Gα subunits have an intrinsic GTPase activity hydrolysing GTP to GDP causing the reformation of the G-protein timer ready for the next round of signalling via the GPCR. Some GPCRs have been described to be pre-associated with G-proteins whereas others have been described to assemble with G-proteins upon activation of the GPCR (Neubig et al., 1988; Hein et al., 2005). It is currently not known whether in its inactive state $GABA_B$ receptors remain pre-assembled with G-proteins or whether assembly occurs post activation

$GABA_B$ receptors couple to pertussis toxin sensitive $G\alpha_{i/o}$ subunit containing G-proteins (Fig. 1.5) and there is evidence that the coupling to the exact isoform of $G\alpha_{i/o}$ is likely to be region or function specific. Increased GABA binding to N-ethylmaleimide (NEM) treated brain membrane has been reported in the presence of $G\alpha_o$ and $G\alpha_{i1}$ but not $G\alpha_{i2}$ by one study (Morishita et al., 1990) whereas another study has reported that $GABA_B$ receptors indeed link to inwardly-rectifying K^+ (GIRK) channels via $G\alpha_{i2}$ (Leaney and Tinker, 2000). Alternatively both $G\alpha_{i1}$ and $G\alpha_{i2}$ in bovine cerebral cortex may couple $GABA_B$ receptors to adenyl cyclase (Nishikawa et al., 1997).

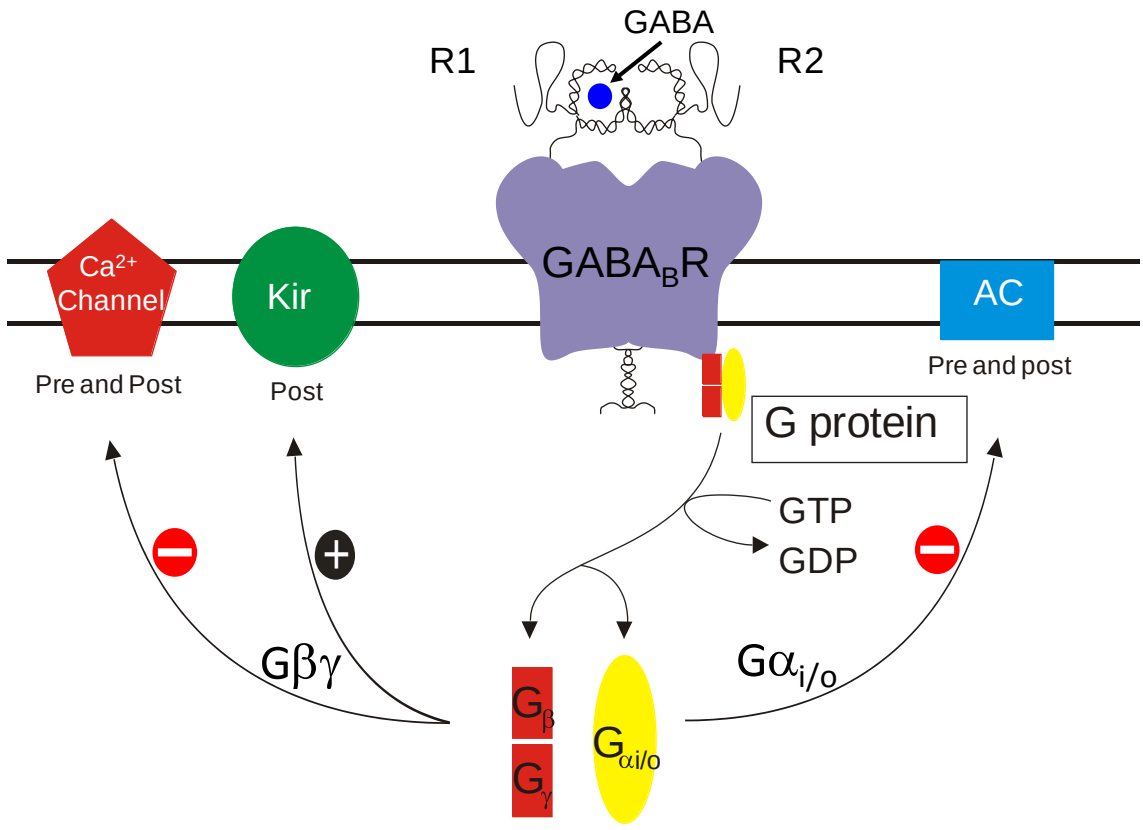

Figure 1.5 – GABA$_B$ receptor signalling.
GABA$_B$ receptors couple to Gα$_{i/o}$ G-proteins and link to three major pathways: activating (+) inward rectifying K$^+$ channels (Kir); inhibiting (-) Ca^{2+} channels; and regulating adenyl cyclase (AC) activity

One of the first effectors identified of GABA$_B$ receptor signalling was voltage-gated calcium channels (VGCCs). Calcium dependent action potentials were impaired by GABA (Dunlap and Fischbach, 1981) in dorsal root ganglion (DRG) neurons. Dissociation of G-proteins upon the activation of GABA$_B$ receptors releases G$_{βγ}$ allowing them to inhibit Ca^{2+} currents. GABA$_B$ receptors couple to P-, Q-, and N-type VGCCs (Guyon and Leresche, 1995; Harayama et al., 1998; Huston et al., 1995; Li and Stern, 2004; Mintz and Bean, 1993). The receptor can therefore inhibit various processes that depend on the influx of Ca^{2+} including the release of neurotransmitters from presynaptic terminals (Huston et al., 1995). GABA$_B$ autoreceptors inhibit the

release of GABA at GABAergic synapses and heteroreceptors inhibit the release of glutamate in excitatory synapses. In the postsynaptic membrane, $GABA_B$ receptors reduce Ca^{2+} signals generated by VGCCs and NMDA receptors in layer 2/3 cell, and VGCCs in layer 5 pyramidal neurons in the prefrontal cortex (Chalifoux and Carter, 2011; Chalifoux and Carter, 2010).

$GABA_B$ receptor activation also leads to activation GIRK channels that are sensitive to Ba^{2+} (Inoue et al., 1985a; Inoue et al., 1985b). $GABA_B$ receptors couple to and activate Kir3.1 and Kir3.2 channels (Misgeld et al., 1995) via $G_{\beta\gamma}$ causing hyper-polarisation of the postsynaptic neuron, underlying the late phase of inhibitory postsynaptic currents (IPSCs).

$GABA_B$ receptors also activate or inhibit adenyl cyclases and can activate phospholipase C (PLC) (Bettler et al., 2004). Adenyl cyclases catalyse the conversion of ATP to the second messenger cAMP (Nishikawa et al., 1997) and PLC cleaves the phospholipid, phosphatidylinositol 4,5-bisphosophate to produce diacyl glycerol and inositol 1,4,5-triphosphate, both second messengers (Rhee and Bae, 1997). $GABA_B$ receptors inhibit adenyl cyclase, reducing cAMP levels in cells, upon activation by GABA. However, in the presence of activated $G\alpha_s$ within in the cell, $GABA_B$ receptor activation can increase cAMP levels. Such elevation of cAMP levels in response to $GABA_B$ activation has been observed in the presence of activated β_2AR which couple to and activate $G\alpha_s$ (Robichon et al., 2004).

1.7 Heterodimerisation of $GABA_B$ receptors

$GABA_B$ receptors function as dimers of R1 and R2 subunits and it was the first GPCR identified that required dimerisation in order to be functionally active (Bowery and Enna, 2000; Marshall et al., 1999). The two subunits interact in at least three different regions: the C-terminal coiled-coil domain, the N-terminal VFTD, and the 7-TM region (Fig. 1.6). Dimerisation is required for at least three reasons. First, the ligand binding site resides in the R1 VFTD where GABA has been described to bind in the cleft between the VFTD's two lobes; whereas G-protein coupling domain resides in the intracellular loops of R2 (Robbins et al., 2001; Duthey et al., 2002; Havlickova et al., 2002). Second, the interaction between the R1 and R2 N-terminal VFTDs is important as the apparent affinity of the receptors for GABA increases upon dimerisation (Galvez et al., 2001) and disruption of the dimerisation interface abolishes G-protein coupling activity of the receptors (Rondard et al., 2008). Finally, when expressed alone in heterologous systems, the R1 subunits do not reach the cell surface (Couve et al., 1998) being retained in the ER, because of the presence of an ER retention motif in the C-terminal coiled-coil domain (Margeta-Mitrovic et al., 2000). However when co-expressed with R2 subunits, R1 can traffic to the cell surface and it has been proposed that an interaction of R2 with the R1 coiled-coil domain masks the ER retention motif in R1 enabling its exit from the ER. Mutation of the ER retention motif from RSR to ASA allows R1 to exit the ER in the absence of R2 subunits and reach the cell surface.

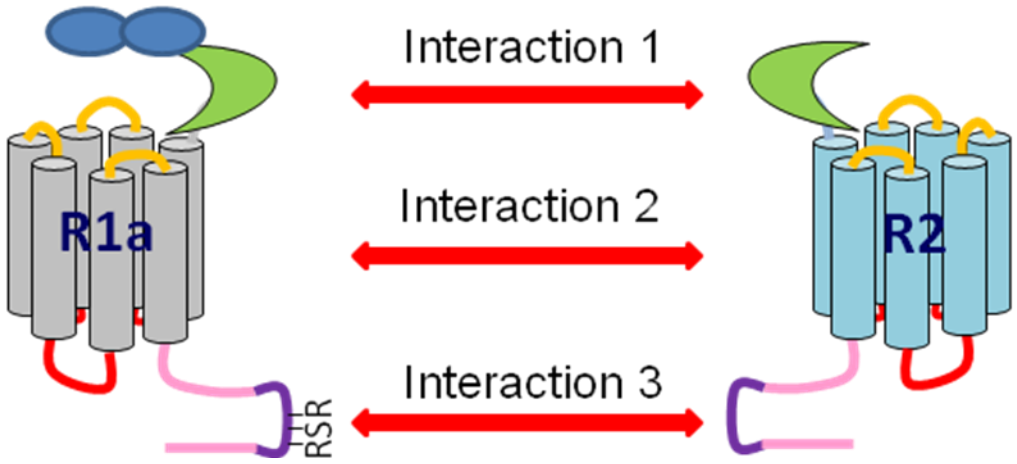

Figure 1.6 – $GABA_B$ receptor heterodimerisation interactions.
Interactions between R1 and R2 have been described to occur in at-least three regions: the N-terminal VFTD (shown as interaction 1), the 7-TM domains and the C-terminal coiled-coil domains

1.8 Isoforms of $GABA_B$ receptor subunits

In humans, the R1 subunits are encoded by a single locus (HGNC: 4070), containing 22 exons (Martin et al., 2001; Goei et al., 1998) (20 exons in rat; (Pfaff et al., 1999)). To date, 6 different R1 isoforms have been described in human and 7 have been described in rat (Fig. 1.7). The different isoforms arise because of alternative promoter usage by RNA polymerase (Vigot et al., 2006) or due to alternative splicing (Pfaff et al., 1999; Martin et al., 2001). The R1 isoforms that have been tested for pharmacology are very similar and are expressed in a wide range of tissues, sometimes in a tissue-specific manner.

In both human and rat, R1a and R1b subunits are the predominant R1 subunit isoforms expressed in the CNS and arise because of the use of different promoters. A relatively less well characterised isoform, R1c is also abundant in human CNS. R1a differs from R1b because of the presence an additional 143 amino acids that form two SDs, also

known as Complement Control Protein or Short Consensus Repeats, in the N-terminus of the mature R1a protein (Fig. 1.3). $GABA_B$ was the first GPCR described to contain SDs, and although several other GPCRs have now been described with SDs (Couvineau and Laburthe, 2011). SDs form the predominant protein modules found in several soluble and cell surface proteins of the Complement activation pathway of the immune system (Kirkitadze and Barlow, 2001). SDs are well known to engage in specific protein-protein interactions. SD1 (proximal to the N-terminus) of R1a has been shown to be less compact in structure than SD2 (Blein et al., 2004), and interacts specifically with the extracellular matrix protein fibulin-2 *in vitro*.

In human R1c, the second SD is removed (Fig. 1.7) by alternative splicing (Martin et al., 2001). Two different R1cs have been reported in rats which arise due to alternative splicing on either the R1a or the R1b template and contain an insertion of 31 amino acids between the second extracellular loop and the fifth transmembrane region (Pfaff et al., 1999; Isomoto et al., 1998). The R1d has a shorter C-terminal tail in which part of the coiled-coil domain containing the ER retention motif has been replaced by 25/26 amino acids (Isomoto et al., 1998).

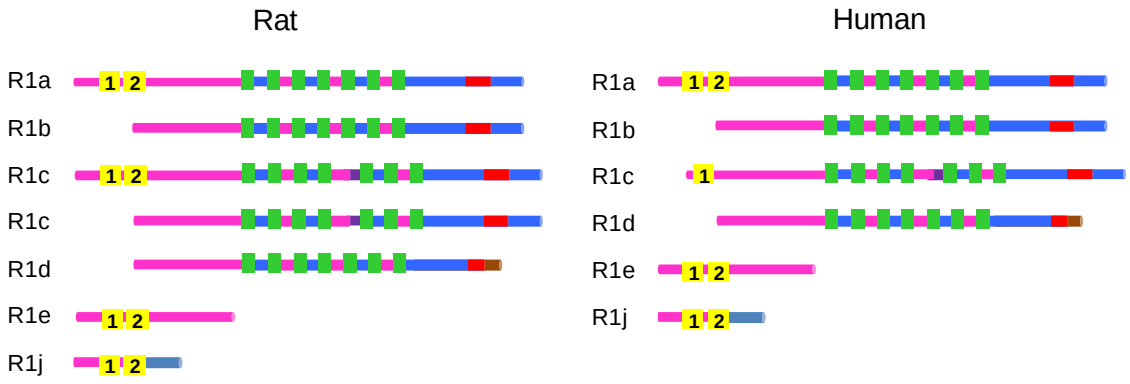

Figure 1.7 - R1 isoforms in rat (left) and human (right).
Linear structure of $GABA_B$ R1 isoforms with extracellular loops and N-terminus (pink), transmembrane regions (green), intracellular loops and C-terminal tail (blue), coiled-coil domain (red), Sushi domains (1 and 2, yellow)

The human R1e isoform arises due to a truncation and is identical to the extracellular domain of R1a (Schwarz et al., 2000). A secreted isoform of the R1 has been reported in rat that contains the two SDs of R1a. This isoform has been named R1j and has been proposed to impair the functioning of $GABA_B$ receptors (Tiao et al., 2008). Recently, the presence of R1j has also been reported in humans (Lee et al., 2010).

By contrast to R1, the $GABA_B$ R2 subunit is encoded by a single coding region (HGNC: 4507) of 19 exons humans (Martin et al., 1999) and there is only one known isoform of this subunit in human and rat.

1.9 GPCR trafficking

Regulation of cell surface receptor numbers by receptor trafficking plays a key role in cellular homeostasis. Such regulation is not only essential in order to prevent over- or under-expression of receptors, but also critical for maintaining precise temporal signalling dynamics imparted by active receptors in response to extracellular cues.

Trafficking of several GPCRs, in particular the β_2AR and the protease activated receptor 1 (PAR1), have been studied extensively and broadly two distinct multi-step modes of trafficking have been described. The first mode of trafficking is initiated by activation of the receptors by agonist, and in the second mode, the receptors are constitutively trafficked in the absence of agonist. Upon activation by agonist, β_2ARs activate intracellular G proteins through their intracellular loops and initiate a sequence of events that lead to their rapid desensitisation mediated by phosphorylation, manifest by a loss of the ability of active receptors to couple to G proteins. GPCR kinases (GRKs)

selectively phosphorylate agonist-bound receptors leading to the recruitment of β-arrestins which in turn recruits clathrin leading to the endocytosis of desensitised receptors (Bonifacino and Traub, 2003; Marchese et al., 2008).

Trafficking of GPCRs have been described to occur via the recruitment of proteins that recognise specific amino acid sequences or motifs in the intracellular domains of the receptors (Bonifacino and Traub, 2003). Among these, di-leucine motifs have been well characterised. Acidic di-leucine motifs have the sequence [E/D]XXXL[L/I] (where X can be any amino acid) and bind to the clathrin adapter protein complex-2 (AP2). AP2 is formed of subunits α, β2, μ2, and σ2, and the two leucine residues bind to a hydrophobic pocket on σ2 to signal recruitment of cargo to the clathrin-coated pits. The hydrophilic residue four positions upstream from the first leucine sits on a positively-charged patch made from residues on the σ2 and α subunits (Kelly et al., 2008). The $GABA_B$ R1 subunit contains one such acidic di-leucine motif ^{885}EKSRLL^{890} (in R1a) that is positioned in the coiled-coil and the role of this motif in endocytosis has not been studied and is therefore of interest.

Trafficking of several neuronal receptors have been studied in detail and among these the ionotropic excitatory AMPA receptors have been studied most extensively using a wide range of techniques (Malenka, 2003; Malinow and Malenka, 2002) and a considerable amount of literature details the role of trafficking of these receptors in long-term potentiation (LTP) and long-term depression (LTD), which form the basis of synaptic plasticity and in turn memory and learning. Among the inhibitory receptors, $GABA_A$ receptor trafficking remains best characterised (Jacob et al., 2008; Moss and Smart, 2001) and is a major determinant of inhibitory synaptic efficacy.

1.10 $GABA_B$ receptor trafficking

The cell surface mobility of $GABA_B$ receptors is important because it could influence the efficacy of inhibition caused by GABA and has therefore been the subject of several studies often with conflicting results. Although initially $GABA_B$ receptors were considered to be being highly stable on the cell surface (Fairfax et al., 2004; Perroy et al., 2003; Balasubramanian et al., 2004) several studies since have shown that they are mobile and rapidly constitutively internalised in the absence of agonist in both HEK-293 cells and neurons (Grampp et al., 2008; Grampp et al., 2007; Hannan et al., 2011; Wilkins et al., 2008; Vargas et al., 2008). Agonist-induced internalisation of $GABA_B$ receptors has also been reported in three studies (Gonzalez-Maeso et al., 2003; Laffray et al., 2007; Wilkins et al., 2008), whereas several others found no change in trafficking in the presence of agonists (Fairfax et al., 2004; Grampp et al., 2007; Vargas et al., 2008). Chronic and prolonged stimulation with agonists has also been described to accelerate the rate of internalisation of the receptors (Fairfax et al., 2004; Gonzalez-Maeso et al., 2003), although the physiological relevance of such long-term treatments are questionable. In addition, changes in allosteric and orthosteric properties of the $GABA_B$ receptors have been observed in cells treated chronically with baclofen (Gjoni and Urwyler, 2009).

Recently, NMDA has been reported to modulate the rate of trafficking of $GABA_B$ receptors (Terunuma et al., 2010; Guetg et al., 2010) by decreasing recycling and increasing lysosomal degradation of the receptors (Maier et al., 2010). NMDA achieves this by initiating phosphorylation of R1 serine 867 by Ca^{2+}/calmodulin-dependent protein kinase II (CaMKII) (Guetg et al., 2010). This effect of CaMKII is more pronounced in the R1bR2 subtype of the $GABA_B$ receptor compared to R1aR2

receptors. In addition, dephosphorylating the AMP-activated protein kinase (AMPK) substrate residue on R2 at serine 783 by the protein phosphatase 2A, (PP2A) redirects recycling $GABA_B$ receptors by recruiting them for lysosomal degradation upon NMDA activation (Terunuma et al., 2010).

Phosphorylation of many GPCRs after agonist treatment leads to rapid desensitisation followed by arrestin or dynamin recruitment, which mediates the internalisation of the desensitised receptors. Arrestins or dynamins form two distinct modes of internalisation for GPCRs (Zhang et al., 1996). $GABA_B$ receptors undergo rapid desensitisation upon agonist treatment which involves GRK4 in a phosphorylation independent manner (Perroy et al., 2003) or NEM sensitive fusion protein (NSF) (Pontier et al., 2006). This process is enhanced by regulators of G-protein signalling (RGS) (Mutneja et al., 2005). Using biochemical and electrophysiological methods, it has been shown that phosphorylation of a single serine residue (S892) on R2 by cAMP-dependent protein kinase A (PKA) stabilises $GABA_B$ receptors on the cell surface (Couve et al., 2002), which is unusual for GPCRs, as phosphorylation is generally regarded to decrease GPCR stability on the cell surface.

$GABA_B$ receptors internalise through the classical clathrin- and dynamin-dependent pathways (Grampp et al., 2007; Laffray et al., 2007; Wilkins et al., 2008), although two studies describe internalisation using non-classical mechanisms (Fairfax et al., 2004; Perroy et al., 2003). Internalised receptors are then targeted to endosomes from where they can either be recycled back to the cell surface (Grampp et al., 2008; Vargas et al., 2008) or degraded in the lysosomes (Grampp et al., 2008). An interaction involving GISP and the tumour susceptibility gene 101 (TSG101) product, a protein involved in lysosomal targeting of proteins, reduces lysosomal degradation the of

$GABA_B$ R2 receptors (Kantamneni et al., 2009). With regard to $GABA_B$ receptors, the recruitment of arrestins have not been found to occur (Fairfax et al., 2004; Perroy et al., 2003). Using a snap-tag technique, $GABA_B$ receptors have recently been described to exist as dimers of R1R2 dimers (Maurel et al., 2008) on the cell surface. Such higher-order oligomerisation may have implications in signalling efficacy and trafficking of the receptors.

1.11 The α-bungarotoxin labelling method

Most studies on $GABA_B$ receptors so far have used cell surface biotinylation or specific antibodies to monitor trafficking, both of which require the cells to be fixed. Recently the cell surface mobility of $GABA_B$ R1 receptors have been studied in GIRK cells and live hippocampal neurons using an α-bungarotoxin (BTX) binding site (BBS) method (Wilkins et al., 2008).

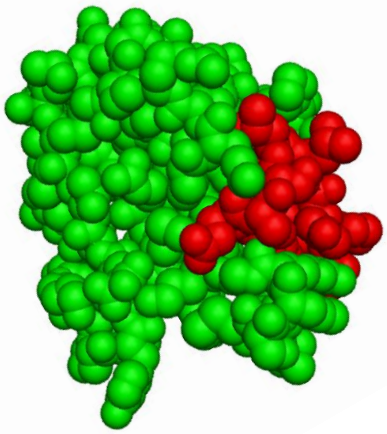

Figure 1.8 – α-bungarotoxin (BTX) bound to the bungarotoxin binding site.
Crystal structure of the α-bungarotoxin (green) bound to the 13 amino acid BBS mimotope (red). The BBS binds to a groove formed on the surface of BTX. The structure was generated form PDB file 1HC9

The 8 kDa (74 amino acid) snake venom neurotoxin, BTX was discovered in 1963 (Chang, 1999) and binds to α7, α8, and α9 nicotinic acetylcholine receptors (AChRs) causing their inhibition (Corringer et al., 2000). There has been considerable effort in crystallizing nicotinic AChRs bound to BTX, but due to its hydrophobic nature this has proved difficult to achieve. Several studies have therefore focused on identifying the residues within the receptor that play a crucial role in binding BTX and based on these studies, the crystal structure of the mimotope WRYYESSLEPYPD bound to BTX with high affinity has been resolved (Harel et al., 2001) (Fig. 1.8). This mimotope has been cloned into several receptors/ ion channels and shown to bind to BTX. These include, $GABA_A$ receptor subunits (Bogdanov et al., 2006), AMPA receptors (Sekine-Aizawa and Huganir, 2004), $GABA_B$ R1 receptors (Wilkins et al., 2008), Ca^{2+} channels (Tran-Van-Minh and Dolphin, 2010), and voltage-gated K^+ channel $K_V4.2$ (Moise et al., 2010).

Several biochemical and fluorescent-tagging techniques are available to study receptor trafficking. One of the most important considerations while studying receptor trafficking is the specificity of the tags for the receptor of interest. For receptors like the α7, α8, and α9 nicotinic AChRs, the high affinity binding of BTX coupled to fluorophores can be used to study the mobility these receptors. For receptors that are not known to bind to an agonist to which a fluorophore can be conjugated, specificity can be achieved by creation of fusion proteins between receptors and fluorescent proteins to provide specificity. However, although fusion proteins have been routinely genetically engineered to integrate into the genomes of simple model organisms such as drosophila and *C. elegans* because of the ease with which their genomes can be genetically modified, this is more of a challenge in higher model organisms. A vast majority of fusion protein studies in vertebrates have therefore used transfection

methods for recombinant fusion protein expression. In addition to this, depending on the location of the insertion of the fluorescent protein on the receptor, the fusion proteins can sometimes alter the normal functioning of the receptor.

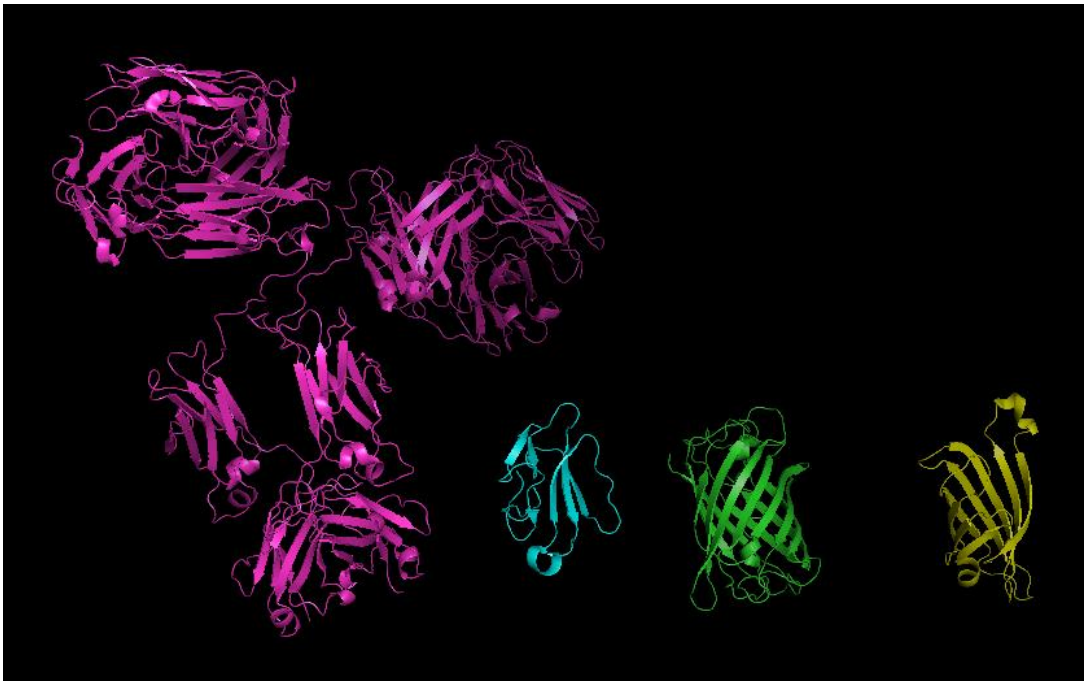

Figure 1.9 – Structures of commonly used tags.
Shown are the structures of an IgG antibody (magenta; PDB ID – 1IGT), α-bungarotoxin molecule (cyan; PDB ID – 1HC9), eGFP molecule (green; PDB ID – 1EMA), and a monomeric streptavidin molecule (yellow; PDB ID – 1STP). The structures are to scale relative to each other.

Tagging specificity can also be achieved by using specific antibodies to receptors or by engineering an antibody tag for example the myc-, flag-, or the HA-tag at a suitable location in the receptor. Antibody labelling strategies have used cell surface biotinylation followed by detection using antibody based biochemical strategies while live cell imaging with antibodies is also common. Other tags that do not depend on the

use of antibodies have also been developed and include a SNAP or CLIP tags (Maurel et al., 2008) and the alkaline phosphatase (AP) tag (Alcor et al., 2009). Strategies that couple specific agonists/ antagonists to fluorescent dyes have also been used to study receptor trafficking. Conjugation of fluorescent dyes to cysteine modification reagents have also been used although these sometimes have issues with specificity and functional neutrality.

While most of the tags described above have not reported changes in the pharmacological profiles of receptors, one has to be mindful of the fact that the size of the tag and pharmacological treatments used could alter the mobility of the receptors. The BTX binding strategy has several advantages over other receptor tagging methods. Firstly, the BBS is small (13 amino acids) compared to the size of other fluorophores, e.g., GFP, which is the most widely used fluorescent protein for the creation of fusion proteins, and is comparable in size to myc-(10 amino acids), flag-(8 amino acids), HA-(9 amino acids), AP-(15 amino acids), SNAP-/ CLIP- (around 180 amino acids: NEB UK pSNAPf/ pCLIPf vectors) tags. In addition, the size of BTX is significantly smaller than antibodies, f(ab)' fragments, eGFP molecules and streptavidin molecules that are commonly used in live cell imaging assays (Fig. 1.9). Live cell imaging using antibodies to date have used various approaches including primary antibodies coupled to fluorophores, primary antibodies followed by secondary antibodies or f(ab)' fragments coupled to fluorophores. Perhaps the most widely used approach is the primary and secondary antibody complex, which would be significantly greater in size compared to the BTX (Fig. 1.9). Another advantage of using the BTX labelling technique compared to fluorescent protein-receptor fusion proteins is that the BTX method allows discrimination of cell surface receptors compared to fluorophore protein tagging

techniques. pH sensitive fluorescent proteins (Ashby et al., 2004) have been developed that allows the detection of only cell surface proteins provided the fluorescent protein is exposed in the extracellular environment, but often the signal-noise achieved at the cell surface is quite low compared to BTX fluorophore conjugates. The advantage of using BTX technique over AP tags is that for the AP tag, an additional bacterial enzyme, BirA, has to be co-transfected with the AP tag containing recombinant receptor.

1.12 Dual-labelling with a minimal tag

Dual-labelling of two different surface receptors with two different fluorophores allows the study of relative mobility of the two receptors simultaneously and has been achieved using several strategies. A method for discriminating cell surface $GABA_B$ receptors from intracellular receptors using antibodies targeted specifically against the R1 and R2 subunits has been used (Vargas et al., 2008). The two receptors were incubated with two different primary antibodies that specifically recognise the R1 and R2 subunits followed by incubation with secondary antibodies coupled to two different fluorophores specific to the primary antibodies. Although this method allowed the detection of the two different cell surface subunits, the size of the antibody complexes could disrupt the normal functioning and mobility of the receptors. Therefore a method that uses a minimal reporter method to simultaneously monitor the trafficking of R1 and R2 subunits would be beneficial.

1.13 Lateral mobility of receptors

The fluid mosaic model of the plasma membrane postulates that the plasma membrane is a highly dynamic structure and lipids and proteins are free to move around within the plane of the cell membrane. For neuronal membranes, specialisation in terms of pre- and postsynaptic membranes is important for synaptic transmission and is achieved by compartmentalisation of receptors and proteins. Once a receptor is inserted into the plasma membrane, it diffuses freely with Brownian motion and a deviation from random diffusion is observed when the molecule enters areas of the cell surface with increased apparent viscosity. Factors that increase the apparent viscosity of membranes include filamentous actin (F-actin), hydrodynamic friction, and lipid domains. In addition to these factors intracellular scaffolds stabilise receptors at the postsynaptic membranes. Introduction of such confinements serves as important means of regulating signalling efficacy at synapses in addition to aiding receptor internalisation.

Given the important role lateral mobility of receptors plays in signalling efficacy, several biochemical, electrophysiological, and imaging approaches (Jaskolski and Henley, 2009) have been employed to study the dynamics of receptors on the plane of the membrane. Fluorescent recovery after photobleaching (FRAP) (Renner et al., 2008) of receptors tagged with genetically encoded fluorescent proteins is one of the most widely used methods to study lateral mobility. This has been used to study the bulk mobility of a population of the receptors although single receptors and different types of diffusion cannot be distinguished using this technique.

Single particle tracking (SPT) methods to study lateral mobility have used latex beads, fluorophores, and Quantum Dots (QDs) (Groc et al., 2007b) and can be used to study the mobility of single receptors in specific cell surface compartments. QDs are semiconductor nanocrystals that fluoresce brightly upon excitation and their photostability makes them suited to the study of lateral mobility. The size of the nano-crystals commercially available can vary between 10-30 nm in diameter and the fluorescence excitation of these crystals is directly related to their sizes. Hence, the emission spectra of these nanocrystals can vary from below 525 nm to just greater than 800 nm, even though the range of the diameter varies only by steps of 5 nm.

The lateral mobilities of several ionotropic receptors including $GABA_A$ (Bannai et al., 2009), Glycine (Dahan et al., 2003), AMPA (Groc et al., 2004), NMDA (Groc et al., 2007a), L-type Ca^{2+} channels (Mercer et al., 2011) along with the GPCR cannabinoid receptor 1 (CB1) (Mikasova et al., 2008) have been studied using QDs. These studies have used several strategies based on antibody labelling techniques to couple QDs to the receptors of interest: primary antibodies to specifically label the receptors in the N-terminus followed by either secondary antibody coupled to a QD or f(ab)' fragment coupled to biotin that reacts to a streptavidin-QD conjugate. An AP tag based method has also been used to study the lateral mobility of GluR2 receptors (Howarth et al., 2008). Recently the lateral mobility of nicotinic α7 AChRs (Burli et al., 2010; Fernandes et al., 2010) has been studied using a BTX based approach. At present there is no information on the lateral mobility of $GABA_B$ receptors on neuronal membranes and given the importance of $GABA_B$ receptors in cellular physiology this information is of interest.

Aims

The efficacy of slow synaptic inhibition in the CNS in response to GABA should depend on the cell surface stability and synaptic localisation of $GABA_B$ receptor hetero-oligomers. Most studies on the $GABA_B$ receptor so far have required the fixation of cells and therefore the mechanism of internalisation in live cells, in real time is less well understood. The roles of heterodimerisation on forward trafficking of R1 subunits from the ER to the cell surface has been relatively well characterised although whether heterodimerisation influences the internalisation profiles of $GABA_B$ receptors is unknown. In addition to this, it is not known whether there is a difference in internalisation and lateral mobility profiles of the two predominant subtypes of the $GABA_B$ receptor in the CNS, R1aR2 and R1bR2. Moreover, little is known about the lateral mobility of single $GABA_B$ receptors on neurons. Therefore, the development of an assay to study the real-time lateral mobility of $GABA_B$ receptors is important as it will enable the study of mechanisms that will could alter the specific synaptic localisations of cell surface $GABA_B$ receptors and therefore influence synaptic efficacy.

The summary of aims of this thesis is as follows:

- To study constitutive internalisation of $GABA_B$ in live GIRK cells and neurons in order to dissect the mechanism of internalisation including clathrin and dynamin dependence
- To study the role of heterodimerisation of $GABA_B$ in modulating trafficking of the $GABA_B$ receptor

- To develop a novel minimal reporter method based on the BBS site for simultaneously studying the internalisation of $GABA_B$ R1 and R2 subunits
- To identify motifs that regulate internalisation of $GABA_B$ receptors
- To study the role of the SDs in trafficking of $GABA_B$ receptors
- To study single $GABA_B$ receptor lateral mobility in hippocampal neurons using the BBS strategy

Chapter II

Materials and Methods

2.1 DNA, cloning and mutagenesis of $GABA_B$ receptor subunits

Myc-tagged rat $GABA_BR1a$ ($R1a^{Myc}$), myc-tagged human $GABA_BR1b$ ($R1b^{Myc}$), BBS-tagged $GABA_B$ R1a ($R1a^{BBS}$), and Flag-tagged $GABA_B$ R2 ($R2^{Flag}$) in pRK5 vector, pEGFP-C1, pEGFP-N1, pDsRed-Monomer-N1, and Rab7-GFP have all been described previously (Wilkins et al., 2008; Arancibia-Carcamo et al., 2009). eGFP-Rab5 and eGFP-Rab11 were a generous gift from José A Esteban and synaptophysin-eGFP was a generous gift from Yukiko Goda.

All oligonucleotides were purchased from Sigma-Genosys (UK) and the sequences have been provided in Table 2.1. The locations to which the oligonucleotide-pairs were designed to anneal to on the $GABA_B$ receptor subunits have been shown in Figure 2.1. $R2^{BBS}$ containing the BBS site was created from $R2^{Flag}$ by sub-cloning sense and antisense oligonucleotides encoding the 13 amino acid BBS (WRYYESSLEPYPD) (Harel et al., 2001) into a NheI site introduced using polymerase chain reaction (PCR; Table 2.2) into the $R2^{flag}$ subunit such that the BBS was placed 27 amino acids from the start of the mature protein (Fig. 4.2A). The $GABA_BR2^{BBS}$ ($R2^{BBS}$) cDNA was subcloned into pRK5. $R1b^{BBS}$ was created from $R1b^{myc}$, using an inverse PCR approach (Table 2.3) in which the 13 amino acids encoding for the BBS were inserted adjacent to the myc-tag,

which resides six amino acids from the start of the mature $GABA_B$ R1b protein (Fig. 5.1A).

Table 2.1 – List of oligonucleotides. All oligonucleotides are in the 5' to 3' direction

Primer Pair	Clone	Template	Method	Forward Primer	Reverse Primer
1	$R2^{Flag}$ ($R2^{Flag-Nhe1}$) with NheI site	$R2^{Flag}$	PCR	GCTAGCCTGCTGCTG TCGCTGCTGCTGT	GGGCAGCAGCAGG CGCGCGGGC
2	$R2^{BBS}$	$R2^{Flag-Nhe1}$	Ligation	CTAGCTGGAGATAC TACGAGAGCTCCCT GGAGCCCTACCCTG ACG	CTAGCGTCAGGGT AGGGCTCCAGGGA GCTCTCGTAGTATC TCCAG
3	$R1b^{BBS}$	$R1b^{myc}$	Inverse PCR	CCCTGGAGCCCTACC CTGACCCGCGGCCTC ACCCGCGGGTCCCC	AGCTCTCGTAGTAT CTCCATAGGTCTTC TTCTGATATTAG
4	$R1a^{BBS-ASA}$	$R1a^{BBS}$	Inverse PCR	GCCTCAGCGCGCCA CCCCCCAACACCCCC AGATC	GAGTTGCTGCCGA GACTGGAGCTG
5	$R1a^{BBS}\Delta CT$	$R1a^{BBS}$	Inverse PCR	TAGTTTAGAGTCGG CCTGCAGAA	CCTGCGCATCTTGG GCACAAAGAG
6	$R1a^{BBS-ASA-L889A,L890A}$	$R1a^{BBS-ASA}$	Inverse PCR	GCAGCAGAGAAGGA AAACCGAGAACTG	TCGGGACTTCTCTT CCTCGTTGTT
7	R2ΔCT	$R2^{BBS}$	Inverse PCR	TAGAAGCTTGGCCG CCATGGCCCAA	GTTTGTCCTCAGAG TGATGAGCTTTG
8	$R1b^{BBS-ASA}$	$R1b^{BBS}$	Inverse PCR	GCCTCCGCGCGCCA CCCACCGACACCCC	GAGCTGCTGCCGA GACTGGAG
9	$R1b^{BBS-ASA-L773A,L774A}$	$R1b^{BBS-ASA}$	Inverse PCR	GCGGCGGAGAAGG AGAACCGTGAACTG	CCGGGACTTCTCCT CCTCGTTG
10	$R1a^{BBS}\Delta$ SD1	$R1a^{BBS}$	Inverse PCR	TCCGAATCTGCTCCA AGTCTTA	CTTCCGAGGTGCTA GCGTCAGG
11	$R1a^{BBS}\Delta$ SD2	$R1a^{BBS}$	Inverse PCR	GAATCGAACGCCAC ACTCAGAACG	ACACAGCGGCTGG GTGTGTCCAT
12	$R1a^{BBS-CC}$	$R1a^{BBS}$	Inverse PCR	TGTTGTCTGGAGCCC TACCCTGACGCTAGC	CTCGTAGTATCTCC AGCTAGCTA
13	$mGluR2^{BBS}$	mGluR2	Inverse PCR	TTTAGAACCATATCC AGATGTGCTGACCCT GGAGGGAGAC	CTACTTTCATAATA TCTCCACTTCTTGG CTGGGCCCTCAGC
14	Insertion of Nhe1 site in $mGluR2^{BBS}$	$mGluR2^{BBS}$	PCR	CATCATGCTAGCGTG CTGACCCTGGAGGG AGAC	CATCATGCTAGCAT CTGGATATGGTTCT AAAC
15	SDs PCR out with Nhe1 site	$R1a^{myc}$	PCR	CATCATGCTAGCGG CGGGGCGCAGACAC CAAA	CATCATGCTAGCAT TCACCTGGCAGTG GGGCT

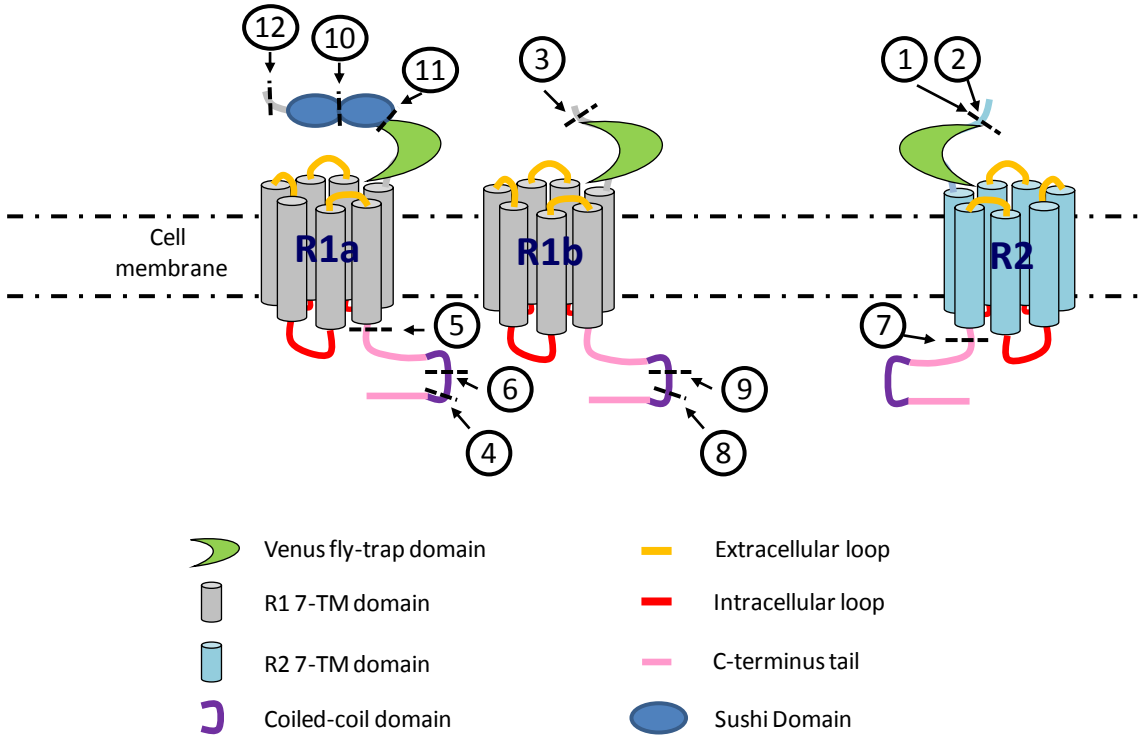

Figure 2.1 – Primer annealing sites on $GABA_B$ cDNAs.
Schematic diagram showing the annealing locations of the primer pairs on $GABA_B$ receptor subunit cDNA equivalents. The circles depict the primer pair number from Table 2.1 and the dotted lines are approximate areas where the primers were designed to anneal to.

The RSR ER retention motifs of $GABA_BR1a^{BBS}$ and $GABA_BR1b^{BBS}$ were mutated to ASA by substituting R922 and R924 in $R1a^{BBS}$ and R806 and R808 in $R1b^{BBS}$ to alanines, leaving serine in situ, using an inverse PCR strategy ($R1a^{BBS-ASA}$; $R1b^{BBS-ASA}$). $R1a^{BBS}$ with a complete truncation of the C-terminal tail (starting after R858; $R1a^{BBS}\Delta CT$), was made from $R1a^{BBS}$ using an inverse PCR method. Two leucines were substituted for alanines (L889A, L890A in $R1a^{BBS-ASA}$ and L773A and L774A in $R1b^{BBS-ASA}$) by inverse PCR to create $R1a^{BBS-ASA-L889A,L890A}$ and $R1b^{BBS-ASA-L773A,L774A}$. R2 with a truncated C-terminal tail (truncation starting after T748; R2ΔCT), was made from $R2^{flag}$ using an inverse PCR method.

Table 2.2- PCR protocol.

Reagent	Stock concentration	Final concentration	Volume
Forward Primer	15 µM	0.3 µM	1 µl
Reverse Primer	15 µM	0.3 µM	1 µl
Phusion® Buffer HF/ GC (Thermo Scientific)	x5	x1	10 µl
Template DNA	10 – 13 pM	0.2-0.26 pM	1 µl
dNTPs (dCTP, dATP, dGTP, dTTP; NEB UK)	10 µM each neucleotide	0.2 µM each neucleotide	1 µl
Phusion® (Thermo scientific)	2 units per µl	0.02 units	0.5 µl
H_20	-	-	35.5 µl
Total			50 µl

In order to study the role of the SDs on trafficking, they were deleted using inverse PCR strategies. R1a^{BBS}ΔSD1 contained a deletion in the first SD of R1a^{BBS}, from amino acids G28 to C95, and R1a^{BBS}ΔSD2 contained a deletion of the second SD in R1a^{BBS}, from amino acids R97 to V185 (both created by inverse PCR).

Two serine residues in the BBS (WRYYE*SS*LEPYPD) were substituted with cysteines in R1a^{BBS} by an inverse PCR method to create modified BBS for double fluorophore labelling (WRYYE*CC*LEPYPD; R1a$^{BBS\text{-}CC}$).

Table 2.3 – Inverse PCR method of mutagenesis.

Step 1
Polymerase chain reaction (as described in table 2.2)
Step 2
Gel purification PCR product run on 1% agarose gel followed by gel purification using Qiaquick gel extraction kit (Qiagen)
Step 3
Ligation - 16 µl of gel extracted DNA heated at 70°C for 2 min to denature the ends - DNA incubated in ice for 2 min - 2 µl X 10 DNA ligase buffer (Roche) - 1 µl (10 units) T4 polynucleotide kinase (NEB UK) - Incubation at 37°C for 30 min - Incubation on ice for 2 min - 1 µl (1 unit) T4 DNA ligase (Roche) - Incubation at 16°C overnight
Step 4
Transformation - 25 µl of One Shot TOP10 cells (Invitrogen) was thawed on ice - 1 µl of ligation product at 4°C added to cells and incubated on ice for 30 min - The cells were heat-shocked at 42°C for 30 s followed by incubation on ice for 1 min - 100 µl super optimal broth (Invitrogen) added and incubated at 37°C for 30 min with shaking at 800 rpm - The mixture was plated on ampicillin (100 µg/ml when liquid) agar plates
Step 5
Extraction of DNA for sequencing - Colonies were picked and grown up overnight as starter cultures in 2.5 ml lysogeny broth (LB; 20 g/l; Sigma) supplemented with 2.5 µl ampicillin (100 mg/ml) at 37°C and shaking at 350 rpm overnight - DNA was extracted using either a QIAprep Spin Miniprep Kit (Qiagen) or a GenElute Plasmid Miniprep Kit (Sigma) according to manufacturer's instructions
Step 6
Large scale extraction of DNA - The starter cultures of clones that contained the desired mutations were grown up in 200 ml LB (supplemented with 100 µg/ml ampicillin) at 37°C and shaking at 350 rpm overnight - DNA was extracted using either a Qiagen Plasmid Midi/ Maxi-prep Kit or a PureYield Plasmid Maxiprep kit (Promega) according to manufacturers' instructions

Human mGluR2 cDNA in the vector pCDNA3.1+ was purchased from Missouri S&T cDNA Resource Centre (www.cdna.org) and a BBS with the sequence WRYYESSLEPYPD was introduced 6 amino acids from the start of mature protein using an inverse PCR strategy (Fig. 5.7A). The two SDs of R1a from amino acids G16 to N159 was inserted

into the N-terminus of mGluR2^{BBS} adjacent to the BBS site by introducing an NheI site at the end of the BBS mGluR2^{BBS} (mGluR2$^{BBS\text{-}NheI}$). The two SDs on R1a^{Myc} were amplified by PCR with primers containing NheI sites at either ends. mGluR2$^{BBS\text{-}NheI}$ was digested with NheI (NEB UK) and the PCR products containing the SDs were cleaned using a Qiagen PCR purification kit according to the manufacturer's instructions, then digested using NheI and gel purified. mGluR2$^{BBS\text{-}NheI}$ digested with NheI was 5' dephosphorylated using shrimp alkaline phosphate (USB) and ligated with the gel purified, NheI digested SDs.

Table 2.4 – Method for restriction digestion and 5' dephosphorylation.

Step 1
Restriction Digestion - 2 µl X10 Buffer 2 (NEB UK) - 1 µl Template DNA (1000 µg/ml for mGluR2$^{BBS\text{-}NheI}$ or 5 µl PCR cleanup product) - 2 µl X10 BSA (NEB UK) - 14 µl H_20 - 1 µl Nhe1 (NEB UK) - Incubation at 37°C for 1 hr
Step 2
5' dephosphorylation - 1 µl shrimp alkaline phosphatase added to the digestion mixture (Step 1) - Incubation at 37°C for 1 hr - Heat inactivation at 65°C for 15 min followed by gel purification (Table 2.3 Step 2)

The protocol for Inverse PCR reactions is provided in table 2.2. The details of digestion, 5'-dephosphorylation are provided in table 2.4. The entire cDNA sequences of all constructs were checked for fidelity.

2.2 Cell Culture and transfection

HEK cells with a stable transformation with Kir3.1 and Kir3.2 channels (GIRK cells) (Leaney and Tinker, 2000) were maintained at 37°C and 95% air/ 5% CO_2 in Dulbecco's modified eagle medium (DMEM) supplemented with 10% v/v fetal calf serum (FCS), penicillin-G/ streptomycin (100U/ 100µg/ml), 2 mM glutamine, and geneticin (0.5 mg/ml) (all from Invitrogen). Cells were seeded onto poly-L-lysine-coated 22 mm glass coverslips and transfected using a calcium phosphate method (Wilkins et al., 2008) with 4 µg of total DNA in the following ratios: R1a (or $R1a^{BBS}$)/R2 (or $R2^{BBS}$) /eGFP reporter, 1:5:1, or R1a (or $R1a^{BBS}$)/ R2 (or $R2^{BBS}$) 1:5. The ratio of the subunits used for transfections was optimised for achieving maximum currents in electrophysiology experiments (Kuramoto et al., 2007). For radioligand binding experiments cells were transfected by electroporation using a GenePulser II electroporator (Bio-Rad) (Donnelly et al., 1999) using 10 µg DNA with R1a/ $R2^{BBS}$ ratio of 1:3 and then plated onto 10 cm dishes at 70% confluency.

Cultured hippocampal neurons were prepared from E18 Sprague-Dawley rat embryos as described previously (Thomas et al., 2005). Briefly this involved dissociation of the dissected hippocampi into single cells followed by plating onto 18 or 22 mm glass coverslips (Assistence/ VWR) coated with poly-D-lysine (Sigma) in a medium containing minimum essential media (MEM; Invitrogen), supplemented with 5% v/v heat-inactivated FCS, 5% v/v heat-inactivated horse serum (Invitrogen), penicillin-G/ streptomycin (10 U/10 µg/ml), 2 mM glutamine, and 20 mM glucose (Sigma). After 2 hours, the media was replaced and the cells were maintained until used for experiments in a media containing Neurobasal-A (Invitrogen), supplemented with 1%

v/v B-27, penicillin-G/ streptomycin (50 U/50 µg/ml), 0.5% v/v Glutamax (Invitrogen), and 35 mM glucose. Neurons were transfected at 8-10 days *in vitro* (DIV) using Effectene (Qiagen) or a calcium phosphate method (Xia et al., 1996). Visually, the efficiency of transfection with three or more constructs was lower than the efficiency of transfection with eGFP only. However, transfection of three constructs was routinely achieved to a satisfactory level in order to carry out experiments as only one neuron per cover-slip was required for imaging. The lab routinely uses transfection of three $GABA_A$ subunits along with eGFP for electrophysiology experiments to satisfactory levels.

2.3 α-bungarotoxin radioligand binding assay

The apparent affinity of BTX for its binding site on the $GABA_BR1aR2^{BBS}$ or $R1b^{BBS}R2$ receptor was determined using ^{125}I-BTX as described previously (Wilkins et al., 2008). GIRK cells expressing BBS containing $GABA_B$ receptors were washed in phosphate buffered saline (PBS) before re-suspension in PBS containing 0.5% w/v bovine serum albumin (BSA; Sigma). Cells were incubated in 150 µl of PBS + 0.5% BSA containing ^{125}I-BTX (200 Ci/mmol; PerkinElmer) for 60 min at room temperature (RT). Nonspecific binding was determined after the addition of a 1000-fold excess higher concentration of unlabelled BTX (UL-BTX; Molecular Probes). Cells were harvested (Brandel) and radioligand binding was assessed by filtration onto 0.5% polyethylenimine pre-soaked Whatman GF/A filters, followed by rapid washing with PBS. The radiolabel retained on the filters was assayed with a Wallac 1261 gamma counter. Scatchard analysis using a non-linear regression fitting algorithm was used to obtain B_{max} and K_d values from:

$$y = (B_{max}X)/ (K_d + X),$$

where X is the ^{125}I-BTX concentration. The same analysis was used for the $\alpha7/5HT_{3a}$ receptor chimera, expressed in GIRK cells, which exhibits high affinity BTX binding (Wilkins et al., 2008).

2.4 Whole-cell electrophysiology

Whole-cell potassium currents activated by GABA were recorded from individual $GABA_B$ receptor expressing GIRK cells using patch clamp recording as indicated previously (Wilkins et al., 2008). Patch pipettes (resistances: 3 – 5 MΩ) contained the following solution (mM): 120 KCl, 2 $MgCl_2$, 11 EGTA, 30 KOH, 10 HEPES, 1 $CaCl_2$, 1 GTP, 2 ATP, 14 creatine phosphate, pH 7.0. The GIRK cells were bathed in a Krebs solution containing (mM): 140 NaCl, 4.7 KCl, 1.2 $MgCl_2$, 2.5 $CaCl_2$, 11 glucose, and 5 HEPES, pH 7.4. To increase the amplitude of the $GABA_B$ receptor-activated K^+ currents, prior to the application of GABA, the KCl concentration in the external solution was increased to 25 mM, with a corresponding reduction in the NaCl concentration to 120 mM. This shifted E_K from -90 mV to -47 mV. The peak amplitude GABA-activated K^+ currents were now inward at a holding potential of -70 mV increasing their amplitude give the inward-rectifying nature of the channels. Membrane currents were recorded from cells 48–72 h post-transfection and filtered at 5 kHz (-3dB, 6th pole Bessel, 36 dB/octave) before storage on a Dell Pentium III computer for analysis with Clampex 8. Changes >10% in the membrane input conductance or series resistance resulted in the recording being discarded.

The GABA concentration-response curves were generated by measuring the potassium current (I) for each GABA concentration applied at 3-min intervals in the absence or presence of 3 µg/ml BTX coupled to Alexa Fluor 555 (BTX-AF555; Molecular Probes). The current amplitudes were normalized to the maximum GABA response (I_{max}) and the concentration response relationship fitted with the Hill equation:

$$I/ I_{max} = [(1 / 1 + (EC_{50} / A)^{n})],$$

where A represents GABA concentration, EC_{50}, the GABA concentration activating 50% of the maximum response, and n, is the Hill slope.

2.5 Double labelling of R1a and R2 with BTX

R1a and R2 subunits containing the Cys mutant ($R1a^{BBS-CC}$) and wild-type ($R2^{BBS}$) versions of the BBS in GIRK cells were exposed to 0.2 mM dithiothreitol (DTT) in PBS for 15 min at room temperature to reduce the di-sulphide bond that forms between the two cysteines on the modified BBS. After washing (3x) in PBS to remove the DTT, cells were incubated with 200 µM Sodium (2-Sulphonatoethyl) methanethiosulfonate (MTSES) in PBS for 5 min at 4°C to selectively block the binding of BTX to $R1a^{BBS-CC}$. MTSES has the advantage of being cell impermeable compared other small MTS reagents such as 2-aminoethyl methanethiosulfonate hydrobromide (MTSEA). Subsequently, after washing in ice-cold PBS (3x) to remove the MTSES, the cells were incubated in 3 µg/ ml BTX coupled to Alexa Fluor 488 (BTX-AF488; Molecular Probes) for 10 min at 4°C to label the $R2^{BBS}$ subunits. The cells were then washed with PBS (3x) to remove the unbound BTX-AF488 and incubated in 2 mM DTT in ice-cold PBS for 5

min at RT to remove the MTSES bound to $R1a^{BBS-CC}$ subunits. The cells were then washed with PBS to remove the DTT and incubated in 3 µg/ml BTX-AF555 for 10 min at 4°C to label the $R1a^{BBS-CC}$ subunits. Finally, PBS was used to remove excess BTX-AF555 prior to dual fluorophore confocal imaging.

2.6 Fixed cell confocal imaging

Cells were fixed in 4% w/v paraformaldehyde (PFA) in PBS for 5 min and quenched with 5% w/v NH_4Cl in PBS for 5 min. After washing (3x), cells were mounted on glass microscope slides using glycerol. A Zeiss Axioskop LSM510 confocal microscope with 3 laser lines (λ = 488, 543 and 643 nm) and a Meta head was used with a Plan Neofluor 40x oil differential interference contrast (DIC) objective (NA 1.3; Zeiss) for confocal imaging. The top and bottom of the imaged cell was determined using a rapid z-stack scan and a mid-stack slice was optimised and acquired as a mean of 4 scans in 8 bits and stored for analysis.

2.7 Live cell confocal imaging

Live transfected GIRK cells and hippocampal neurons at 14-21 days *in vitro (*DIV) were imaged using the confocal microscope with an Achroplan 40x water immersion DIC objective (NA 0.8; Zeiss). To label $R1a^{BBS}$ or $R2^{BBS}$ with BTX, transfected GIRK cells were washed in (3x) Krebs and incubated in 3 µg/ml BTX-AF555. Transfected hippocampal neurons were similarly washed and incubated in 1 mM d-tubocurarine (d-TC) for 5

min, to prevent BTX binding to native nicotinic AChRs (Wilkins et al., 2008; Sekine-Aizawa and Huganir, 2004), followed by incubation with 3 µg/ml BTX-AF555 in Krebs for 10 min. Labelled cells were superfused with Krebs at 16-18°C, 22- 24°C, or 30-32°C.

To start imaging at t = 0, the mid-optical slice was optimised as described above and imaged as a mean of 4 scans in 8 bits using the 543 nm Helium-Neon laser (560 nm long-pass filter) for BTX-AF555, or the 488 Argon laser (505-530 nm band-pass filter) for imaging eGFP or BTX-AF488. For later time points all the confocal settings (detector gain, amplifier offset, optical slice thickness, laser intensity) were unaltered from those used at t = 0. For fixed and live cell imaging at low temperatures, cells were co-transfected with eGFP and $GABA_B$ receptor subunit constructs. For single fluorophore live cell confocal imaging at room and near physiological temperatures, the cells were only transfected with the receptor subunits. Thus the only fluorophore excited during live cell imaging was AF555, conjugated to BTX. This minimised the exposure time of the cells to the laser. During live imaging, transmitted light or eGFP images were captured simultaneously with BTX-AF555 images to check for change to cell morphology. The majority of cells showed no sign of phototoxicity, such as surface blebbing, over 1 hr periods of imaging and those that did, were excluded from analysis.

2.8 Photobleaching profile

To ensure the rate and extent of $R1a^{BBS}R2$ receptor internalisation could be accurately measured using the BTX-linked fluorophores required that the fluorophore emissions are not significantly affected by photobleaching. To determine the extent of any

photobleaching for BTX-AF555, live GIRK cells, transfected with R1a^{BBS}R2 were tagged with BTX-AF555 and then exposed to 8 scans (pixel time = 1.6 µs) performed consecutively every 8 s up to a total of 120 (total laser exposure time per pixel = 192µS) at 7-9°C and 30-32°C. A loss of approximately 10% fluorescence intensity was evident over 120 scans, which was unaffected by temperature. However, this rate of scanning far exceeds that used in all the live cell experiments which required 4 scans at 5 time points over 1 hr, giving a total of just 20 scans. Therefore, photobleaching was negligible and did not affect the surface fluorescence measurements.

2.9 Confocal image analysis

Confocal images were analysed using ImageJ (Ver 1.40g). The mean fluorescence was determined for 3 regions of interest (ROIs), selected for each cell - surface membrane, intracellular compartment, and total cell fluorescence. Background fluorescence was set by imaging a region of the coverslip devoid of cells. This was subtracted from the ROI fluorescence yielding a mean background-corrected fluorescence. For live cells, the mean background-corrected fluorescence per unit area (µm^2) at each time point was then normalised to the mean background-corrected fluorescence per µm^2 at t = 0. These values were then fitted with an monoexponential decay function using Origin (ver 6).

2.10 Labelling BBS containing receptors with QDs

Hippocampal neurons expressing BBS tagged receptors were incubated in 1 mM d-TC for 5 min and incubated in 2 μg/ml biotinylated BTX (BTX-B; Molecular Probes) for 2 min at 37°C. The cells were washed with Krebs (3x) and incubated in 10 pM Quantum Dot 655 conjugated to streptavidin (QD655; Molecular Probes) for 1 min at 37°C in QD binding buffer, essentially as described previously (Levi et al., 2011). This contained BSA (2% w/v), sodium azide (1 mM; Sigma), sucrose (215 mM; Sigma), and sodium borate (2.5 mM; Sigma). The cells were washed thoroughly in Krebs and either fixed, in 4% w/v PFA in PBS for 5 min followed 5% w/v NH_4Cl in PBS and mounted on glass microscope slides, for fixed cell imaging or mounted in a recording chamber at 37°C (Solent Scientific) for live cell imaging in Krebs.

2.11 Fixed cell wide-field imaging

A wide-field imaging setup was used to image specificity of QD655 labelling in fixed neurons using a Olympus IX71 inverted microscope, with a 60X objective (NA – 1.35; Olympus) and halogen lamp illumination (PhotoFluor-II Metal Halide illumination system. Images were acquired using a back-illuminated cooled electron-multiplying charge coupled device (EMCCD) camera (iXon3 885; Andor Technology). eGFP was imaged with a 457-487 nm (Semrock) band-pass excitation filter, a 496 nm long-pass emission filter, and 495 nm dichoric beamsplitter. QD655 was imaged with a 415-455 nm band-pass excitation filter, a 647.5 - 662.5 nm band-pass emission filter, and a 510 nm dichoric beamsplitter. Images were acquired with minimum exposure (typically 30-

100 ms) in 16 bits using Cairn-Metamorph Meta Imaging software (Molecular Devices; version 7.7.10) and stored for analysis.

2.12 Real-time imaging of single $GABA_B$ receptors

Real-time imaging of single $GABA_B$ receptors tagged with QD655 was carried out using the wide-field setup described in the previous section. To start imaging, a suitable area was selected and at first, an image of the eGFP marker would be captured with a suitable exposure time (typically around 30-150 ms based on the levels of expression). Next the filters were changed to image QD655 without changing the field of view and an image sequence of 300 frames captured at 33 Hz would be taken and stored for later analysis.

2.13 Single particle tracking

SPT of $GABA_B$ receptors was carried out as described previously for other receptors (Levi et al., 2011; Dahan et al., 2003; Renner et al., 2009; Groc et al., 2007a; Bannai et al., 2009). Single $GABA_B$ receptors coupled to QD655 via the BBS site were identified by their characteristic blinking (Dahan et al., 2003). Matlab (MathWorks) based software, SPTrack (Ver 5), was a gift from Antoine Triller (Paris) and was used to track the QDs. For every image in sequence, the centre of the QD spot fluorescence was determined by a two-dimensional Gaussian fit with a spatial resolution of $\sim$10 – 20 nm. This was undertaken for all QDs. The Gaussian peaks in a given frame were next associated with the Gaussian peaks from the previous frame based on estimated diffusion co-efficients

and the likelihood of the two Gaussian peaks in consecutive frames belonging to the same QD. QDs which appear in at least 15 consecutive frames were used for tracking analysis and the shorter ones discarded. The mean square displacement (MSD) of each QD was calculated using the following equation:

$$\mathrm{MSD}\,(ndt) = (N-n)^{-1}\Sigma_{i=1}^{N-n}((x_{i+n}-x_i)^2 + ((y_{i+n}-y_i)^2)$$

where x_i and y_i are the spatial co-ordinates of a QD on any image frame i, N is the total number of points in the trajectory, dt is the time interval between two successive frames (33 ms), and ndt is the time interval over which the displacement is averaged. From the MSD plot, the diffusion coefficient, D, for a QD was calculated by fitting the first two to five points of the MSD plot against time with the following equation:

$$\mathrm{MSD}(t) = 4D_{2-5}\,t + 4\sigma_x^{\,2}$$

where σ_x is the QD localization accuracy in one direction. D was determined from the slope of the relationship. Given the inherent noise in CCD imaging systems and the errors in precise pointing accuracy that results to, trajectories with $D < 10^{-4}$ $\mu m^2/s$ were considered immobile.

Synaptic terminals were identified and thresholded using a multidimensional image analysis plug-in based on MetaMorph (Molecular Devices) software in Paris (Professor Antoine Triller; (Racine et al., 2007)). QD trajectories that co-localised with synaptic markers were defined as synaptic.

QD data was analysed using Origin (Ver 6) and built-in functions in Matlab.

Chapter III

Constitutive internalisation of $GABA_B$ receptors in live cells

3.1 Introduction

Molecular cloning of the two $GABA_B$ receptor subunits in 1997 and 1998 (Kaupmann et al., 1998; Kaupmann et al., 1997; White et al., 1998) heralded a new era in the study of the molecular properties of $GABA_B$ receptors including trafficking of these receptors. Soon after the first report on the cloning of the R1 subunit was published (Kaupmann et al., 1997), a study reported the failure of this subunit to reach the cell surface due to retention within the ER in heterologous expression systems (Couve et al., 1998). Thus, the earliest trafficking studies of the $GABA_B$ receptor were focused on anterograde trafficking of R1 subunits. After the R2 subunit was cloned, it became clear that heterodimerisation of the two subunits was required for cell surface expression of a functional $GABA_B$ receptor because of the presence of a RXR-type ER retention motif in the C-terminal coiled-coil domain of R1 (Margeta-Mitrovic et al., 2000; Restituito et al., 2005; Margeta-Mitrovic et al., 2000). Interaction of the C-terminal coiled-coil domain of R2 masks this retention motif, RSR, thereby enabling R1 subunits to exit the ER and travel to the cell surface to form functional receptors (Margeta-Mitrovic et al., 2000; Villemure et al., 2005; Calver et al., 2001; Vargas et al., 2008).

Several studies so far have focused on the internalisation of $GABA_B$ receptors. Three of the earliest studies on internalisation of $GABA_B$ receptors reported these receptors as

highly resistant to internalisation on the cell surface in COS-7 cells (Perroy et al., 2003), HEK-293 cells (Balasubramanian et al., 2004) and cortical and hippocampal neurons in primary culture (Fairfax et al., 2004) with very little basal (constitutive) internalisation determined using cell surface biotinylation and fixed-cell antibody-labelling techniques. These studies neither observed a change in the internalisation profile of $GABA_B$ receptors in the presence of the $GABA_B$ receptor specific agonist baclofen nor a recruitment of β-arrestins to the cell surface in response to the agonist. Since these reports, several studies (Vargas et al., 2008; Wilkins et al., 2008; Grampp et al., 2008; Grampp et al., 2007; Guetg et al., 2010; Terunuma et al., 2010; Laffray et al., 2007; Gonzalez-Maeso et al., 2003) have described $GABA_B$ receptors as being highly mobile on the cell surface with rapid constitutive internalisation properties using a range of fixed cell antibody labelling techniques in combination with confocal imaging, or cell surface biotinylation. Some studies have observed agonist induced internalisation (Wilkins et al., 2008; Laffray et al., 2007) whereas others have observed no baclofen/ GABA induced changes to internalisation kinetics suggesting that the $GABA_B$ receptors have only one mode of internalisation unlike several other GPCRs including the β_2AR that undergo rapid agonist-mediated internalisation in response to the specific agonist isoprenaline (Scarselli and Donaldson, 2009). However, one study has reported increased internalisation of $GABA_B$ receptors in response to chronic agonist stimulation (Gonzalez-Maeso et al., 2003) where the difference between levels of constitutive internalisation and agonist-induced internalisation becomes statistically significant after two hours.

$GABA_B$ receptors have been reported to constitutively internalise via clathrin- (Grampp et al., 2007; Vargas et al., 2008; Grampp et al., 2008) and dynamin-dependent

(Grampp et al., 2007; Vargas et al., 2008; Guetg et al., 2010) pathways in fixed cells. In addition, the presence of $GABA_B$ receptors in lipid rafts has been reported by two studies (Becher et al., 2001; Becher et al., 2004) although no effect in $GABA_B$ receptor internalisation has been observed in the presence of blockers of caveolin-mediated endocytosis (Grampp et al., 2007; Laffray et al., 2007).

$GABA_B$ receptors are recruited to early endosomes (Grampp et al., 2008) after internalisation from where a proportion of the receptors move to recycling endosomes (Grampp et al., 2008; Laffray et al., 2007; Vargas et al., 2008) and are subsequently re-inserted into the plasma membrane to form cell-surface receptors (Laffray et al., 2007; Vargas et al., 2008) and the rest are targeted to lysosomes for degradation (Grampp et al., 2008; Grampp et al., 2007; Kantamneni et al., 2008; Kantamneni et al., 2009) via late-endosomes (Grampp et al., 2008). Baclofen has been reported to speed up the rate of recycling of $GABA_B$ receptors (Grampp et al., 2008). Inhibition of lysosomal degradation by the protease inhibitor leupeptin causes accumulation of $GABA_B$ receptors in the cytosol (Grampp et al., 2008) further supporting the lysosomal degradation hypothesis of these receptors.

Most studies on $GABA_B$ receptor trafficking, so far, have used cell surface biotinylation or antibody labelling techniques both of which require the cells to be fixed. Recently the internalisation of $GABA_B$ R1 receptors have been studied in fixed GIRK cells and live hippocampal neurons using a BBS inserted at the N-terminus of the receptor (Wilkins et al., 2008). Here the same strategy has been applied to monitor the trafficking of $GABA_B$ receptors using optimised live cell imaging strategies to report the kinetics of constitutive internalisation of $GABA_B$ receptors.

3.2 Results

3.2.1 Constitutive internalisation of bungarotoxin tagged $GABA_B$ $R1a^{BBS}$ R2 receptors in live GIRK cells

A clear staining of cell surface $GABA_B$ $R1a^{BBS}$ receptors was observed in live GIRK cells when cells transfected with cDNAs encoding for $R1a^{BBS}$, R2 and eGFP were incubated in 3 µg/ml BTX-AF555 for 10 min at RT and imaged using a water immersion objective (Fig 3.1A; upper panel). Fluorescence staining was specific as it was not observed when the transfected cells were incubated either in UL-BTX (Fig 3.1A; middle panel) or when cells transfected with cDNA encoding for eGFP only were incubated in BTX-AF555 (Fig. 3.1A; lower panel) prior to imaging.

Having established the fluorescence staining specificity of BBS containing receptors, constitutive internalisation of $R1a^{BBS}$R2 receptors was studied in live GIRK cells in order to understand the kinetics of $GABA_B$ receptor internalisation and to identify factors that influenced them. Selectively labelled $GABA_B$ $R1a^{BBS}$R2 receptors were imaged in Krebs solution at specific time points for an hour at low (16-18°C; LT), room (22-24°C; RT), or near physiological (30-32°C; PT) temperatures. During live cell imaging, transmitted light or eGFP images were captured simultaneously along with BTX-AF555 images and the cell surface membrane was identified by drawing a region of interest around the eGFP/ transmitted light images. This region of interest was then transferred to BTX-AF555 image and checked for overlap with the surface staining observed in the BTX-AF555 channel. The mean cell surface fluorescence per unit area at each time point was calculated and normalised to the cell surface fluorescence at t=0 and these were fitted to a mono-exponential decay to determine the rates of

internalisation of $R1a^{BBS}R2$ receptors. The percentage of receptors at t = 0 remaining on the cell surface at t = 60 was used as an indicator of the extent of internalisation. The decrease in cell surface fluorescence observed (Fig. 3.1B) at RT and PT is due to internalisation of BBS-AF555 tagged $GABA_B$ $R1a^{BBS}R2$ receptors.

At LT, which are non permissive for internalisation (Connolly et al., 1999), very little constitutive internalisation of $R1a^{BBS}R2$ receptors was observed in GIRK cells (Fig 3.1B; upper panels). After 1 hr, a large proportion of the original cell surface fluorescence at t = 0 remained on the cell surface (85.7%, n= 6) (Fig 3.1B; 3.1C; 3.1D), indicating that $GABA_B$ receptor internalisation is an active process.

At RT and PT, $R1a^{BBS}R2$ receptors rapidly constitutively internalised in GIRK cells (τ = 13.4 ± 1.4, n=12 at RT; τ = 12.4 ± 1.1, n=15 at PT; Fig. 3.1B; middle and lower panels) and in 5 min, intracellular compartments were filled with internalised BBS tagged receptors (Fig 3.1B; arrows). There was no statistical difference between the membrane fluorescence decay constants, according to a single exponential process, at RT and PT ($P>0.05$; Fig. 3.1C) but the receptors have a tendency to internalise at a faster rate as the temperature increases. The extent of internalisation was greater at the higher temperature (35.2 ± 1.9, n=15; $P<0.001$; Fig 3.1C; 3.1D) compared to RT (50.5 ± 2, n=12; Fig 3.1C; 3.1D) and the extents of internalisation at both RT and PT were greater than the extent of internalisation at LT ($P<0.001$; Fig 3.1D).

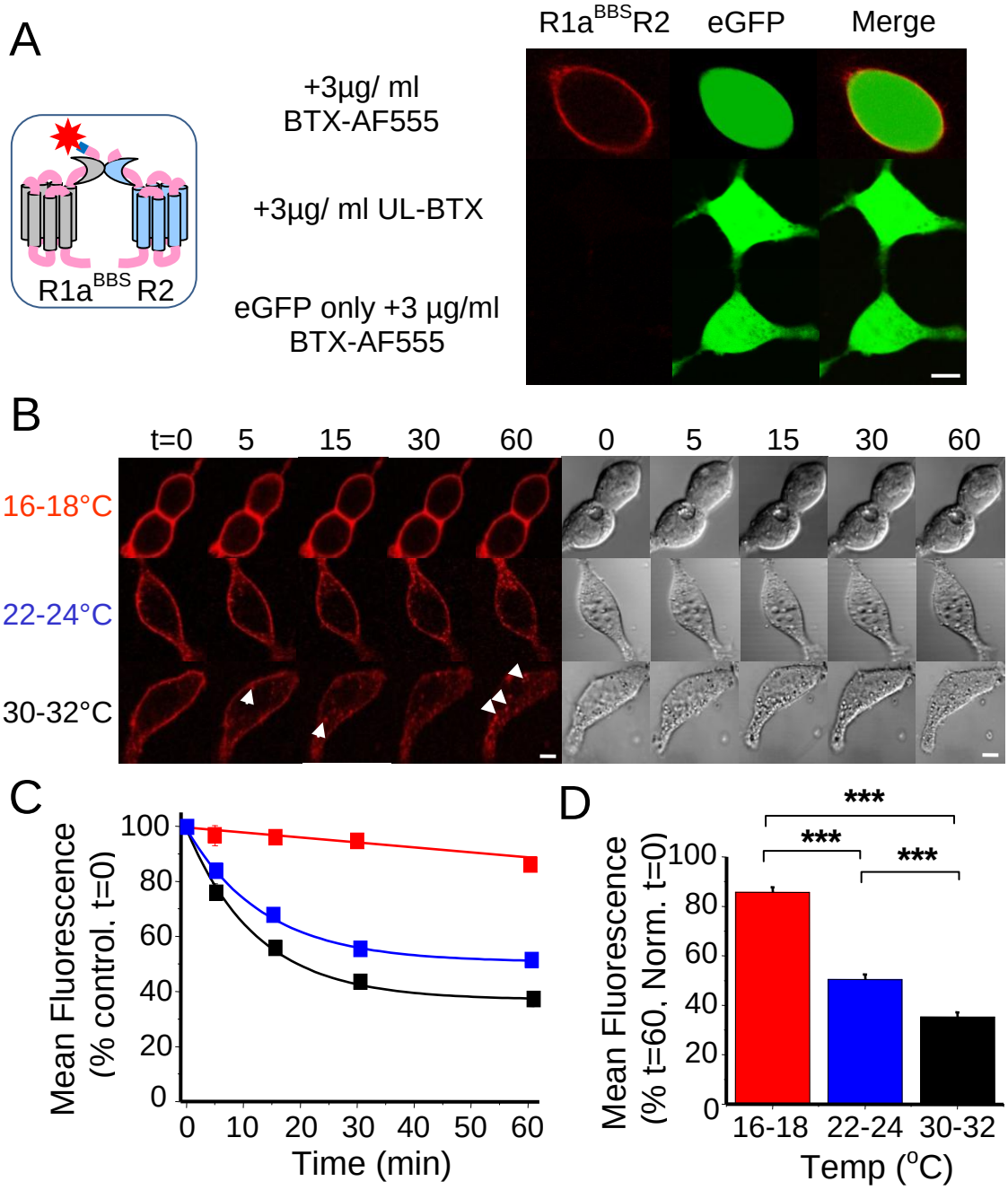

Figure 3.1 - Constitutive internalisation of R1a^{BBS}R2 receptors in live GIRK cells.

A GIRK cells expressing eGPF with (upper and middle panels) or without R1a^{BBS} and R2 (bottom panel) cDNAs were incubated either in 3 µg/ml BTX-AF555 or 3µg/ ml unlabelled BTX. Scale bar 5 µm. *B* GIRK cells expressing R1a^{BBS}R2 receptors were incubated in 3 µg/ml BTX-AF555 for 10 min at RT and then imaged over 0 – 60 min at 16-18°C, 22-24°C, and 30-32°C. Arrowheads locate internalised R1a subunits. Scale bar = 5 µm. *C and D*, Rate (C) and extent (D) of internalisation of BTX-AF555 tagged R1a^{BBS}R2 at 16-18°C (red), 22-24°C (blue), and 30-32°C (black), n = 6 - 15, *** P<0.001. In this and proceeding figures, all points and bars represent means ± s.e.m. n = 6 - 12 ***P<0.001.

The transmitted light or eGFP images captured simultaneously along with BTX-AF555 images allowed identification of changes in cellular morphology due to phototoxicity or poor cellular physiology that was introduced during live cell imaging. A vast majority of cells showed very little change in morphology in the presence of a correct osmolarity of the Krebs media and slow rate of perfusion (Fig 3.1B). In cases where the morphology changed significantly, the images were discarded and not used for analysis. Additionally, classical signs of photo-toxicity such as blebbing were not observed over the one hour period of imaging. The differences in morphology observed between cells at different temperatures (Fig. 3.1B) is possibly due to properties of the cell membrane which causes them to be more fluid at higher temperatures compared to lower temperatures.

3.2.2 Constitutive internalisation of bungarotoxin tagged $GABA_B$ $R1a^{BBS}R2$ receptors in live primary hippocampal neurons

Having studied constitutive internalisation of $GABA_B$ receptors in GIRK cells, constitutive internalisation of $R1a^{BBS}R2$ receptors was studied in primary hippocampal neurons in culture. Similar to GIRK cells, a clear and selective staining of $R1a^{BBS}$ subunits was achieved in neurons, pre-incubated in 1 mM d-TC for 5 min, when cells transfected with cDNAs encoding for $R1a^{BBS}$, R2 and eGFP were incubated in 3 µg/ml BTX-AF555 for 10 min at RT and imaged (Fig 3.2A; upper panel). Such staining was not observed when the transfected cells were incubated either in UL-BTX (Fig 3.2A; middle panel) or when cells transfected with cDNA encoding for eGFP only were incubated in BTX-AF555 (Fig 3.2A; lower panel).

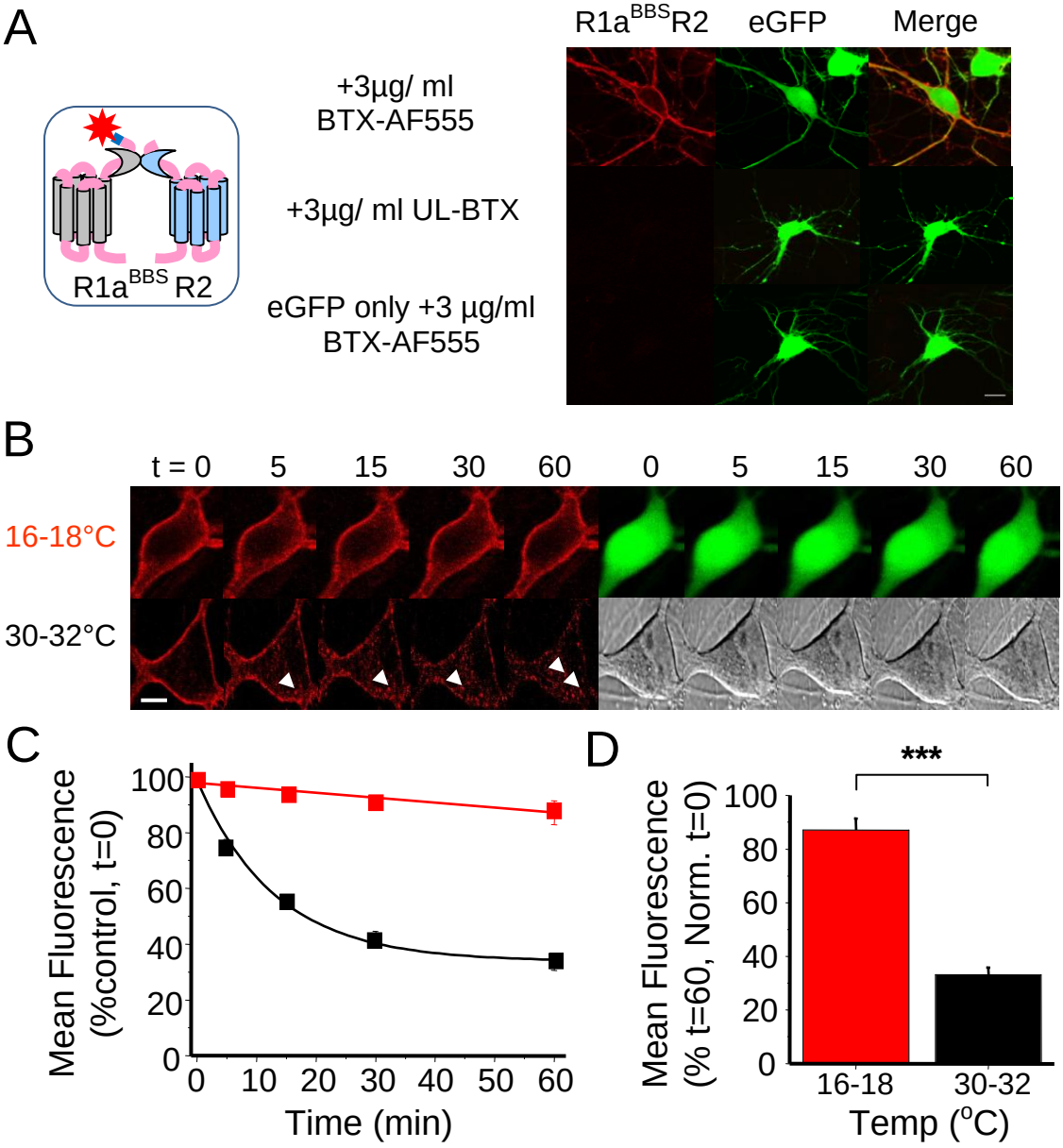

Figure 3.2 - Constitutive internalisation of R1a^{BBS}R2 receptors in live hippocampal neurons.

A. Hippocampal neurons in culture (14-21 DIV) expressing eGPF with (upper and middle panels) or without R1a^{BBS} and R2 (bottom panel) cDNAs were incubated in 1 mM d-TC for 5 min and then either in 3 µg/ml BTX-AF555 or 3 µg/ml UL- BTX. *B.* Hippocampal neurons (14-21 DIV) expressing R1a^{BBS}R2 and eGFP were incubated in 1 mM d-TC for 5 min followed by 3 µg/ml BTX-AF555 for 10 min at RT and imaged at different time points at 16-18°C or 30-32°C. Arrowheads indicate internalised R1aR2 receptors. C *and D,* Rate (C) and extent (D) of internalisation of BTX-AF555 tagged R1a^{BBS}R2 receptors at 16-18°C (red), and 30-32°C (black) in live hippocampal neurons, n = 6 - 12 ***P<0.001. Scale bars = 10 µm.

At LT, very little constitutive internalisation of BTX-AF555 labelled $R1a^{BBS}R2$ receptors was observed in hippocampal neurons (Fig 3.2B; upper panel) with a large proportion of the original cell surface fluorescence at t = 0 remaining on the cell surface after 1 hr (85.7%, n= 6; Fig 3.2C; 3.2D). However, at PT constitutive internalisation $R1a^{BBS}R2$ receptors preceded at a rapid rate and intracellular structures filled with BTX-AF555 tagged receptors could be detected within 5 min (Fig 3.2B; lower panel; arrows). The time constant for the rate of decay of membrane fluorescence according to a single exponential process was 13.1 ± 1.7 (n=12; Fig 3.2C) and after 1 hr the extent of receptor internalisation was greater (33.2 ± 2.6, n=12, $P<0.001$) than that was observed at LT (Fig 3.2D). Transmitted light or eGFP images revealed no change in cellular morphology due to phototoxicity during live cell imaging of hippocampal neurons (Fig. 3.2B).

3.2.3 Photobleaching of BTX-AF555

To accurately reflect the rate and extent of receptor internalisation by using a fluorophore reporter requires that the fluorophore is stable and not subject to significant photo-bleaching. Thus, photo-bleaching can become a limiting factor in all live cell imaging studies the rate of photo-bleaching of BTX-AF555 was determined under the experimental conditions used. GIRK cells, transfected with $R1a^{BBS}R2$ were tagged with BTX-AF555 and superfused in Krebs and imaged. An average of 8 (pixel time 1.6 μS) scans were performed consecutively every 8 seconds to give a total of 120 scans in order to construct the bleaching profile of BTX-AF555 under the live cell imaging conditions at two different temperatures, 7-9°C (Fig 3.3A; 3.3B) and 30-32°C

(Fig. 3.3B). No discrimination was made in choosing the cells for imaging and cells with a wide range of starting levels of fluorescence were selected. Most cells irrespective of the initial levels of fluorescence behaved in similar ways. There was a loss of about 10% fluorescence intensity over 120 scans and the bleaching profile did not appear to be influenced by temperature. For live cell experiments, an average of 4 scans at 5 time points were acquired over an hour giving a total of 20 scans and therefore photobleaching should play a negligible role in the differences of membrane fluorescence that was observed in the internalisation profiles. The approximately 10-14% loss of fluorescence that was observed for experiments at LT can be attributed in part to photobleaching and the rest to non-regulated forms of internalisation.

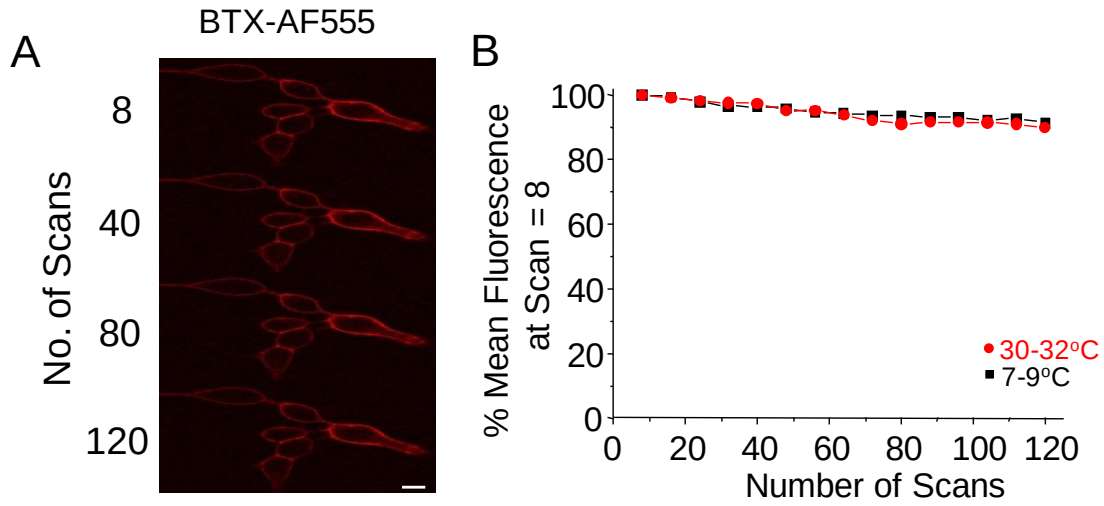

Figure 3.3 – Photobleaching time profile of BTX-AF555 in Krebs.
A, B. Images (A) and time profiles (B) of membrane fluorescence taken from GIRK cells expressing $R1a^{BBS}R2$ and labelled with BTX-AF555. Cells were superfused in Krebs and imaged using an average of 8 consecutive scans every 8 s to a total of 120 scans at 7-9°C and 30-32°C. Scale bar 5 µm.

3.2.4 Agonist induced internalisation of $GABA_B$ receptors

GPCRs undergo agonist mediated internalisation where the application of an agonist specific for the receptor accelerates the internalisation kinetics of the receptor. The effect of the $GABA_B$ receptor specific agonist baclofen on internalisation was studied in primary hippocampal neurons at PT. Cells transfected with cDNAs encoding for $R1a^{BBS}$, R2 and eGFP were tagged with BTX-AF555 in the presence of 100 µM baclofen. Additionally cells were imaged in the presence of 100 µM baclofen in perfusion (Fig. 3.4A; upper panel). The time constant for the rate of internalisation of $GABA_B$ receptors in the presence of baclofen was 13.4 ± 1.3 (n=6; Fig. 3.4B) and there was no significant difference in the rate of internalisation in the presence of baclofen compared to controls in Krebs ($P>0.05$; Fig. 3.4C). In addition to this, the extent of internalisation in the presence of baclofen (27.6 ± 2.2) was not statistically different to untreated controls in Krebs ($P>0.05$; Fig. 3.4D).

The effect of a selective antagonist CGP55845 on the internalisation of $GABA_B$ receptors was also studied in live hippocampal neurons. Cells transfected with cDNAs encoding for $R1a^{BBS}$, R2 and eGFP were tagged with BTX-AF555 in the presence of 1 µM CGP55845 and the cells were imaged during the perfusion of 1 µM CGP55845 (Fig. 3.4A; lower panel). The time constant for the rate of internalisation of $GABA_B$ receptors in the presence of CGP55845 was 12.9 ± 3.1 (n=5; Fig. 3.4B) and there was no significant difference in the rate of internalisation in the presence of CGP55845 compared to controls in Krebs ($P>0.05$; Fig. 3.4C). In addition to this, the extent of internalisation in the presence of CGP55845 (35.3 ± 3.1) was not statistically different to untreated controls in Krebs ($P>0.05$; Fig. 3.4D). This data is in contrast to studies of

BBS tagged $GABA_B$ $R1a^{BBS}R2$ receptors (Wilkins et al., 2008) where an increase of internalisation rates has been observed in fixed GIRK cells in the presence of GABA at 37°C and a decrease of internalization extent has been observed in live primary hippocampal neurons in the presence of CGP55845 at RT. These differences could be due to experimental variations such as the use of different BTX fluorophores, use of fixed cells, and temperatures at which the experiments were carried out.

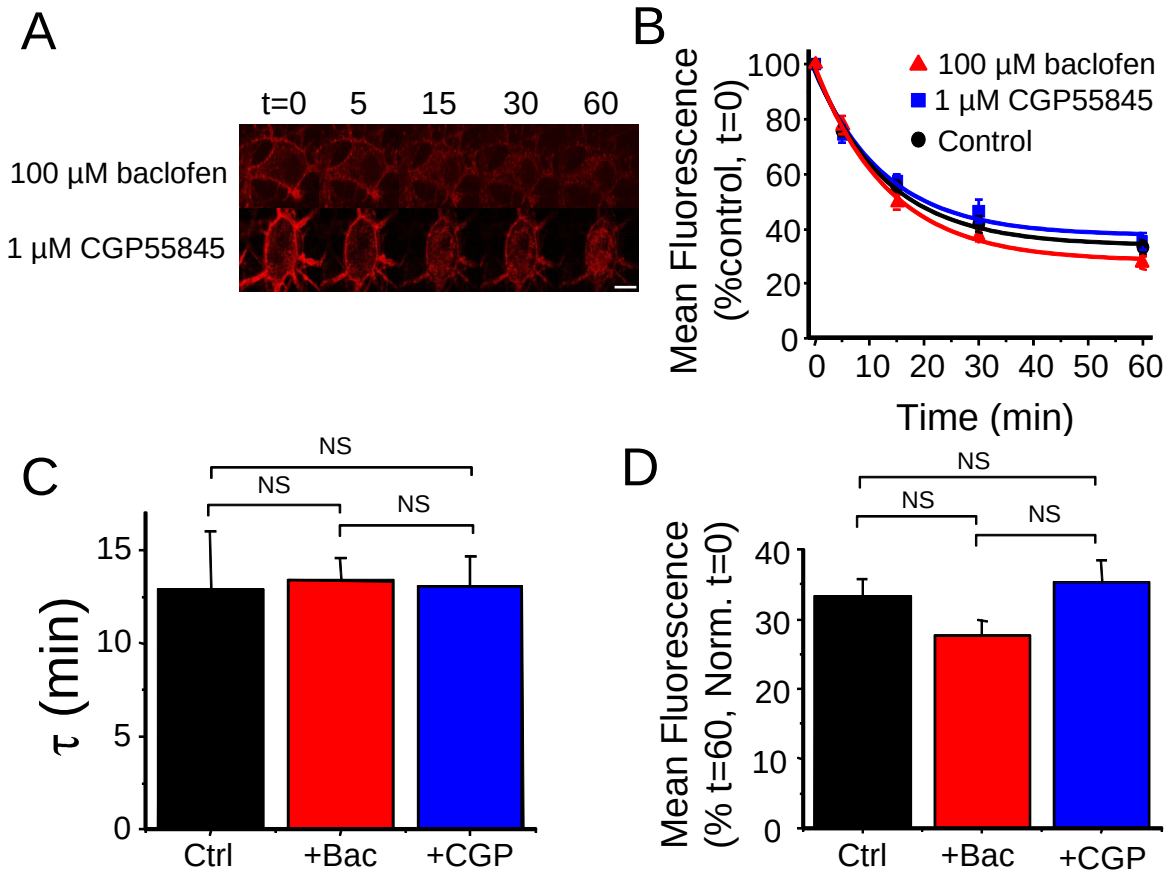

Figure 3.4 – Agonist induced internalisation of $GABA_B$ receptors.
A. Hippocampal neurons (14-21 DIV) expressing $R1a^{BBS}R2$ and eGFP were incubated in 1 mM d-TC for 5 min followed by 3 µg/ml BTX-AF555 or 3 µg/ml BTX-AF555 in the presence of 100 µM baclofen or 1 µM CGP55845 for 10 min at RT and imaged at different time points at 30-32°C with Krebs or 100 µM baclofen or 1 µM CGP55845. *B, C and D,* Rate (B, C) and extent (B, D) of internalisation of BTX-AF555 tagged $R1a^{BBS}R2$ receptors in the presence of Krebs (Ctrl; black), 100 µM baclofen (Bac; red) or 1 µM CGP55845 (CGP; blue) in live hippocampal neurons, n = 5 – 12, NS - not significant. Scale bar = 10 µm.

3.2.5 $GABA_B$ receptors are constitutively internalised via clathrin- and dynamin-dependent mechanisms

$GABA_B$ receptors have been reported to internalise through clathrin- and dynamin-dependent mechanisms in fixed cells. The BBS method was therefore used to study the clathrin- and dynamin-dependence of internalisation in real-time in live cells. A clathrin pit formation blocker, chlorpromazine (Wang et al., 1993), previously used to block internalisation of $GABA_B$ receptors (Grampp et al., 2007), was used to study the effect of blocking clathrin on $GABA_B$ receptor internalisation in live GIRK cells. Similarly, the cell permeable inhibitor of dynamin, dynasore (Macia et al., 2006), was used to study the effect of blocking dynamin on $GABA_B$ receptor internalisation in live GIRK cells. GIRK cells transfected with $R1a^{BBS}R2$ were tagged with BTX-AF555 and the cells were superfused with Krebs containing either 50 µg/ml chlorpromazine (Grampp et al., 2007) or 80 µM dynasore (Macia et al., 2006) in perfusion and imaged for an hour at PT (Fig. 3.5A).

The rate of constitutive internalisation of $R1a^{BBS}R2$ receptors was not altered in the presence of either chlorpromazine or dynasore in perfusion compared to controls in Krebs media (Fig. 3.5B; $\tau_{chlorpromazine}$ = 10.4 ± 1.9 (n=5), $\tau_{dynasore}$ = 13.7 ± 2.7, (n=11), $P>0.05$). However, the extent of internalisation in presence of chlorpromazine (52.4 ± 4.1, n=5, $P<0.01$) or dynasore (49.3 ± 3.6, n=11, $P<0.01$) was significantly lower compared to $R1a^{BBS}R2$ controls (Fig. 3.5C). This difference could be due to the slow onset of the drugs used as the rate of internalisation is calculated from a monexponential decay function and value of the time constant achieved is influenced by the initial time points. Therefore, for slower-acting drugs an change of rates of

internalisation may not be observed. The fact that, the extents are different in the presence of chlorpromazine and dynasore at the end of an hour suggests that the internalization of $GABA_B$ receptors is clathrin- and dynamin-dependent.

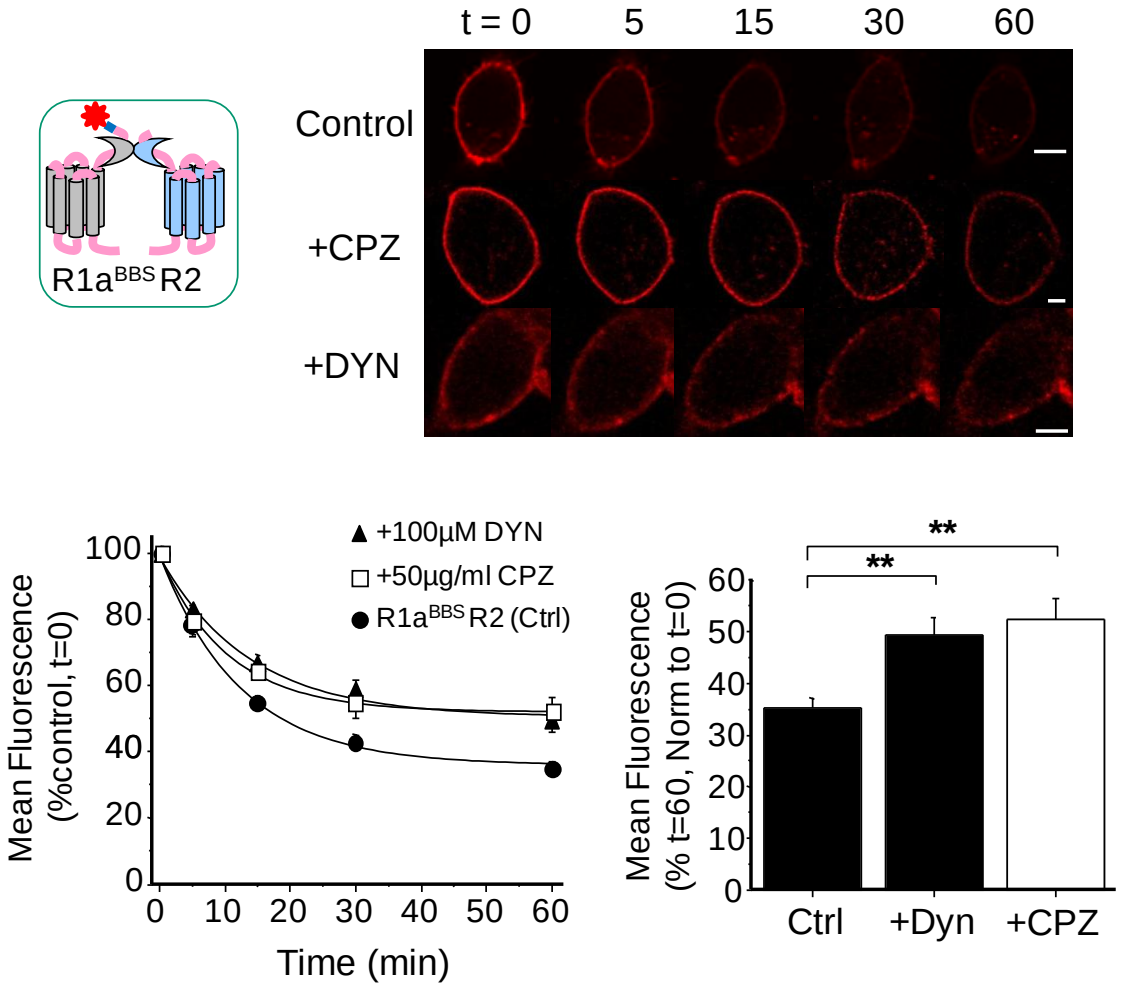

Figure 3.5 - $GABA_B$ receptors are internalised via clathrin- and dynamin-dependent mechanisms.

A, GIRK cells expressing $R1a^{BBS}R2$ receptors were incubated with 3 µg/ml BTX-AF555 for 10 min at RT and imaged over 0 – 60 min at 30-32°C in Krebs or in the presence of either 50 µg/ml chlorpromazine (CPZ) or 80 µM dynasore (DYN) or vehicle control. Scale bars = 5 µm. *B and C*, Rate (B) and extent (C) of constitutive internalisation of BTX-AF555 tagged $R1a^{BBS}R2$ receptors in the absence (●) and presence of dynasore (▲) or chlorpromazine (□), n = 5 - 11, **P<0.01 (one-way ANOVA).

3.2.6 Constitutively internalised $GABA_B$ receptors are sorted in endosomes and degraded in lysosomes

In order to study the fate of the internalised $R1a^{BBS}R2$ receptors, GIRK cells and hippocampal neurons were co-transfected with cDNAs encoding for $R1a^{BBS}$, R2 and

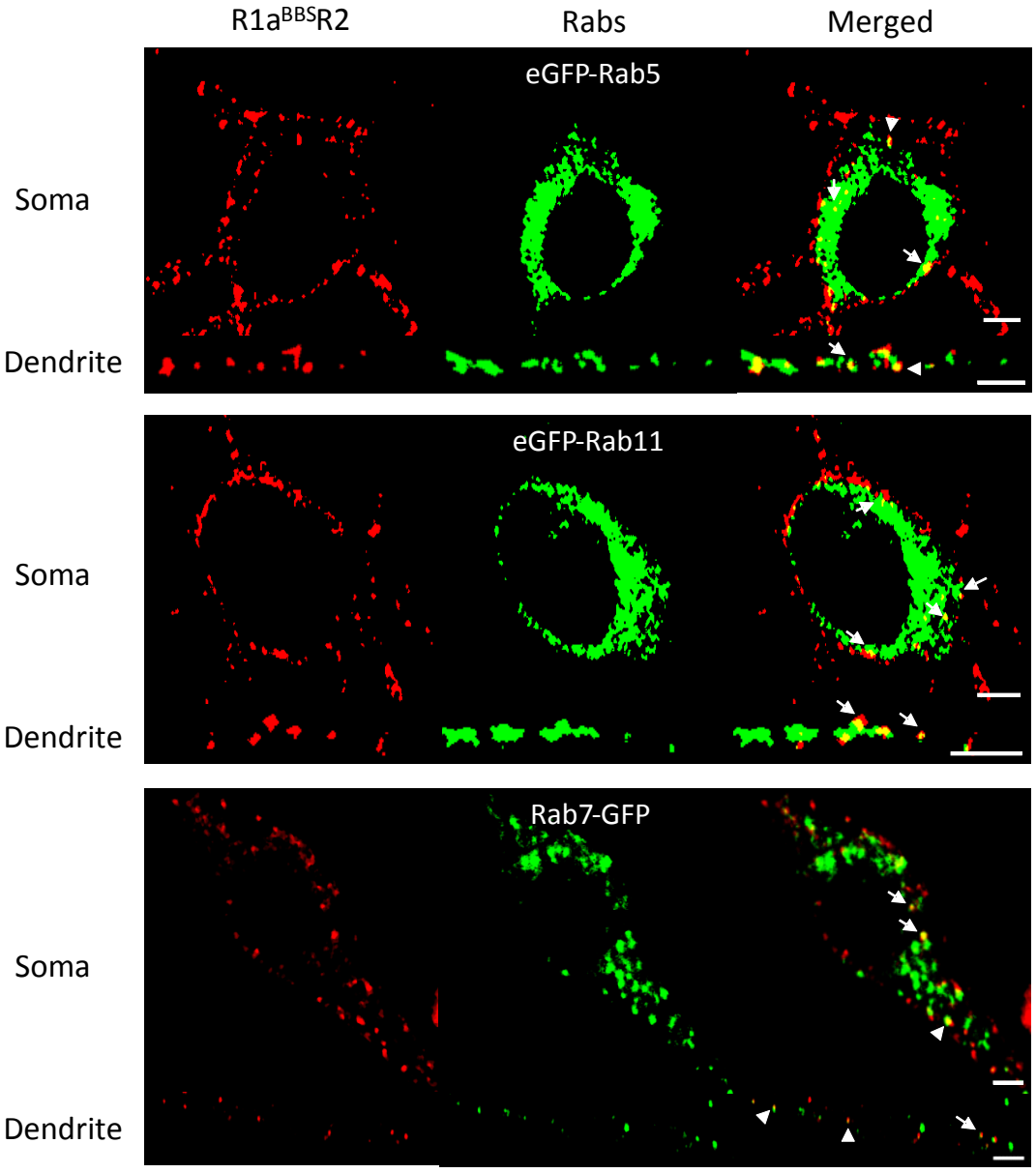

Figure 3.6 - $GABA_B$ receptors are recruited to endosomes and lysosomes in hippocampal neurons.
Hippocampal neurons (14-21 DIV) expressing $R1a^{BBS}R2$ and eGFP-Rab5, or eGFP-Rab11, or Rab7-eGFP were incubated in 1 mM d-TC for 5 min followed by 3 µg/ml BTX-AF555 for 10 min at RT. Cells were incubated at 37°C for 30 – 60 min, then fixed and imaged. Arrowheads depict co-localisation in the soma (upper panel) and a dendrite (lower panel). Scale bar = 5 µm.

eGFP-Rab5, a marker for early endosomal compartments (de Hoop et al., 1994;Mohrmann and van der, 1999), or eGFP-Rab11, a marker for recycling endosomes (Zerial and McBride, 2001;Stenmark and Olkkonen, 2001) , or Rab7-GFP, a marker for late endocytic/ lysosomal compartments (Bucci et al., 2000;Meresse et al., 1995). The cells were incubated in 3 µg/ml BTX-AF555 for 10 min at RT to label the surface receptors and washed three times in PBS to remove the unbound BTX-AF555 and incubated at 37°C/ 5% CO_2 in PBS for 60 min for Rab7-GFP and 30 min for eGFP-Rab5 or eGFP-Rab11 to allow the BTX tagged receptors to internalise. After the incubation, the cells were fixed and imaged and BTX-AF555 tagged $R1a^{BBS}R2$ were found to co-localise with eGFP-Rab5, eGFP-Rab11, and Rab7-eGFP containing intracellular compartments in the soma (Fig. 3.6, upper panels) and dendrites (Fig.3.6, lower panels) of hippocampal neurons in culture and in GIRK cells (Fig. 3.7).

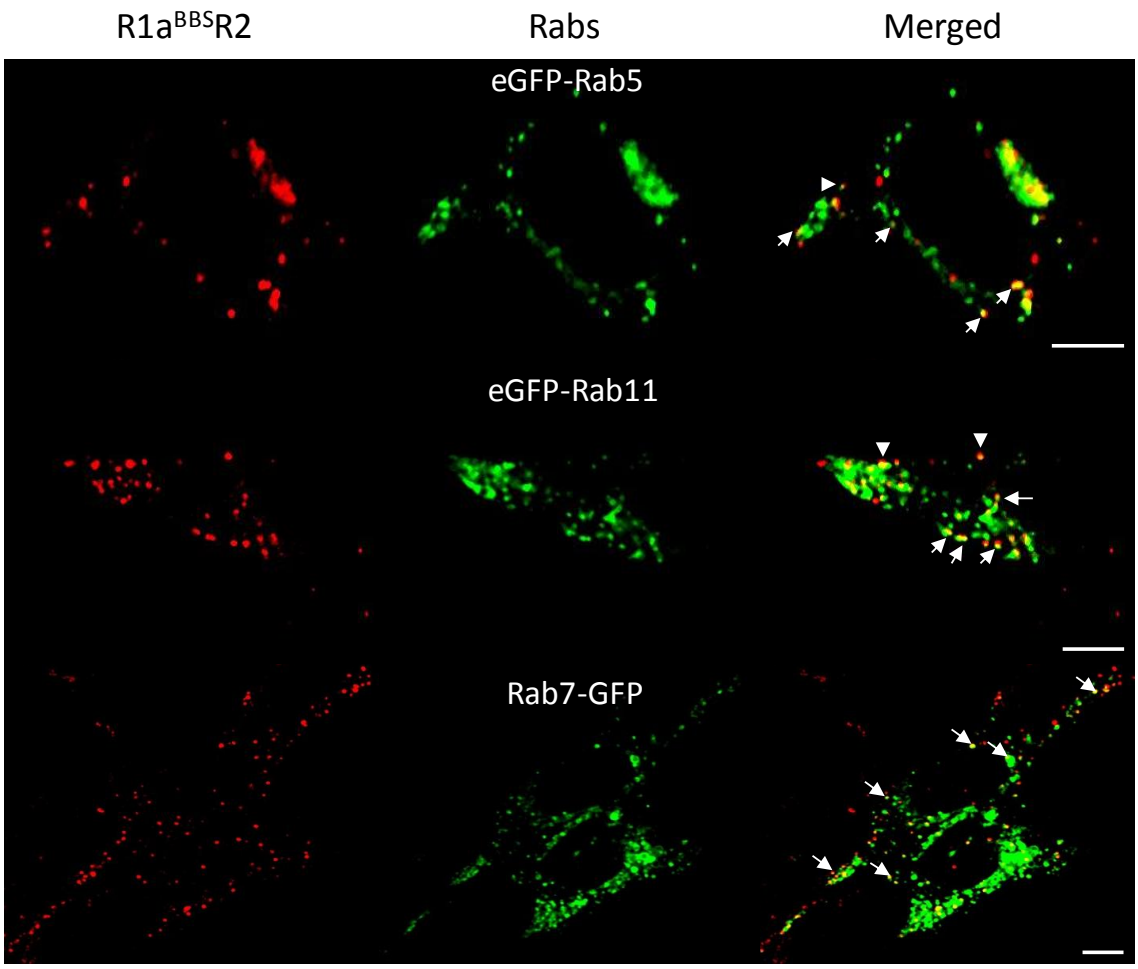

Figure 3.7 - $GABA_B$ receptors are recruited to endosomes and lysosomes in GIRK cells.

GIRK cells expressing $R1a^{BBS}R2$ and eGFP-Rab5, or eGFP-Rab11, or Rab7-eGFP were incubated in 3 µg/ml BTX-AF555 for 10 min at RT. Cells were incubated at 37°C for 30 – 60 min, then fixed and imaged. Arrowheads depict co-localisation. Scale bar = 5 µm.

3.3 Discussion

$GABA_B$ receptors mediate slow and prolonged synaptic inhibition in the nervous system in response to GABA and given the importance of receptor trafficking for maintaining signalling efficacy, several studies so far have focused on the trafficking of these receptors using methods that require fixation of cells. However, these studies

can not reveal real-time dynamics of internalisation of these receptors and therefore the BBS tagging approach was extended to study the internalisation of $GABA_B$ receptors in live GIRK cells and hippocampal neurons. Moreover, fixed cell imaging techniques are subjective because of the variability associated with the levels of fluorescence staining observed between cells due to differences in expression levels and other factors. Thus, a live cell imaging strategy that monitors changes in fluorescence levels at different time points in the *same* cell was developed.

The BBS site on the $GABA_B$ $R1a^{BBS}$ has been previously reported to be functionally silent using whole cell patch-clamp techniques in which no change was observed in the GABA binding affinity between the recombinant BBS containing receptors ($R1a^{BBS}R2$) and wild-type receptors (R1aR2) both in the presence and absence of BTX bound to $R1a^{BBS}$ (Wilkins et al., 2008). In addition to this, BTX was found to bind to $R1a^{BBS}$ with a high affinity of 9.8 ± 2.6 nM (Wilkins et al., 2008) which meant that the BBS could be efficiently used to monitor the mobility of $GABA_B$ receptors in live cells over a prolonged period of time.

The use of near-physiological temperatures (30-32°C) instead of physiological temperatures (37°C) for studying internalisation meant that the real-time kinetics described here is more accurate as the internalisation of $GABA_B$ receptors at physiological temperatures proceeds at a fast rate and imaging the first time point, to which all successive time points are normalised, accurately is challenging because of the time it takes to configure confocal imaging settings for acquiring an optimal image. However, although 30-32°C is closer to physiological temperature compared to room temperature one cannot fully rule out the possibility that the receptors would behave

differently at physiological temperatures without direct verification. The use of a water immersion NA 0.8 objective compared to the oil immersion NA 1.3 objective that has been used previously for fixed cell imaging (Wilkins et al., 2008) also meant a significant reduction of background fluorescence was achieved.

3.3.1 Constitutive internalisation of $GABA_B$ receptors in live cells

A clear and selective staining of $R1a^{BBS}R2$ receptors was achieved in live GIRK cells and hippocampal neurons with BTX-AF555 and this allowed the study of constitutive internalisation kinetics of these receptors in both these cell types. The rates of internalisation, as measured by fluorophore-conjugated α-BTX labelling of $GABA_B$ receptors, is likely to accurately reflect receptor trafficking in GIRK and neuronal cells for three reasons. Firstly, BTX binds with relatively high affinity to the BBS inserted in the R1a subunit. The dissociation constant compares well (11-fold lower; (Wilkins et al., 2008)) with that measured for the native BTX binding site located on the nicotinic ACh $\alpha7/5HT_{3A}$ chimeric receptor. This suggests that significant dissociation of the fluorophore from the $GABA_B$ receptor is unlikely. Secondly, there is very little constitutive internalisation of $GABA_B$ receptors at low temperatures, which are conditions that are considered to be non-permissive for internalisation. At RT and PT, $GABA_B$ receptor internalised rapidly, and the extent of internalisation was dependent on temperature although the lack of significance to the rates could be due to the small difference between the two temperatures. Thirdly, the reduction in cell surface fluorescence at RT and PT is not a consequence of photobleaching of BTX-AF555 at either low or near physiological temperatures, as the photobleaching profile of BTX-

AF555 shows negligible (<10%) reductions of surface fluorescence with the scanning protocols used to follow receptor movement.

Although constitutive internalisation of GPCRs has been described for several receptors to date including PAR1; (Paing et al., 2006)**,** melanocortin-4 receptor (MC4) (Mohammad et al., 2007), CB1 (McDonald et al., 2007a), alpha1b-adrenergic receptors (Stanasila et al., 2008), the role of constitutive internalisation in cellular physiology is not clear. One possibility is that constitutive internalisation could be a result of basal activity of the receptor. For the $GABA_B$ receptor, the absence of an inverse agonist makes this possibility difficult to probe. $GABA_B$ heteroreceptors have been hypothesised to be activated by ambient GABA that is found in some areas of the brain where the levels of endogenous GABA has been estimated between 65-120 nM (Bohlen et al., 1979; Bist and Bhatt, 2009; Paredes et al., 2009). Therefore the $GABA_B$ receptors could have evolved to constitutively internalise at rapid rates in order to remove activated receptors from the cell surface to prevent over-signalling. Another reason for the requirement of constitutive internalisation and recycling could be to introduce polarity in the cell membrane and to recruit receptors to specific locations on the membrane. For the CB1, one study has reported constitutive internalisation of these receptors in somatodendritic compartments but not in the axons (McDonald et al., 2007a) allowing accumulation of CB1 in the axons. Similarly, $GABA_B$ receptors have been reported to constitutively internalise in somatodendritic compartments but not in the axons (Vargas et al., 2008) but the physiological consequences of this difference has not been investigated.

3.3.2 $GABA_B$ receptors do not undergo agonist induced internalisation

Simulation of GPCR endocytosis upon agonist stimulation has been observed for several receptors. In this activity dependent internalisation mechanism, GPCRs are internalised with faster internalisation kinetics compared to basal internalisation levels in order to remove activated cell surface receptors and prevent over-signalling. The $GABA_B$ receptor specific agonist baclofen does not affect the internalisation profile of the receptor in hippocampal neurons as addition of the agonist had no effect on either the rate or the extent of internalisation compared to controls in Krebs. The fact that baclofen failed to effect the internalisation of $GABA_B$ receptors could mean that these receptors are constitutively active or are activated by GABA released by neurons and are therefore being internalised in response to paracrine activation. The use of the antagonist CGP55845 had no effect on the rate or the extent of internalisation suggesting that for the $GABA_B$ receptor, activation is not required for endocytosis as observed for the internalisation of the β_2AR (Scarselli and Donaldson, 2009). In addition to this, similar experiments conducted in GIRK cells (data not shown as the data in neurons is more physiologically relevant) where the cells are known not to produce GABA revealed that there was no change in internalisation in the presence or absence of baclofen verifying that the $GABA_B$ receptor does not undergo agonist induced internalisation. One study has described high concentrations of GABA (100 µM; saturating concentration for $GABA_B$ receptors) having an effect on the internalisation of $GABA_B$ receptors (Gonzalez-Maeso et al., 2003) where prolonged/ chronic incubation in GABA accelerated the rate of internalisation of these receptors with statistical significance in rates appearing after 2 hours of treatment with GABA. Physiologically, $GABA_B$ receptors have been described to be activated by high

concentrations of GABA when GABA spills-over into the perisynaptic regions upon GABA release at the synapses. However, in order for $GABA_B$ receptors to be active, strong stimulation is required to release GABA and often in addition to this, the vesicular GABA transporters GAT1 have to be blocked to prevent the reuptake of GABA from the synapses so that can spill-over to activate $GABA_B$ receptors, but this will only occur briefly. These studies suggest that $GABA_B$ receptors are not exposed to high concentrations of GABA for a prolonged period of time and therefore the modulation of rate of internalisation in response to incubation of cells in baclofen for more 2 hr is of questionable physiological relevance. In addition to this, incubation of $GABA_B$ receptors in GABA for two hours causes pharmacological changes in the orthosteric and allosteric ligand binding properties of the receptor (Gjoni and Urwyler, 2009). The assay used here determines the rate of internalisation over a period of one hour at five different time-points and therefore the possibility of very fast agonist induced-internalisation coupled with recycling (less than 5 min) cannot be ruled out.

The $GABA_B$ receptor is different from the prototypical GPCR the β_2AR which has a low rate of constitutive internalisation (20% at 37 in 30 min) and undergoes faster internalisation in response to the specific agonist 1 mM isoprenaline (75% at 37 in 30 min) (Scarselli and Donaldson, 2009). The finding that the $GABA_B$ receptor has a higher rate of constitutive internalisation and does not undergo agonist induced internalisation suggests that different mechanisms of trafficking have evolved within the GPCR super-family.

3.3.3 $GABA_B$ receptors internalise via clathrin- and dynamin-dependent mechanisms

Chlorpromazine was found to reduce the extent of internalisation suggesting that $GABA_B$ receptors are internalised via the clathrin-dependent pathways. This data is consistent with studies where $GABA_B$ receptors have previously been reported to co-localise with β-adaptin (Grampp et al., 2008) and clathrin (Ramoino et al., 2006) and internalisation has been blocked by 450 mM sucrose (Vargas et al., 2008; Grampp et al., 2007), 100 µg/ml chlorpromazine (Grampp et al., 2007), and K^+ depletion (Laffray et al., 2007; Vargas et al., 2008) all of which prevent the formation of clathrin-coated pits (Ivanov, 2008). At the end of an hour in the presence of chlorpromazine, 50% of the receptors remained on the cell surface compared to 85% of receptors that remain at LT at the same time point. This raises the possibility that perhaps a portion of the difference of 35% receptors undergo clathrin-independent endocytosis as previously reported (Ramoino et al., 2006). The BBS binding site strategy and live cell imaging can be used in future to study the effect of blocking these clathrin-independent pathways using chemical blockers or by co-expressing dominant negative proteins that would block these pathways.

Clathrin-dependent pathways are one of the major forms of regulated endocytosis pathways in living cells. Several GPCRs have been described to internalise via this pathway in response to agonists (Wolfe and Trejo, 2007) including the β_2AR (Scarselli and Donaldson, 2009), M3 muscarinic receptor (Scarselli and Donaldson, 2009), CB1 (McDonald et al., 2007b), and in the absence of agonist, including PAR1 (Paing et al., 2006) and MC4 (Mohammad et al., 2007). One systematic study (Scarselli and

Donaldson, 2009) on internalisation of two Class I GPCRs, β_2AR and M3 muscarinic receptors, found they were internalised via clathrin-independent pathways in the absence of agonists. Addition of agonists switched endocytosis from a clathrin-independent pathway to one dependent on clathrin. Other studies have found clathrin-independent endocytosis of several GPCRs including the M2 receptor (Delaney et al., 2002) in the presence of agonists. Whether the clathrin-dependent constitutive internalisation property of $GABA_B$ receptors is unique to $GABA_B$ receptors or a feature of Class III GPCRs remains to be studied, but it is clear that GPCRs constitutively internalise via diverse mechanisms.

The cell permeable inhibitor of dynamin, dynasore was also observed to block the internalisation of $GABA_B$ receptors. Similar to extents of internalisation in the presence of clathrin inhibition, about 50% of receptors remained on the cell surface at the end of an hour. This is not unexpected as dynamin functions as a scission protein for clathrin-coated pits enabling them to pinch-off from the cell surface (Conner and Schmid, 2003). A dominant negative form of the GTP-ase dynamin, dyn-1-K44A, has been described to also block internalisation of $GABA_B$ receptors (Grampp et al., 2007;Vargas et al., 2008) consistent with data presented here.

3.3.4 $GABA_B$ receptors are sorted in endosomes

Sorting of GPCRs into the endosomal compartments and their degradation in lysosomes provides an important means of receptor signalling modulation (Marchese et al., 2008). After internalisation, $GABA_B$ receptors were observed to co-localise with

eGFP-Rab5, eGFP-Rab11, and Rab7-GFP. Therefore it is likely that the $GABA_B$ receptors are recruited to early endosomes immediately after internalisation as observed for the transferrin receptor (Naslavsky et al., 2003) from where they are either recycled back to the plasma membrane via Rab11 containing recycling endosomes or are recruited to Rab7 containing late endosomes and lysosomes for degradation. In addition to this, the presence of the endocytic markers in dendrites raises the possibility of local processing of dendritic $GABA_B$ receptors. These results are consistent with studies that have reported co-localisation of $GABA_B$ subunits with markers for early endosomes (EEA1, Rab5; (Grampp et al., 2008)), late endosomes (Lamp1; (Grampp et al., 2008)), re-cycling endosomes (Rab4, Rab11, TGN38-IR; (Laffray et al., 2007; Vargas et al., 2008; Grampp et al., 2008; Ramoino et al., 2005)), and lysosomes (Lamp1; (Grampp et al., 2008; Ramoino et al., 2005)) using antibody labelling and imaging in dendrites.

Thus, in conclusion cell surface $GABA_B$ receptors are constitutively-internalised in live GIRK cells and hippocampal neurons in clathrin- and dynamin-dependent pathways and the addition of the specific agonist baclofen does not alter the rates or the extents of internalisation (Fig. 3.8). After being internalised, they are recruited to Rab5 containing early endosomes from where they are recycled back via Rab11 containing recycling endosomes to the plasma membrane or are degraded in lysosomes via Rab7 containing late endosomes (Fig. 3.8).

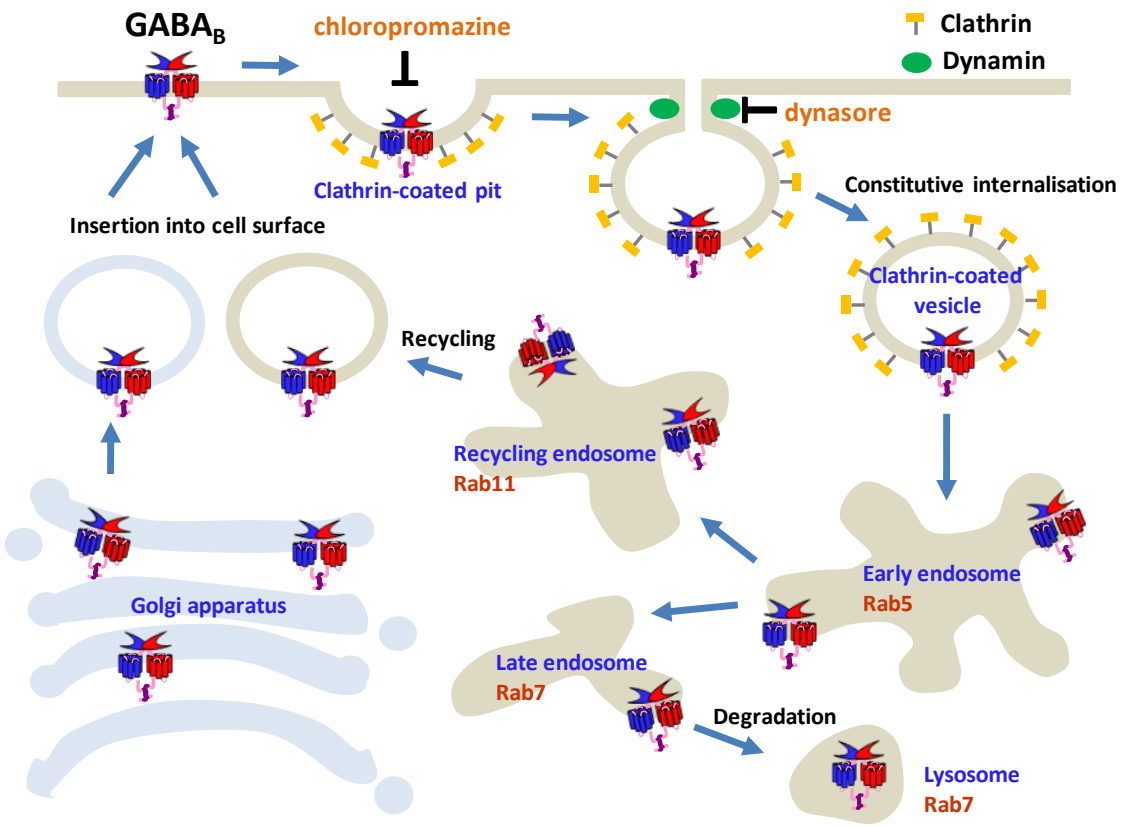

Figure 3.8 – Constitutive internalisation of $GABA_B$ receptors.
Cell surface $GABA_B$ receptors are constitutively-internalised at permissive temperatures in a temperature dependent manner in clathrin-coated pits, a process that requires dynamin. The clathrin inhibitor chloropromazine and the dynamin inhibitor dynasore reduce the extent of internalisation. Internalised clathrin coated vesicles fuse with early endosomes and from here the $GABA_B$ receptors can be routed to recycling endosomes from where they can recycle back to the cell surface to form cell surface receptors or sent to lysosomes for degradation.

3.4 Summary

- $GABA_B$ receptors are constitutively-internalised at a rapid rate in GIRK cells and hippocampal neurons in culture at permissive temperatures
- $GABA_B$ receptors do not undergo agonist-induced internalisation
- $GABA_B$ receptors constitutively internalise via clathrin- and dynamin-dependent mechanisms
- After internalisation $GABA_B$ receptors enter early endosomes from where they can either enter recycling endosomes from where they can be recycled back to the plasma membrane or are degraded in lysosomes via late endosomes

Chapter IV

R2 subunit stabilises $GABA_B$ receptors on the cell surface

4.1 Introduction

The $GABA_B$ receptor was the first GPCR described to require heterodimerisation between R1 and R2 subunits in order to be functionally active (Kaupmann et al., 1998; White et al., 1998). Heterodimerisation is not only important for the cell surface expression of a functional $GABA_B$ receptor, but also for coupling of the receptor to G-proteins and signalling to related downstream effectors. Therefore it is of no surprise that several studies to date have focused on the effect of heterodimerisation on the signalling of $GABA_B$ receptors (Duthey et al., 2002; Galvez et al., 2001; Havlickova et al., 2002; Rondard et al., 2008; Margeta-Mitrovic et al., 2001a; Margeta-Mitrovic et al., 2001b; Filippov et al., 2000; Robbins et al., 2001; Thuault et al., 2004). $GABA_B$ receptors have been reported to form higher order oligomers using biochemical and bioluminescence resonance energy transfer (BRET) approaches (Rondard et al., 2008; Villemure et al., 2005; Comps-Agrar et al., 2011; Maurel et al., 2004). More recently, TR-FRET techniques have also demonstrated the formation of 'dimers of dimers' (Maurel et al., 2004). The formation of such a tetrameric configuration causes a reduction in receptor signalling efficacy compared to heterodimers (Comps-Agrar et al., 2011) creating a mechanism to modulate signalling by heterodimerisation.

$GABA_B$ receptors have been described as “obligate” heteromers for coupling to GIRK channels, VGCCs, and adenyl cyclase, although other forms of signalling and trafficking that do not involve the formation of the heterodimer have been described. R1 can activate the ERK 1/2 MAP kinase pathway directly in the absence of R2 (Richer et al., 2009) and regulate Leptin mRNA and blood leptin levels also in the absence of R2 (Nakamura et al., 2011). In addition, the localization of $GABA_B$R1 and R2 in the brain does not universally overlap. For example, in the caudate-putamen R2 is undetectable whereas R1 is highly expressed and yet a functional $GABA_B$ response is still discernable (Durkin et al., 1999). In terms of trafficking, R1 subunits have has been described to reach the cell surface in the absence of R2 chaperoned by $GABA_A$ γ2S subunits (Balasubramanian et al., 2004). Together, these results suggest the $GABA_B$ receptor is as obligate heteromer may not be universal and other forms of atypical signalling by this receptor may exist.

Oligomerisation of GPCRs is important for receptor signalling and the properties of the monomeric subunits are often modified as a result of the formation of the oligomers. For the $GABA_B$ receptor, although the role of heterodimerisation in determining the forward trafficking (from ER to cell membrane) properties of the monomeric subunits have been studied, the role of heterodimerisation in determining the internalisation properties has received little attention and therefore the BBS approach was used for this purpose.

4.2 Results

4.2.1 R1a homomers constitutively internalise at a faster rate and greater extent than R1aR2 heteromers

R1a subunits contain an RSR ER retention motif in the C-terminal tail which prevents their trafficking to the cell membrane in the absence of R2 subunits. To investigate the role of heterodimerisation on $GABA_B$ receptor constitutive internalisation, the trafficking of the R1a subunit was studied in isolation. In order to enable the R1a subunit to internalise in the absence of R2 and be tracked by BTX labelling requires the removal of the ER retention motif and therefore the RSR motif was substituted for ASA, forming $R1a^{BBS\text{-}ASA}$, by site-directed mutagenesis.

$R1a^{BBS\text{-}ASA}$ receptors were targeted to the cell surface in the absence of R2 subunits in GIRK cells and bound to BTX-AF555 when the cells expressing $R1a^{BBS\text{-}ASA}$ were incubated in 3 µg/ml BTX-AF555 for 10 min at RT (Fig. 4.1A; upper panel). At RT, $R1a^{BBS\text{-}ASA}$ constitutively internalised in the absence of R2 subunits (Fig. 4.1*A*). Notably, intracellular structures were decorated with BTX-AF555 even at t = 0, indicating active receptor internalisation during BTX-AF555 binding. The loss of surface fluorescence for $R1a^{BBS\text{-}ASA}$ was significantly faster (τ = 7.2 ± 1.5 min; n = 10; Fig. 4.1*B, C*; $P<0.05$) and also more extensive after 60 min (30 ± 3 %, n = 10; Fig. 4.1*D*; $P<0.001$) compared to that for $R1a^{BBS}R2$ heterodimers.

As constitutive internalisation of $R1a^{BBS}R2$ proceeds more slowly than $R1a^{BBS\text{-}ASA}$, this could be due to a dominant-internalisation signal on R1a and, following heterodimerisation, the R2 subunit could mask this signal slowing the rate of R1aR2

internalisation. R2 subunits interact with R1a in the C-terminal coiled-coil domain, 7-TM region, and the VFTD.

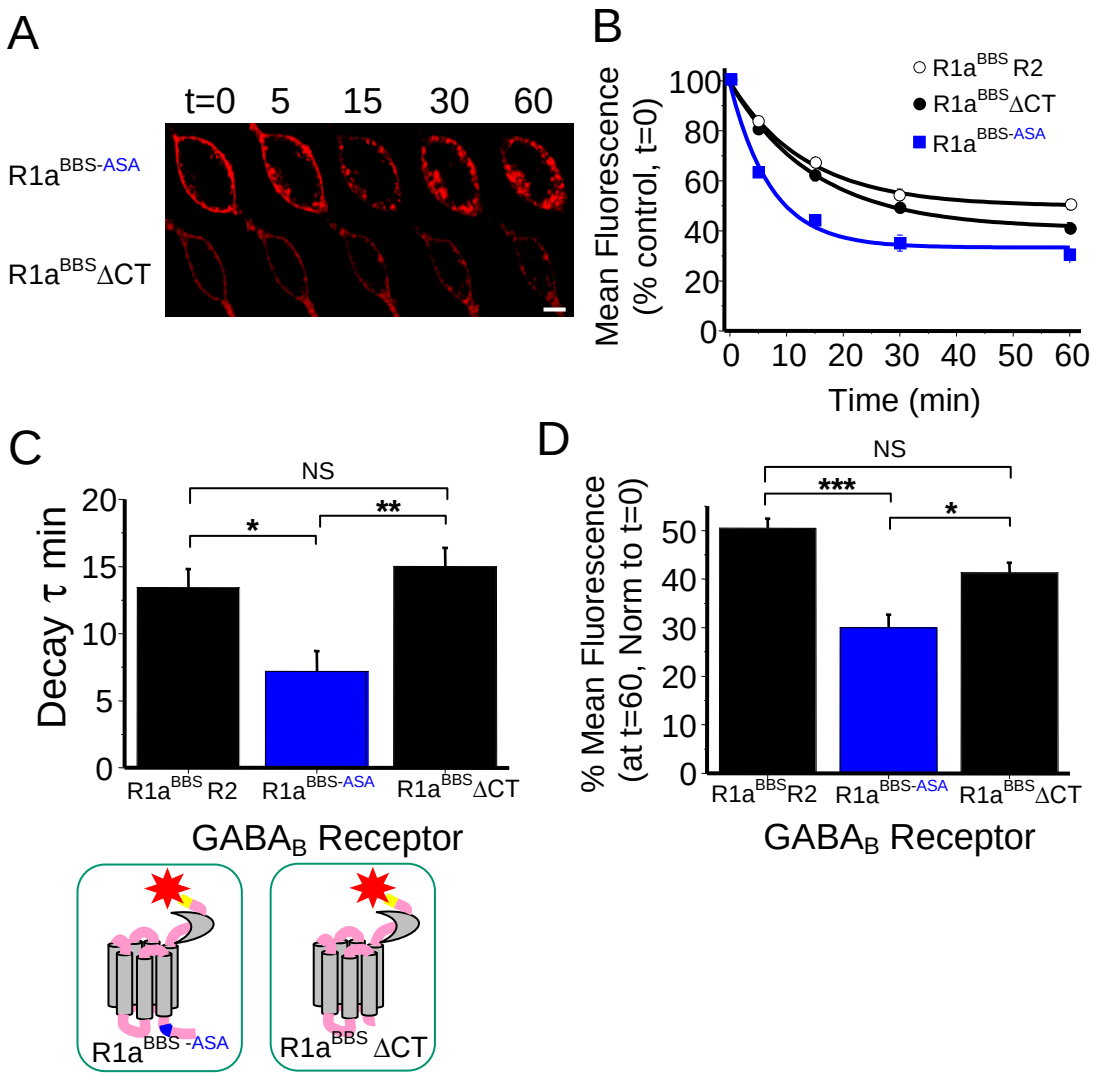

Figure 4.1 - Faster and more extensive internalisation of $R1a^{BBS-ASA}$ compared to $R1a^{BBS}R2$.

A, GIRK cells expressing either $R1a^{BBS-ASA}$ (upper panel) or $R1a^{BBS}\Delta CT$ (lower panel) were incubated in 3 µg/ml BTX-AF555 for 10 min at RT to label surface $GABA_B$ receptors and imaged over 0 – 60 min at RT. *B*, The rate of internalisation of BTX-AF555 tagged $R1a^{BBS}R2$ heteromers, and $R1a^{BBS-ASA}$ and $R1a^{BBS}\Delta CT$ homomers at RT (n = 6 - 10). The inset shows the relative positions of the ASA motif (blue) and C-terminal truncation (ΔCT). *C*, Exponential decay time constants for the rate of decay of membrane fluorescence for $R1a^{BBS}R2$, $R1a^{BBS-ASA}$ and $R1a^{BBS}\Delta CT$. *D*, Extent of internalisation for $R1a^{BBS}R2$ receptors, and $R1a^{BBS-ASA}$ or $R1a^{BBS}\Delta CT$ homomers. One-way ANOVA *P<0.05, **P<0.01, ***P<0.001 Scale bar = 5 µm.

To determine if the R1a C-terminal tail contains a dominant-internalisation signal, a tailless $R1a^{BBS}$ receptor was generated in which the C-terminus was truncated from and including L859 ($R1a^{BBS}\Delta CT$). This subunit was expressed on the GIRK cell surface without R2, since the C-terminal truncation included the ER retention motif. After labelling with BTX-AF555, $R1a^{BBS}\Delta CT$ constitutively internalised in the absence of R2 (Fig. 4.1A, B). Both the rate of internalisation (τ = 15.0 ± 1.4 min, n = 6, P>0.05) and the extent (41 ± 2 %, n = 6, P>0.05) were not significantly different compared to $R1a^{BBS}R2$ (Fig. 4.1*C*, *D*) but the internalisation rate (P<0.01; Fig. 4.1C) was slower and less extensive (P<0.05; Fig. 4.1D) compared to $R1a^{BBS\text{-}ASA}$. The levels of expression of the constructs varied but this should not alter the predictions of rates or extents of internalisation as studies were carried out in live cells and the membrane fluorescence of individual cells was measured at specific time-points for an hour and normalised to the membrane fluorescence at t = 0. A cell expressing a smaller number of receptors should therefore give the same rates and extents of internalisation compared to cells where expression is higher provided that the endocytosis machinery of the cells is not being saturated.

Taken together, these data suggest that R2 subunits are a major determinant of the rate of trafficking for R1a when these subunits co-assemble as a heterodimer, and that the R1a C-terminal tail contains an endocytic signal that in the absence of R2, causes R1a subunits to constitutively internalise at a faster rate and to a greater extent than the heteromer.

4.2.2 Inserting a BBS on $GABA_B$ R2

To directly establish that R2 subunits are determining the rate of internalisation of R1aR2 heterodimers required a separate BBS to be inserted into the R2 subunit. This was placed in the N-terminus, 27 residues from the start of the mature R2 protein (Fig. 4.2*A*). Clear and specific labelling with BTX-AF555 (3 µg/ml) was observed in GIRK cells co-transfected with cDNAs encoding for $R1aR2^{BBS}$ or $R2^{BBS}$ and eGFP (Fig. 4.2*B*, *C*). Such labelling was absent for cells incubated in UL-BTX or for cells transfected with just eGFP alone (data not shown).

Whole-cell patch clamp recording was used to ascertain whether including the BBS in $GABA_B$ R2 had any functional consequences. GIRK cells stably expressing inwardly-rectifying Kir3.1 and Kir3.2 channels were transiently transfected to also express eGFP and either $R1aR2^{BBS}$ or R1aR2. Concentration response curves for GABA activation of Kir3.1 and 3.2 via the $GABA_B$ receptor were similar for R1aR2 and $R1aR2^{BBS}$ receptors reflecting similar potencies for GABA with EC_{50}s of 0.5 ± 0.1 µM ($R1aR2^{BBS}$; n = 6 - 7) and 0.4 ± 0.04 µM (R1aR2; n = 7 - 13, P>0.05; Fig. 4.2*D*).

GIRK cells expressing either $R1a^{BBS}R2$ or $R1aR2^{BBS}$ were next exposed to BTX-AF555 for 10 min before whole-cell recording. Occupation of the BBS by BTX did not affect the GABA concentration response curves or the GABA EC_{50}s ($R1a^{BBS}R2$: 0.53 ± 0.01 µM, n = 5; $R1aR2^{BBS}$: 0.8 ± 0.1 µM, n = 5), which were also similar to those for wild-type R1aR2 $GABA_B$ receptors. Therefore, the insertion of the BBS in the R2 subunit had no significant effect on the functional properties of R1a $R2^{BBS}$ receptors.

The apparent affinity of BTX for the BBS site on R1a was determined previously (Wilkins et al., 2008) and a similar radioligand binding approach with ^{125}I-BTX was used to determine the apparent affinity of BTX for the BBS on R2. The binding curve for ^{125}I-BTX to GIRK cells, expressing R1aR2^{BBS} saturated at approximately 100 nM (Fig. 4.2*E*) and the Scatchard analysis revealed a K_d for BTX binding of 45.5 ± 4.8 nM (n = 6). This was 4-fold lower than the K_d for BTX binding to the R1a^{BBS}R2 receptor (9.8 ± 2.6 nM; n = 6) (Wilkins et al., 2008). As a control, ^{125}I-BTX binding to the nicotinic α7/5HT_{3a} chimeric receptor was determined. This chimera possesses an innate high affinity BTX binding site (Eisele et al., 1993), and the determined K_d was 3.92 ± 2.4 nM (n = 3) agreeing closely with that previously published (Wilkins et al., 2008).

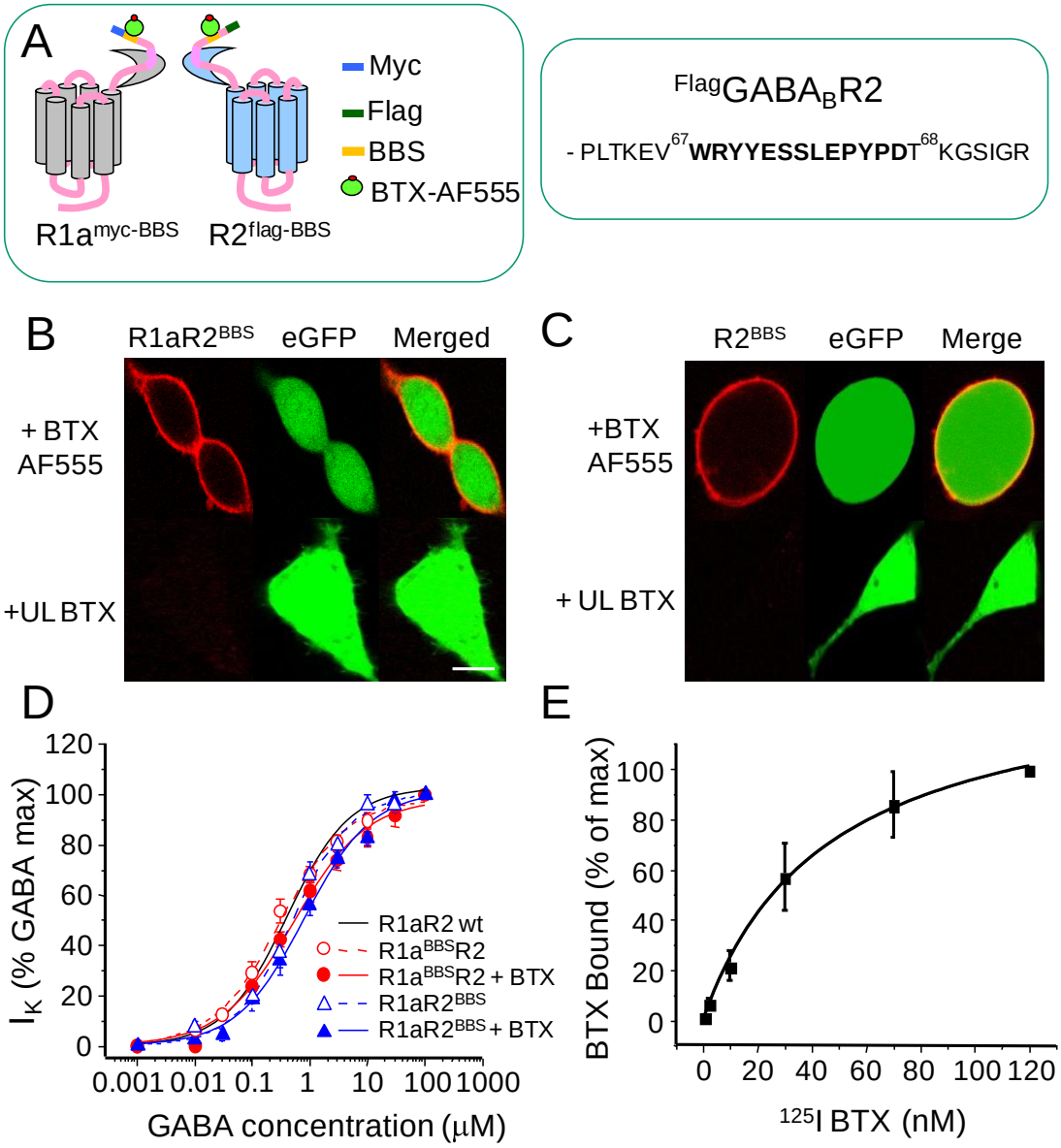

Figure 4.2 - Silent incorporation of the BBS into R2 subunits.

A, Schematic diagram showing the relative locations for the BBS and the Myc and Flag epitopes in $GABA_BR1a$ and R2 subunits. For the R2 subunit, the BBS was inserted between Val67 and Thr68 as shown in the segment of the primary sequence. *B,* Images of GIRK cells expressing $R1aR2^{BBS}$ and eGFP were incubated with 3 μg/ml BTX-AF555 or 3 μg/ml UL-BTX for 10 min at RT. *C*, Images of GIRK cells expressing $R2^{BBS}$ and eGFP, incubated with 3 μg/ml BTX-AF555 or 3 μg/ml UL-BTX for 10 min at RT. Scale bars = 5 μm. *D*, GABA concentration response curves for R1aR2, $R1aR2^{BBS}$, $R1a^{BBS}R2$ receptors and BTX bound $R1aR2^{BBS}$ and $R1a^{BBS}R2$ receptors all expressed in GIRK cells (n = 5 - 13). *E*, Whole-cell radioligand binding experiments with ^{125}I-BTX for the $R1aR2^{BBS}$ receptor (n = 6). Data presented in (D) was acquired by Dr. M.E. Wilkins

4.2.3 R2 homomers internalise at the same rate as R1aR2 heteromers

As R2 subunits can form homomeric surface receptors (Villemure et al., 2005), GIRK cells expressing $R2^{BBS}$ were used to determine the rate and extent of constitutive R2 internalisation and to establish its regulatory role in heterodimer internalisation. Although the formation of homomers was not directly tested using the BBS strategy, one possible line of investigation for the existence of homomers could involve the cross-linking of two monomers and then studying the kinetics of internalisation to check how it compares to non-cross-linked receptors.

R2 subunits, labelled with 3 µg/ml BTX-AF555 at RT, showed a clear expression pattern on the cell surface. At LT, internalisation of $R2^{BBS}$ was minimal (85 ± 2%, n = 5, Fig. 4.3*A, C*) and comparable to $R1a^{BBS}R2$ (P>0.05). At RT and PT, $R2^{BBS}$ homomers rapidly internalised (Fig. 4.3A) with rates (τ_{RT} = 18 ± 3 min, n = 8; τ_{PT} = 12.4 ± 1.1 min, n = 10) and extents (RT: 47 ± 2 %, n = 8; PT: 31 ± 1 %; n = 10; Fig. 4.3*C*) of constitutive internalisation which were again comparable to those for $R1a^{BBS}R2$ (P>0.05). By contrast, the rate of internalisation for $R2^{BBS}$ was slower (P<0.01) and its extent reduced (Fig. 4.3*D*; P<0.001) compared to that for $R1a^{BBS\text{-}ASA}$ at RT.

To ensure that there was no contamination from unforeseen innate expression of R1a in GIRK cells, GABA was applied during whole-cell patch clamp recording of cells expressing $R2^{BBS}$ and identified by BTX-AF555. Even at 1 mM GABA no K^+ currents were activated (n = 6; data not shown) indicating the absence of endogenous R1 subunits. Therefore the rates of internalisation of $R2^{BBS}$ subunits in these cells are unaffected by the presence of R1 subunits.

To determine the influence of $R2^{BBS}$ on the internalisation of the R1aR2 heterodimer, the rate of internalisation of $R1aR2^{BBS}$ heterodimers was established (Fig. 4.3*B*, *C*). This rate was very similar to that for $R1a^{BBS}R2$ heterodimers, and $R2^{BBS}$ homomers. Low temperatures slowed the internalisation of $R1aR2^{BBS}$, similar to $R1a^{BBS}R2$ and $R2^{BBS}$ (90 ± 2 %; n = 7; P>0.05; Fig. 4.3C), whilst at RT and PT, $R1aR2^{BBS}$ rapidly internalised (Fig. 4.3C) at rates similar to those for $R1a^{BBS}R2$ and for $R2^{BBS}$ (τ_{RT} = 18.8 ± 2.2 min; n = 13; P>0.05; τ_{PT} = 16.4 ± 2.2 min; n = 6; P>0.05; Fig. 4.3D).

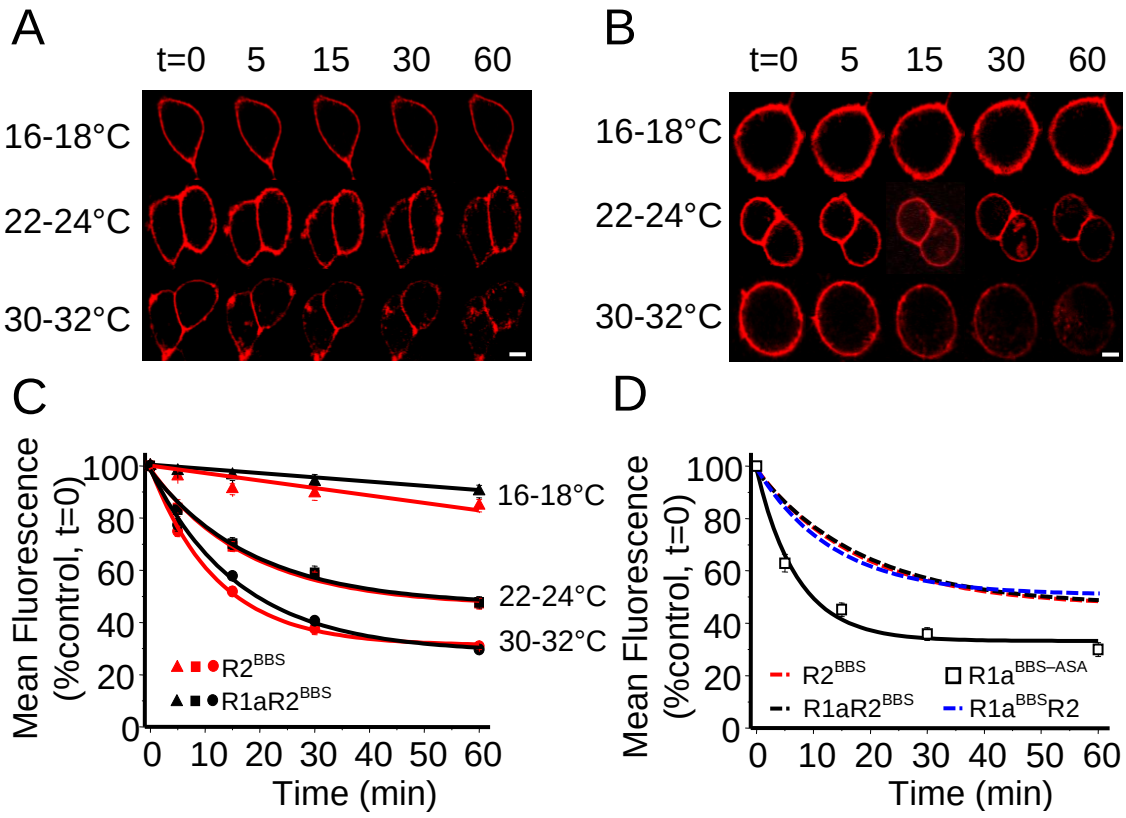

Figure 4.3 - **R2 subunits determine the rate of internalisation of $GABA_B$ heteromers.** *A and B,* GIRK cells expressing $R2^{BBS}$ homomers (A) or $R1aR2^{BBS}$ heteromers (B) were incubated in 3 µg/ml BTX-AF555 for 10 min at RT prior to imaging over 0 – 60 min at 16-18°C, 22-24°C, and 30-32°C. *C*, Rate and extent of internalisation of BTX-AF555 tagged $R2^{BBS}$ (red) or $R1aR2^{BBS}$ (black) at 16-18°C (▲), 22-24°C (■), and 30-32°C (●) (n = 5 – 13). *D*, Comparison of rates and extents of internalisation for: $R1a^{BBS}R2$ (data taken from Fig 3.1C), $R1aR2^{BBS}$ and $R2^{BBS}$ (data from panel C), and $R1a^{BBS-ASA}$ receptors (data taken from Fig 4.1B) at 22-24°C.

The extent of internalisation for $R1aR2^{BBS}$ was similar to that for $R1a^{BBS}R2$ and $R2^{BBS}$ at both RT (48 ± 2 %, n = 13) and PT (30 ± 1 %; n = 6; P>0.05). However, the rate of internalisation for $R1aR2^{BBS}$ was slower (P<0.001) and the extent reduced (P<0.001) compared to $R1a^{BBS-ASA}$. These data suggest R2 subunits play a dominant role in determining the rate and extent of constitutive internalisation of R1a subunits when co-assembled in a heterodimer.

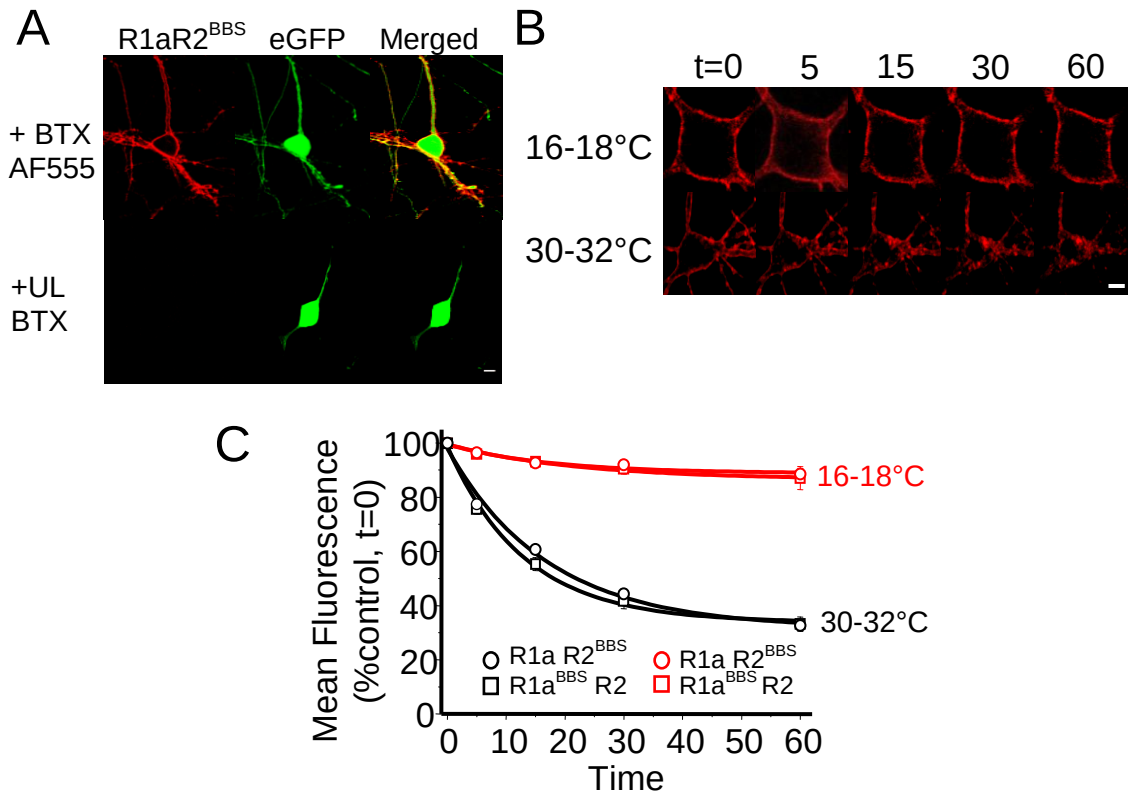

Figure 4.4 – Constitutive internalisation of $R1aR2^{BBS}$ receptors in hippocampal neurons.

A, Images of rat hippocampal neurons in culture expressing $R1aR2^{BBS}$ and eGFP, incubated with 1 mM d-TC for 5 min followed by incubation with or without 3 µg/ml BTX-AF555 for 10 min at RT. Scale bars = 5 µm. *B*, Hippocampal neurons (14-21 DIV) expressing $R1aR2^{BBS}$ and eGFP were incubated in 1 mM d-TC for 5 min followed by 3 µg/ml BTX-AF555 for 10 min at RT before imaging at 16-18°C or 30-32°C. *C*, Rate of internalisation of BTX-AF555 tagged $R1a^{BBS}R2$ (□) and $R1aR2^{BBS}$ (○) receptors at 16-18°C (red), and 30-32°C (black) in live hippocampal neurons (n = 6 – 14).

$R1aR2^{BBS}$ expressed well in the soma of hippocampal neurons in culture and bound BTX-AF555 specifically when neurons expressing R1a, $R2^{BBS}$, eGFP were incubated in 1 mM d-TC for 5 min at RT followed by incubation in BTX-AF555 (3 µg/ml) for 10 min at RT (Fig. 4.4*A*; upper panel). Such staining was not observed for cells incubated in UL-BTX (3 µg/ml; Fig. 4.4*A*; lower panel) or cells transfected with eGFP only and, incubated in 3 µg/ml BTX-AF555 (data not shown). Constitutive internalisation of $R1aR2^{BBS}$ receptors was also evident in the soma of 14-21 DIV cultured hippocampal neurons. As expected from GIRK cell data, internalisation of $R1aR2^{BBS}$ rapidly increased from LT (89 ± 2 % surface fluorescence after 1hr, n = 7) to PT, where τ = 17.1 ± 3.2 min, leaving only 33 ± 2 % (n = 14, Fig. 4.4*B, C*) on the cell surface. These profiles are very similar to those of $R1a^{BBS}R2$ receptors indicating that the receptors are probably internalised as heterodimers (Fig. 4.4*C*).

4.2.4 Di-leucine motif on R1a is a dominant-positive signal for internalisation

A mechanism by which R2 subunits could regulate the rate of internalisation of the R1aR2 receptor on the cell surface may involve an interaction of R2 with a dominant endocytic sorting signal on the R1a C-terminus. As a di-leucine motif in the R1a coiled-coil domain (L889, L890) can affect the surface availability of $GABA_B$ receptors (Margeta-Mitrovic et al., 2000; Restituito et al., 2005), the consequences of their replacement by alanines was investigated on the background of $R1a^{BBS-ASA}$ by forming $R1a^{BBS-ASA, L889A, L890A}$.

GIRK cells expressing $R1a^{BBS\text{-}ASA,\ L889A,\ L890A}$ exhibited surface labelling with BTX and constitutive internalisation at RT (Fig. 4.5*A, B*) with a rate (τ = 11.4 ± 2.6 min; n = 6; Fig. 4.5*B*) and extent of internalisation (47 ± 4 %; n = 6; Fig. 4.5*B*) similar to that for $R1a^{BBS}R2$, $R1aR2^{BBS}$ and $R2^{BBS}$ (Fig. 4.5*C, D*; P>0.05). However, the extent but not the rate of internalisation for $R1a^{BBS\text{-}ASA,\ L889A,\ L890A}$ was significantly less when compared to $R1a^{BBS\text{-}ASA}$ (Fig. 4.5*D*; P<0.001). Thus, conceivably, the di-leucine motif may act as a dominant endocytic signal in the absence of R2 and upon heterodimerisation, this motif is inactivated via an interaction with the R2 coiled-coil domain increasing the stability of the R1aR2 heterodimer on the cell surface.

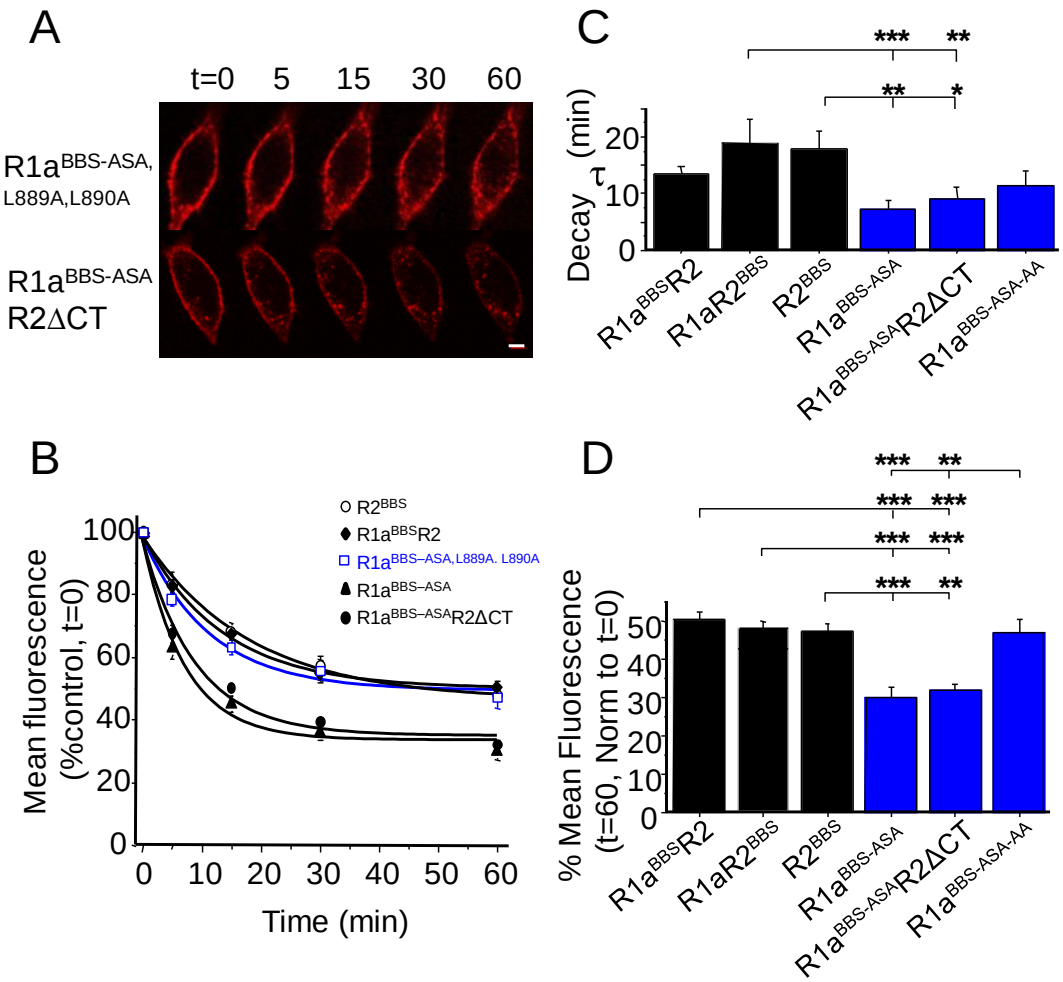

Figure 4.5 - Di-leucine motif on R1a determines the extent of internalisation.
A, GIRK cells expressing $R1a^{BBS\text{-}ASA,L889A,L890A}$ ($R1a^{BBS\text{-}ASA\text{-}AA}$; upper panel) or $R1a^{BBS\text{-}ASA}R2\Delta CT$ (lower panel) were incubated in 3 µg/ml BTX-AF555 for 10 min at RT and

imaged over 0 – 60 min at RT. Scale bar = 3 μm. *B*, Rates of constitutive internalisation for $R2^{BBS}$, $R1a^{BBS}R2$, $R1a^{BBS\text{-}ASA,L889A,L890A}$ ($R1a^{BBS\text{-}ASA\text{-}AA}$), $R1a^{BBS\text{-}ASA}$, and $R1a^{BBS\text{-}ASA}R2\Delta CT$ receptors (n = 6). *C*, Decay time constants for the surface membrane fluorescence for the subunits indicated, where $R1a^{BBS\text{-}ASA\text{-}L889A,L890A}$ = $R1a^{BBS\text{-}ASA\text{-}AA}$. *D*, Extent of internalisation for the subunits indicated. *P<0.05, **P<0.01 ***P<0.001 one way ANOVA.

4.2.5 R2 tail and R1aR2 internalisation

To examine the potential role of the R2 C-terminal tail in determining the rate of internalisation of R1a subunits, the C-terminal tail was truncated (R2ΔCT) starting from and including N749. The $R1a^{BBS\text{-}ASA}R2\Delta CT$ receptors should still interact via their N-terminal VFTDs and the 7-TM regions, but the di-leucine motif on R1 will be free, unable to interact with a missing R2 C-terminal tail. Co-expression of $R1a^{BBS\text{-}ASA}$ and R2ΔCT in GIRK cells revealed co-localisation of the subunits on the cell surface by immunostaining for the myc-tag on R1a and the flag-tag on R2 (data not shown). The $R1a^{BBS\text{-}ASA}R2\Delta CT$ receptors constitutively internalised at RT at a rate (9.0 ± 2.0 min; Fig. 4.5*A*-*C*) and to an extent (32 ± 2 %; n = 6; Fig. 4.5*D*) that was indistinguishable from $R1a^{BBS\text{-}ASA}$ (P>0.05). This rate was significantly faster than that for $R1aR2^{BBS}$ (P<0.01) and $R2^{BBS}$ (Fig. 4.5*C*; P<0.05), and the extent of internalisation for $R1a^{BBS\text{-}ASA}R2\Delta CT$ was significantly greater compared with $R1a^{BBS}R2$ (P<0.001), $R1aR2^{BBS}$ (P<0.001), $R2^{BBS}$ (P<0.01), and $R1a^{BBS\text{-}ASA,\ L889A,\ L8890A}$ (P<0.01; Fig. 4.5*D*).

Therefore these results strongly suggest that R2 subunits determine the rate of constitutive internalisation of the heterodimer most likely by masking a dominant di-leucine motif internalisation signal on the R1a coiled-coil domain by interaction between the C-terminal tails of R1a and R2.

4.2.6 Tracking R1a and R2 using dual labelling and different BTX-linked fluorophores

The rates and extents of internalisation for $GABA_B$ receptor heterodimers monitored with a BBS tag on either R1a ($R1a^{BBS}R2$) or R2 ($R1aR2^{BBS}$) are very similar, suggesting the majority of $GABA_B$ receptors are internalised as heteromers. To unequivocally demonstrate this required the simultaneous labelling of R1a and R2 with BTX linked to different fluorophores. However, to enable dual labelling, the BBS on one of the subunits must be protected from labelling by BTX whilst the BBS on the other subunit remains accessible. The advantage of the BBS over an epitope tagging method using antibodies is that an antibody molecule is six times the size of BTX. A primary antibody F(ab)' complex will be smaller but still about four times the size of BTX.

Differential binding of BTX was achieved by protecting the BBS on one of the $GABA_B$ receptor subunits. Such approaches have been used extensively in structure-function relationship studies of ion channels and in studies for assessment of ion channel membrane topology (Karlin and Akabas, 1998). Chemical protection was achieved by substituting two serine residues in the centre of the BBS on $R1a^{BBS}$ (WRYYE**SS**LEPYPD) for cysteines (WRYYE**CC**LEPYPD; Fig. 4.6) forming $R1a^{BBS\text{-}CC}$. The two cysteines were chosen for replacement because these two residues replace the serines in a mimotope of the BBS that has been described to block the association of BTX to the torpedo AchR (Kasher et al., 2001). By prior covalent labelling of these cysteine residues using a sulphydryl reagent, the binding of BTX to R1a was prevented whilst binding to the unmodified BBS on R2 could proceed unhindered. BTX binding to R1a was subsequently restored by removing the protective sulphydryl reagent using DTT.

The structural integrity of the BBS on $R1a^{BBS\text{-}CC}$ was confirmed by BTX-AF555 binding to $R1a^{BBS\text{-}CC}R2$ expressed in GIRK cells. The binding was selective and the fluorescence intensity lower compared to that observed with BTX-AF555 bound to $R1a^{BBS}R2$ receptors (data not shown). To prevent BTX-AF555 binding to $R1a^{BBS\text{-}CC}$, the two vicinal cysteine residues must be prevented from oxidising and forming a disulphide bond (Fig. 4.6). For $R1a^{BBS\text{-}CC}R2$, Cys bridge formation was prevented using 200 µM DTT for 30 min at RT before the application of 200 µM MTSES for 5 min at 4°C. Under these conditions, the surface labelling by BTX-AF555 was minimal (18 ± 2 % of control; $P<0.001$; n = 9, Fig. 4.7*A, B*).

Having established that BTX binding to $R1a^{BBS\text{-}CC}$ was prevented by MTSES, the protecting group was then removed with 5 mM DTT for 5 min at RT. Subsequent incubation with 3 µg/ml BTX-AF555 for 10 min at 4°C significantly recovered the surface fluorescence indicating that surface $R1a^{BBS\text{-}CC}R2$ receptors had recovered their ability to bind BTX-AF555 via the BBS on R1a (68 ± 6 % of control; n=9; Fig. 4.7*A*, *B*; $P<0.001$). Although there is a difference between the fluorescence intensity of the MTSES block and control, around 20% fluorescence that cannot be blocked means that a small proportion of the receptors will not be labelled specifically. For this reason, high resolution intracellular co-localisation studies will not be possible using this method.

Whole-cell patch clamp recording was used to determine the impact of the cysteine residues in the BBS on the function of $R1a^{BBS\text{-}CC}R2^{BBS}$. Following serine substitution there is a small reduction in GABA potency for activating inwardly-rectifying potassium currents with an 8-fold shift in the EC_{50} to 3.2 ± 0.37 µM (n = 6; Fig. 4.7*C*) compared to

$R1a^{BBS}R2$. This small change in sensitivity was insufficient to affect its use as a tag for monitoring the movement of $GABA_B$ receptors.

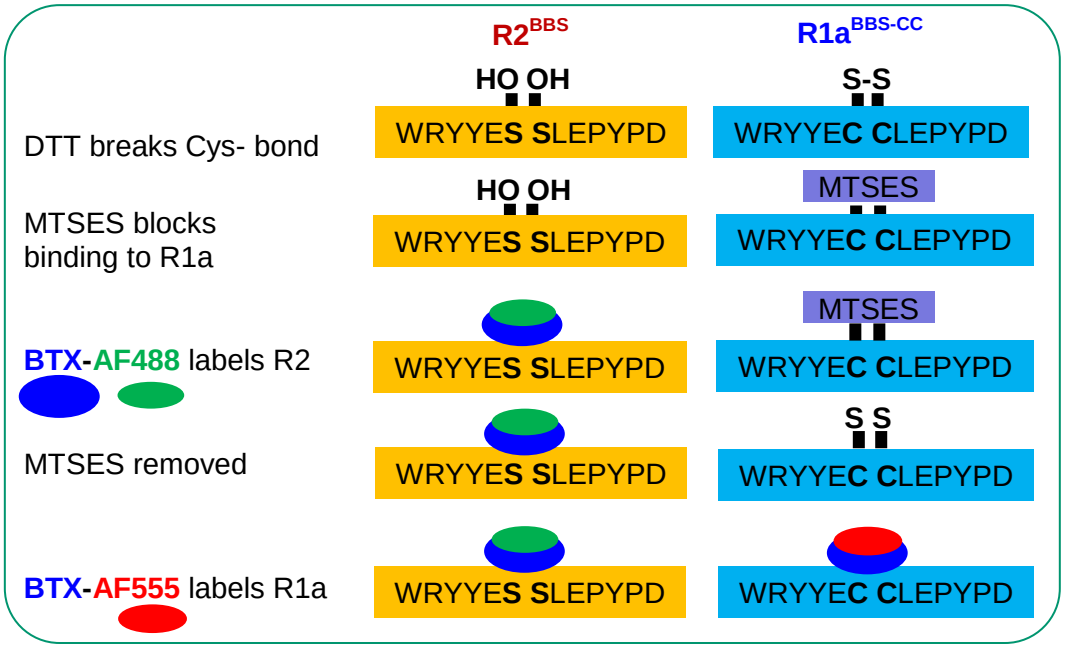

Figure 4.6 - Dual BBS-based fluorophore labeling of R1a and R2 subunits.
Diagram of the steps used for the dual labelling strategy for R2 (normal BBS, left) and R1a (mutant BBS, right) subunits.

Once the binding of BTX to BBS-CC could be blocked by MTSES and reversed with DTT, we used dual BTX labelling to study whether the two $GABA_B$ receptor subunits were internalised as heteromers in hippocampal neurons. Neurons expressing $R1a^{BBS-CC}R2^{BBS}$ were pre-incubated with 1 mM d-TC for 5 min and RT and incubated with 200 µM DTT for 30 min at RT followed by washes in PBS prior to the addition of 200 µM MTSES for 5 min at 4°C to block the binding of BTX to $R1a^{BBS-CC}$. After PBS washes, 3 µg/ml BTX-AF488 was applied for 10 min at 4°C to label the surface $R2^{BBS}$ receptors. The excess was removed by PBS washing and the cells re-incubated in 2 mM DTT for 5 min at RT to remove the MTSES. Finally, after further washing, 3 µg/ml BTX-AF555 was applied for 10 min at 4°C to label surface $R1a^{BBS-CC}$.

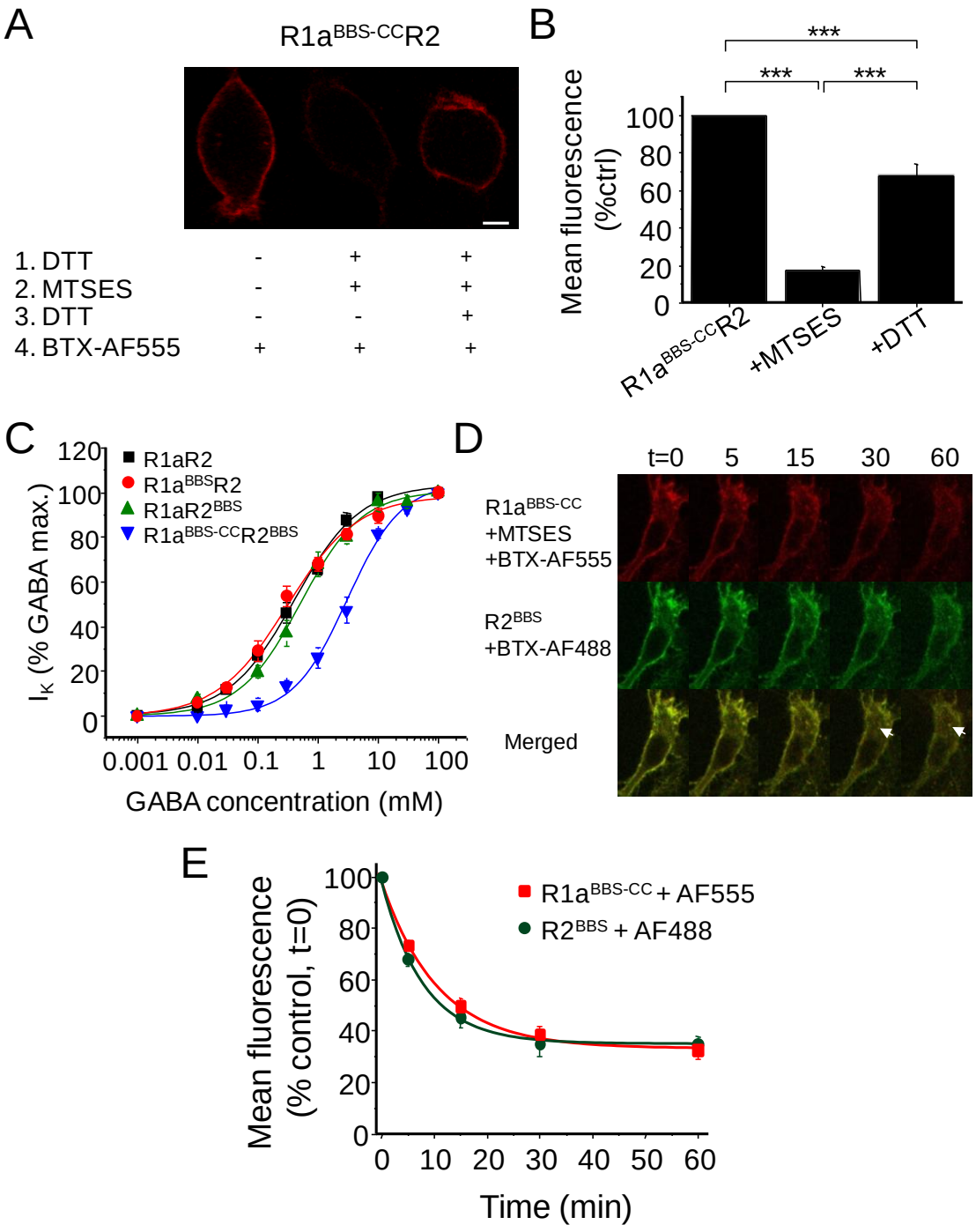

Figure 4.7 - Dual BBS-based fluorophore labeling of R1a and R2 subunits.
A, GIRK cells expressing $R1a^{BBS-CC}R2$ receptors were incubated in: 3 µg/ml BTX-AF555 for 10 min at RT alone (left); with BTX-AF555 after incubation in 200 µM DTT for 30 min at RT and 200 µM MTSES for 5 min at 4°C (middle); or with BTX-AF555 after 200 µM DTT for 30 min at RT and 200 µM MTSES for 5 min at 4°C followed by 5 mM DTT for 5 min at RT. Cells were imaged after fixation. Scale bar = 5µm. *B*, Inhibition of BTX-AF555 binding by MTSES and recovery of fluorescence following removal of MTSES by DTT compared to $R1a^{BBS-CC}R2$ controls (n = 9). *C*, GABA concentration response curves for R1aR2, $R1aR2^{BBS}$, $R1a^{BBS}R2$ and $R1a^{BBS-CC}R2^{BBS}$ expressed in GIRK cells (n = 7 – 13). *D*, Hippocampal neurons (14-21 DIV) expressing $R1a^{BBS-CC}R2^{BBS}$ were incubated in 1 mM d-TC for 5 min followed by 200 µM DTT for 30 min at RT, 200 µM MTSES for 5 min, 3 µg/ml BTX-AF488 for 10 min at 4°C, 2 mM DTT for 5 min at RT, and 3 µg/ml BTX-AF555

for 10 min at 4°C and imaged at different times at 30-32°C. Arrowheads indicate some examples of co-localised and internalised R1a and R2 subunits. *E*, Rate of constitutive internalisation of BTX-AF488 tagged $R2^{BBS}$ and BTX-AF555 tagged $R1a^{BBS-CC}$ receptors (n = 6). ***P<0.001 one way ANOVA. Data presented in (C) was acquired by Dr. M.E. Wilkins

Live cell imaging of cells was carried out at 30-32°C in Krebs. Notably, R2 (+BTX-AF488) and R1a (+BTX-AF555) were co-localised over the same period to intracellular compartments at 15 - 60 min (Fig. 4.7D). No intracellular compartments were decorated with only one or other of the fluorophores. The rates and extents of internalisation for the labelled R1a (τ = 11 ± 1 min; extent = 32 ± 3; n = 5) and R2 subunits (τ = 8 ± 1 min; extent = 35 ± 3; n = 5, P>0.05; Fig. 4.7E) were also similar. Taken together, these data strongly suggest that the majority of R1a and R2 subunits are internalised as heterodimers and rules out the possibility that the subunits disassemble from the heteromeric complex prior to recruitment into the endocytic pathway. NSF (discussed previously) which has been described to play a role in the desensitisation process of $GABA_B$ receptors has been reported to disassemble other receptor complexes such as the AMPA receptor GluR2 subunits and effect synaptic availability and therefore signalling of AMPA receptors (Hanley et al., 2002).

4.3 Discussion

Since the discovery of heterodimerisation of $GABA_B$ receptors, oligomerisation of GPCR subunits is now considered an important mechanism for the modulation of signalling and trafficking properties of GPCRs. Such modulation has been best described for the opioid receptor (Rozenfeld and Devi, 2010) for which dimerisation and higher order oligomerisation of the μ and δ receptors causes the opiod receptor to exhibit different pharmacological profiles and signalling properties to the receptors expressed individually (George et al., 2000). For example, μ and δ receptors complex has a 10-fold lower affinity for the μ- and δ- selective agonists DAMGO ([D-Ala^2, N-$MePhe^4$, Gly-ol]- enkephalin) and ([d-Pen^2, d-Pen^5]-enkephalin) DPDPE, respectively compared to individual receptors and the heteromers are more stable on the cell surface compared to individual monomers. In addition, the dopamine D1 and D2 receptors are unable to couple to Gq as monomers but can do so in their heteromeric forms (Lee et al., 2004) resulting in the activation of PLC.

Similar to these GPCRs, slow synaptic inhibition in the CNS relies on the hetero-oligomerisation of R1 and R2 $GABA_B$ receptor subunits. This links the transmitter binding site on R1 with the G-protein signalling properties possessed by R2. Although it is well established that heterodimerisation enables the trafficking of R1 subunits to the cell surface, what controls $GABA_B$ receptor surface stability thereafter is less well understood. $GABA_B$ receptors have been described to form dimers of dimers (Maurel et al., 2008) with the interaction interface between heterodimers being formed by two R1 subunits. In addition to heterodimerisation, such oligomeric assembly could also affect the internalisation profiles of the $GABA_B$ heteromers. The ability to track the

real-time movement of R1 and R2 subunits in live cells using the BBS and the fluorophore-conjugated BTX provides opportunities for investigating the role of R2 in the molecular mechanisms underlying cell surface receptor stability for $GABA_B$ receptors.

4.3.1 R2 is a regulator of $GABA_B$ receptor internalisation

The fast rate of internalisation of $R1a^{BBS\text{-}ASA}$ homomers became evident once the ER retention motif had been substituted allowing R1a access to the surface membrane. The modulatory influence of R2 was apparent by extending the use of the BBS tagging strategy to insert a functionally silent, high affinity BBS into the N-terminal domain of R2 subunits. Tracking the real-time movement of R2 subunits, for the first time independently from R1a, revealed its internalisation rate was notably slower. Indeed, the rates of internalisation for $R1a^{BBS}R2$, $R1aR2^{BBS}$ and $R2^{BBS}$, were comparable and significantly slower than for $R1a^{BBS\text{-}ASA}$. Independent of which subunit was tagged with the BBS, the R2 subunit slowed the rate and reduced the extent of internalisation. Thus heterodimerisation will slow down the rate of internalisation and if the rate of recycling and rates of insertion of newly synthesised receptors remain the same, this will impart greater stability to cell surface $GABA_B$ receptors thereby enhancing inhibition. Attempts made to study constitutive internalisation of $R1a^{BBS\text{-}ASA}$ homomers at near physiological temperatures demonstrated clearly that these homomers internalised at a quicker rate and to a greater extent compared to $R2^{BBS}$ homomers, and $R1a^{BBS}R2$ or $R1aR2^{BBS}$ heteromers at the higher temperature. However, the rapid

rate of internalisation for $R1a^{BBS-ASA}$ receptors at near physiological temperatures made it difficult to accurately measure kinetic parameters. In addition, given that the rate and extent of internalisation of $R2^{BBS}$ homomers is similar to those of the $R1a^{BBS}R2$ or $R1aR2^{BBS}$ heteromers, the possibility that the rates and extents of constitutive internalisation of the heteromers is a weighted mean of the monomers can be discounted.

Whether the ASA serves as a dominant endocytic signal was investigated by creating a C-terminal tail truncation of $R1a^{BBS}$ starting at R922 and this mutant had similar rates and extents of constitutive internalisation as the $R1a^{BBS-ASA}$ receptors discounting the possibility that ASA serves as an endocytic signal.

4.3.2 Structural motif promoting rapid $GABA_B$ receptor internalisation

The rapid internalisation of $R1a^{BBS-ASA}$ compared to $R2^{BBS}$ was likely to be caused by one or more intracellular motifs specifically located on the R1a subunit. The C-terminal tail was designated as the prime location for controlling receptor internalisation because of its length and its engagement with the equivalent tail in the R2 subunit, which also influences the rate of internalisation of the heteromer.

By truncating the C-terminal tail of $R1a^{BBS-ASA}$ after the seventh transmembrane domain, the rate of internalisation was reduced towards that of $R1^{BBS}R2$, identifying the location of an endocytic motif that increased the rate of constitutive internalisation of $R1a^{BBS-ASA}$ compared to R1aR2. By replacing the di-leucine motif

(L889, L890) in $R1a^{BBS\text{-}ASA,L889A,L890A}$, the rate and extent of constitutive internalisation became comparable to that for $R2^{BBS}$ and R1aR2. By contrast, co-assembly of $R1a^{BBS}$ with R2ΔCT produced receptors exhibiting similar rates and extents of internalisation to $R1a^{BBS\text{-}ASA}$ again discounting the possibility that the ASA motif was serving as an endocytic signal. For the R1aR2 heteromer, the di-leucine motif did not increase the rate of internalisation. This may be a consequence of the R2 subunit C-terminal tail. Its truncation in R2ΔCT and co-expression with $R1a^{BBS\text{-}ASA}$, no longer slowed the rate and extent of internalisation to that of the R2 homomer, but proceeded at the same rate and to the same extent as that of $R1a^{BBS\text{-}ASA}$ homomers. The most plausible explanation is that the R2 subunit determines the rate and extent of internalisation of heterodimers by masking the di-leucine motif upon coassembly with residues from its C-tail. The di-leucine motif is suitably positioned in the coiled-coil domain, a major site of interaction between R1 and R2 (White et al., 1998; Kuner et al., 1999).

The importance of the di-leucine motif on R1a trafficking is exemplified by its previous description as an interaction motif for msec7-1 (Restituito et al., 2005), which is a GEF of the ADP-ribosylation factor (ARF) proteins. These proteins are known to play an important role in vesicular trafficking in all eukaryotic cells (Jackson et al., 2000). Indeed, the overexpression of msec7-1 upregulates the levels of $R1^{ASA}$ on the cell surface of COS-7 cells via an interaction with the di-leucine motif. It is conceivable that msec7-1 could serve as an adapter for $GABA_B$ receptor internalisation by interacting with the di-leucine motif causing $R1a^{ASA}$ receptors to be internalised faster and to a greater extent than R1aR2. An isoleucine-leucine pair is also present on the R2 subunit (I853, L854), but this motif appears to play no role in $GABA_B$ receptor trafficking despite the R2 subunit C-terminal tail influencing the destination of assembled

receptors to specific neuronal compartments (Pooler et al., 2009). Therefore in the absence of R2, R1a subunits internalise at a faster rate and greater extent than they do in the presence of R2 as the dominant positive di-leucine motif internalisation signal in the coiled-coil domain of R1a remains exposed to the cytosol where a yet unknown interaction partner could recruit R1a for internalisation. As part of the heteromer, R2 slows down the internalisation kinetics of R1a by masking the di-leucine motif on R1a and overriding this signal. The finding that internalisation profiles of R2 homomers and R1aR2 heteromers are similar implies that once a part of the heteromeric complex an internalisation signal on R2 subunits could determine the internalisation profiles of the heteromers. A direct evidence of this hypothesis is yet to be established and further work is required to validate this hypothesis including the identification of a motif on R2 that would recruit the heteromers for clathrin- and dynamin-dependent internalisation.

4.3.3 Cycling of $GABA_B$ receptors

The rate and extent of internalisation was notably increased for R1a homomers when the RSR retention motif was removed. Co-expression with R2 nullified this effect unless the C-terminal tail for R2 was truncated. By combining the rates of receptor movement measured in this study with others, it is possible to construct a kinetic model for the trafficking life cycle of $GABA_B$ receptors (Fig. 4.8*A*). The main elements of the model include, rates for $GABA_B$ receptor endocytosis from the surface membrane (k_{endo}, this study), synthesis and insertion of new receptors from the Golgi stack/ER (k_{in}, taken

from (Wilkins et al., 2008)), degradation of endocytosed receptors (k_{degrad}), recycling of receptors back to the surface membrane (k_{recyc}), and photobleaching of the BTX attached fluorophore (k_{pb}, this study; Fig. 4.8*A*). The removal of $GABA_B$ receptors from the surface membrane (as measured by the loss of surface fluorescence) was a function of the rate of insertion (τ = 7.8 min (Wilkins et al., 2008)) and the rate of endocytosis (τ = 15 min for R1aR2 heteromers) with photobleaching (τ = 98 min) having a negligible contribution. To ensure a plateau phase develops requires that a proportion of receptors must recycle back to the cell surface. This rate was empirically determined to reproduce the experimental data, being set to τ = 25 min with up to 40 % of internalised receptors being returned to the surface. A proportion are considered to be degraded from the internalised pool and this was set empirically at 20% with a τ = 120 min. Given these boundary conditions, and apart from changing the rate of endocytosis, the plateau steady-state phases of the decay curves involving, $R1a^{BBS\text{-}ASA}$, $R1a^{BBS\text{-}ASA}R2\Delta CT$, compared to R1aR2 and $R2^{BBS}$ (Fig. 4.5*B*) are most easily accounted for by changes in receptor recycling (Fig. 4.8*B*). Although increased receptor insertion will also affect the steady-state, when the rates are increased, this slows the rate of internalisation often causing an inflection on the decay phase that is not observed experimentally. Changes to the rate of degradation can also affect the steady-state, but under the conditions of the model, large excursions in the extent of degradation have minimal effect on the steady-state. Overall, receptor recycling appears the likeliest cause for the plateau phase observed in the internalisation profiles.

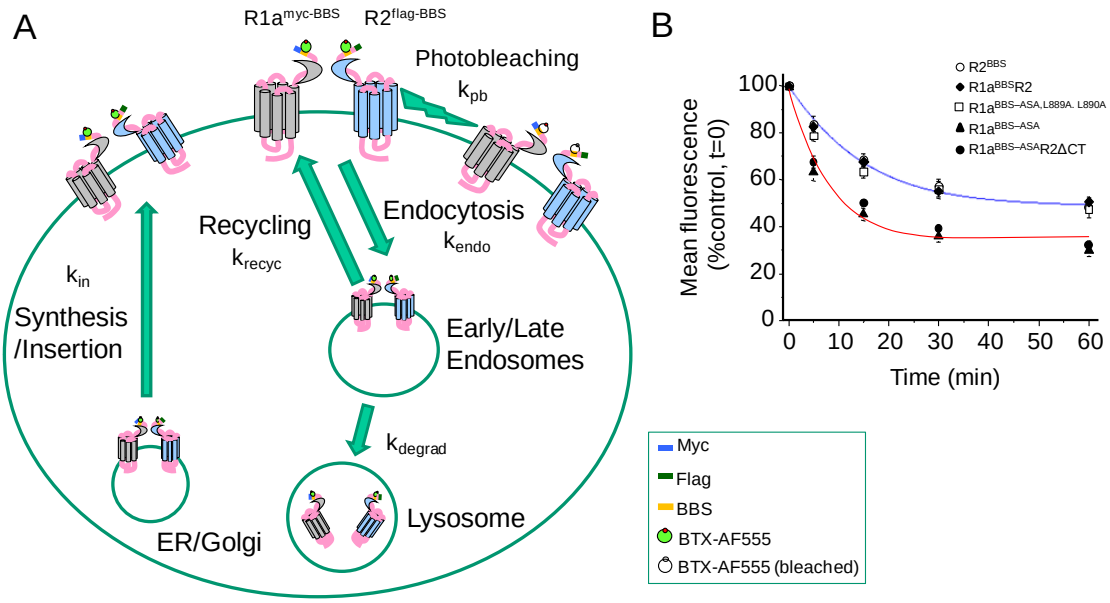

Figure 4.8 - Trafficking model for $GABA_B$ receptors.

A, Schematic diagram that illustrates the trafficking of $GABA_B$ receptors from the cell surface to early/late endosomes and onto lysosomes. The surface replenishment pathway involves the recycling of receptors and the synthetic pathway from the Golgi stack. The respective rate constants and key for the $GABA_B$ receptors are indicated. *B*, Rates of constitutive internalisation for $R2^{BBS}$, $R1a^{BBS}R2$, $R1a^{BBS\text{-}ASA,L889A,L890A}$, $R1a^{BBS\text{-}ASA}$, and $R1a^{BBS\text{-}ASA}R2\Delta CT$ receptors, taken from Fig. 4.5*B*. The curve fits are generated using the model in *A* with k_{endo} = 0.067 min^{-1}, k_{in} = 0.128 min^{-1}, k_{pb} = 0.01 min^{-1}, k_{recyc} = 0.04 min^{-1}, k_{degrad} = 0.0083 min^{-1} (for R1aR2, blue), with 45% of receptors recycling, and k_{endo} = 0.11 min^{-1}, k_{in} = 0.128 min^{-1}, k_{pb} = 0.01 min^{-1}, k_{recyc} = 0.04 min^{-1}, k_{degrad} = 0.0083 min^{-1} (for $R1a^{BBS\text{-}ASA}$, red) with 30% of receptors recycling.

4.3.4 Multiple roles for $GABA_B$ receptor heterodimerisation

The $GABA_B$ receptor was the first example of a GPCR that required heterodimerisation to support ligand binding and G protein coupling (Kaupmann et al., 1998; White et al., 1998). Although the precise subunit stoichiometry(ies) for $GABA_B$ receptors has not been resolved, primarily heterodimerisation between R1 and R2 performs at least three distinct roles. Firstly, to link ligand binding to downstream signalling, the ligand binding site located in the VFTD of R1, needs to be co-assembled with the G-protein coupling domain located in the intracellular loops of R2 (Margeta-Mitrovic et al.,

2001a; Duthey et al., 2002; Havlickova et al., 2002; Robbins et al., 2001). Secondly, an interaction between the VFTDs of R1 and R2 is important to create a high affinity GABA binding site (Galvez et al., 2001), and any disruption to this extracellular interaction abolishes subsequent G-protein coupling (Rondard et al., 2008). Thirdly, R1 requires R2 to act as a chaperone to reach the cell surface (Couve et al., 1998) because of the ER retention motif in R1 (Margeta-Mitrovic et al., 2000). Here, a fourth important role for heterodimerisation has been added in which R2 determines the rate and extent of internalisation of heterodimers by masking the di-leucine motif in the C-terminal tail coiled-coil domain of R1a.

The coupling between R1a and R2 is sufficiently tight such that both subunits are internalised together dispensing with the need to dissociate beforehand in the plane of the cell surface (Kammerer et al., 1999). This aspect was demonstrated by extending the versatility of the BBS tagging method to enable dual labelling of the R1a and R2 subunits with BTX conjugated to discrete fluorophores.

Thus, in conclusion, the new role for R2 subunits in determining the rate of internalisation of R1aR2 denotes R2 as a major determinant of cell surface $GABA_B$ receptor stability. This will influence the efficacy of slow synaptic inhibition in the CNS by slowing the removal of receptors from the cell surface. This is a desirable property for G-protein coupled receptors that are generally considered to perform a housekeeping role in providing background, low efficacy inhibition following GABA spillover from inhibitory synapses.

4.4 Summary

- BBS technique can be applied to study the trafficking of $GABA_B$ R2 subunits
- R2 subunits stabilise R1a subunits at the cell surface
- R2 subunits achieve this by occluding a di-leucine motif in the C-terminal tail of R1, which in the absence of R2, acts as a dominant endocytic signal
- Dual labelling is possible using the BBS approach
- $GABA_B$ receptors are internalised as heteromers

Chapter V

Sushi Domains confer distinct trafficking profiles on $GABA_B$ receptors

5.1 Introduction

Functional $GABA_B$ receptors in the CNS require heterodimerisation (Jones et al., 1998; White et al., 1998; Kaupmann et al., 1998) between R1 subunits that contain the agonist binding domain (Malitschek et al., 1999) and R2 subunits that provide the link to G-protein signalling (Galvez et al., 2001; Margeta-Mitrovic et al., 2001a) in order to couple to GIRK channels and VGCCs. To date, only one isoform of R2 has been reported. By contrast several isoforms of the R1 subunit have been described (R1a, R1b, R1c, R1e, R1j) (Bettler et al., 2004). Amongst these, R1a and R1b are the predominant isoforms found in the CNS and arise because of different promoters (Kaupmann et al., 1998; Kaupmann et al., 1997) of the GABBR1 gene. These isoforms differ in the N-terminus due to the presence in R1a of an additional 143 amino acids forming two SDs which are replaced by 18 unique amino acids in R1b.

Heteromers formed from the R1 spice variants, R1aR2 and R1bR2, are thought to play distinct roles in neurotransmission following studies with R1a and R1b knock-out mice (Perez-Garci et al., 2006; Gassmann et al., 2004; Shaban et al., 2006; Vigot et al., 2006; Ulrich and Bettler, 2007; Guetg et al., 2009). These studies revealed that R1aR2 contributes to presynaptic heteroreceptors, which inhibit glutamate release, whilst

both R1aR2 and R1bR2 are found postsynaptically in dendrites. Here, R1bR2 receptors are more abundant in spines where they couple to K^+ channels. Knocking out R1b, unlike R1a, subunits reduced postsynaptic K^+ currents, suggesting they form the majority of postsynaptic heteroreceptors. R1b is also responsible for inhibiting dendritic Ca^{2+} spikes, possibly via direct inhibition of VGCCs (Chalifoux and Carter, 2011). The two heteromeric subtypes also show different subcellular compartmentalisation with the SDs acting as an axonal targeting sequence to deliver R1aR2 more efficiently to axons compared to R1bR2 receptors (Biermann et al., 2010).

Although $GABA_B$ receptor function can be regulated by the differential targeting of R1aR2 and R1bR2 receptors, it remains unknown how the SDs affect the lateral mobility and internalisation kinetics of R1aR2 receptors - aspects that will play a critical role in determining the efficacy of $GABA_B$ receptor signalling. Here, the role of the SDs on trafficking has been studied by inserting the BBS into the $GABA_B$ receptor R1b splice variant.

5.2 Results

5.2.1 Bungarotoxin tagging of $GABA_B$ $R1b^{BBS}$ is functionally silent

Constitutive internalisation of the R1bR2 receptor, was followed by inserting a BBS site into the N-terminus of R1b subunits. This was inserted adjacent to a myc tag, six amino acids from the start of the mature protein (Fig 5.1*A*). The ability of $R1b^{BBS}$ to bind specifically to BTX-AF555 was demonstrated in GIRK cells and cultured hippocampal neurons (14-21 DIV), transfected with cDNAs encoding for either $R1b^{BBS}$, R2 and eGFP, or just eGFP (Fig. 5.1*B*).

Radioligand binding studies with ^{125}I-BTX was used to assess the apparent affinity of BTX for $R1b^{BBS}$. Increasing concentrations of ^{125}I-BTX were applied to GIRK cells, expressing $R1b^{BBS}$R2 receptors, for 1 hr at RT, with ^{125}I-BTX binding in a concentration-dependent saturable manner (Fig. 5.1*C*). Scatchard analysis was used to determine a K_d of 32.6 ± 5.1 nM (n = 6) for BTX binding, which is 8-fold lower than the K_d for BTX binding to the $\alpha7/5HT_{3a}$ 3.92 ± 2.4 nM (n = 3). Therefore dissociation of BTX from $R1b^{BBS}$ will not affect prolonged live cell imaging of the $GABA_B$ receptors.

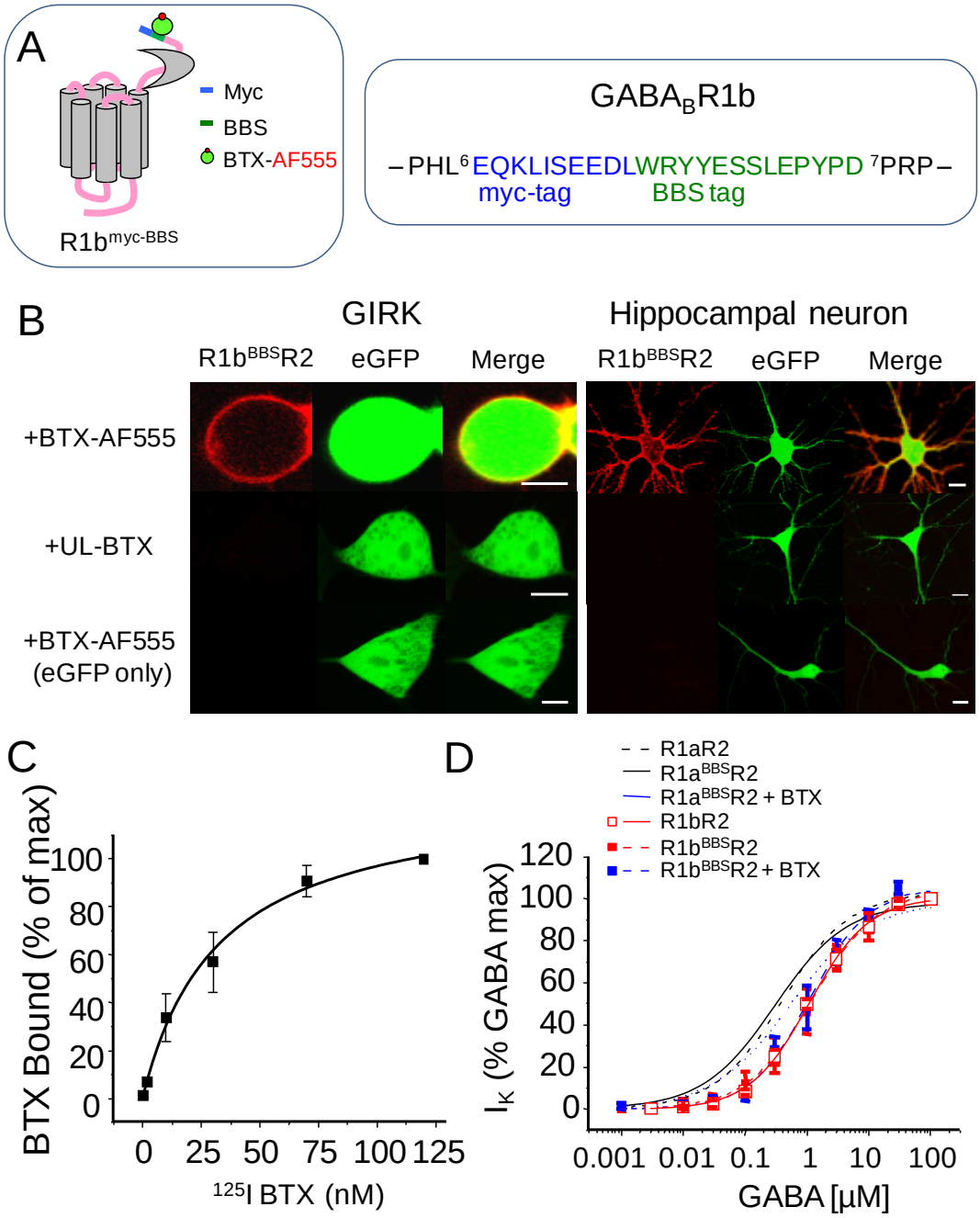

Figure 5.1 - BBS on R1b binds to BTX coupled to AF555 and is functionally silent.
A, Schematic diagram showing the relative locations for the BBS and the myc epitopes in R1b subunits. The BBS was inserted between Leu6 and Pro7. *B (left),* Images of GIRK cells expressing $R1b^{BBS}R2$ and (or) eGFP incubated with 3 µg/ml BTX-AF555 or UL-BTX for 10 min at RT. Scale bars = 5 µm. *(Right)* Images of rat cultured hippocampal neurons expressing $R1aR2^{BBS}$ and (or) eGFP, incubated with 1 mM d-TC for 5 min followed by incubation with 3 µg/ml BTX-AF555 or UL-BTX for 10 min at RT. Scale bars = 10 µm. *C*, Whole-cell radioligand binding experiments with ^{125}I-BTX for the $R1b^{BBS}R2$ receptor (n = 6).*D*, GABA concentration response curves for R1bR2, $R1b^{BBS}R2$, and BTX bound $R1b^{BBS}R2$ receptors all expressed in GIRK cells (n = 5-6). Data presented in (D) was acquired by Dr. M.E. Wilkins

The functional neutrality of the BBS tag on $R1b^{BBS}$ was assessed using whole-cell patch clamp electrophysiology with GABA concentration response curves for the activation of Kir 3.1 and 3.2 channels using wild-type (R1bR2) and $R1b^{BBS}R2$ receptors in the presence and absence of 3 μg/ml BTX-AF555 (Fig. 5.1*D*). The insertion of the BBS on R1b had no effect on the shape of the concentration response curves, or GABA potency, as determined from the EC_{50} values with $R1b^{BBS}R2$ receptors in the absence (1.2 ± 0.1 μM, n = 5) or presence (1.1 ± 0.1 μM, n = 6) of BTX-AF555 compared to the wild-type receptor (1.1 ± 0.1 μM; n = 5; $P > 0.05$; Fig. 5.1D).

These results suggest, as previously for $R1a^{BBS}$ and $R2^{BBS}$, that insertion of the BBS site into R1b enables high affinity binding of BTX, and when co-expressed with R2, the pharmacological profile of the receptor is similar to wild-type. Therefore, the BBS tag approach and a range of imaging strategies can be applied to study the real-time trafficking of R1bR2 receptors.

5.2.2 R2 subunits slow the internalisation rate of R1b homomers but not the extent

R2 subunits have been previously demonstrated to stabilise R1a subunits on the cell surface by interacting with a di-leucine motif (L889, L890) in the C-terminal coiled-coil domain of R1a. Since R1a and R1b have identical C-terminal coiled-coil domain sequences, we expected that R2 would also stabilise R1b by similarly interacting with the homologous R1b di-leucine motif (L773, L774). To study the movement of $R1b^{BBS}$ alone, the ER retention motif (-RSR-) in the coiled-coil domain was replaced by ASA to

create $R1b^{BBS-ASA}$. Cell labelling with BTX-AF555 (3 µg/ml) in GIRK cells expressing $R1b^{BBS-ASA}$ indicated receptor trafficking to the cell surface (Fig. 5.2*A*). Rapid constitutive internalisation to intracellular compartments of BTX-AF555 tagged $R1b^{BBS}R2$ and $R1b^{BBS-ASA}$ was also evident at RT (Fig. 5.2*A*). However, the monoexponential rate of decay in surface membrane fluorescence that marks the progress of constitutive internalisation was much faster for $R1b^{BBS-ASA}$ (τ = 8.6 ± 1.1 min; n = 8) compared to $R1b^{BBS}R2$ (τ = 14.6 ± 1.4 min; n = 9; P<0.05; Fig. 5.2*B, C*), indicating that R2 slows the internalisation of R1b following heterodimerisation.

The importance of the R1b di-leucine motif (L773, L774) in this process was investigated by its replacement with alanines. Using BTX-AF555 labelling, $R1b^{BBS-ASA-AA}$ trafficked to the cell surface (Fig. 5.2*A*), but the rate of internalisation was significantly slower (14.1 ± 1.9 min; n = 8, P<0.05) compared to that for $R1b^{BBS-ASA}$, and comparable to the rate for $R1b^{BBS}R2$ (Fig. 5.2*B, C*). However, differences were not observed between the extents of constitutive internalisation for $R1b^{BBS-ASA}$ (25.9 ± 2 %; n = 8) compared to either $R1b^{BBS}R2$ (23.9 ± 2.1 %; n = 9; P>0.05) or $R1b^{BBS-ASA-AA}$ receptors (21.8 ± 1.7 %; n = 8; P>0.05). This differs from the earlier comparison of R1a homomers and heteromers, where the extent of internalisation was greater for $R1a^{BBS-ASA}$ compared to that for R1aR2 heterodimers (Fig. 5.3*B;* dotted lines; data taken from Fig 3.1C, 4.1B).

Thus whilst the R2 subunit slows the internalisation of both R1aR2 and R1bR2 by interacting with the di-leucine motif in the R1 coiled-coil domain, the disparity between the relative extents of internalisation for R1aR2 and R1bR2 implies that the greater stability of R1aR2 on the surface membrane may be a consequence of the SDs

present in R1a. The fact that the internalisation profiles of R1a and R1b homomers are similar suggests that the SDs in R1a do not interact to stabilise the R1a homomers and that the SDs to impart increased stability to R1a containing receptors, R2 subunits are required.

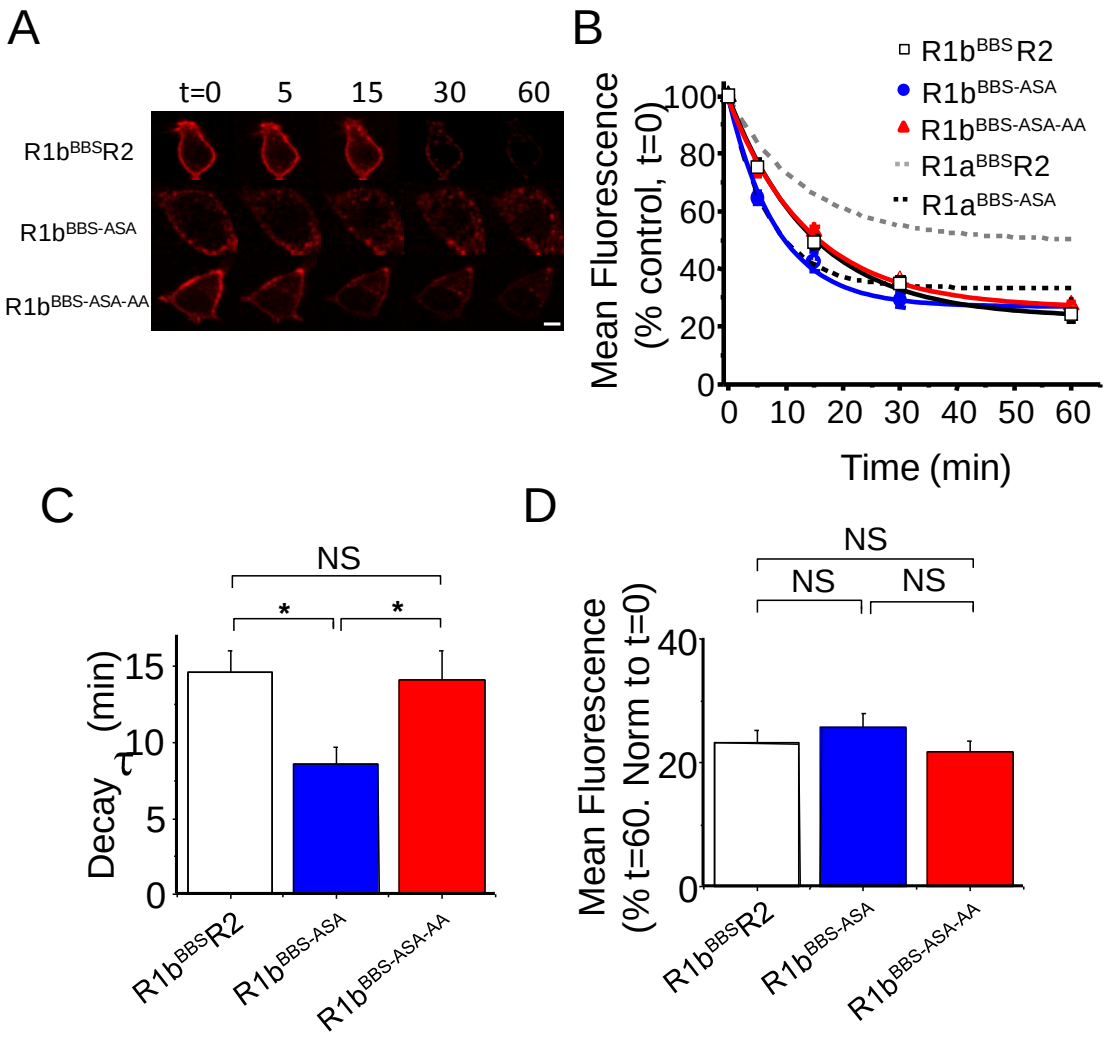

Figure 5.2 - R2 stabilises R1b subunits by altering the rate of internalisation.
A, GIRK cells expressing either $R1b^{BBS}R2$ (upper panel), $R1b^{BBS-ASA}$ (middle panel) or $R1b^{BBS-ASA-AA}$ (lower panel) were incubated in 3 µg/ml BTX-AF555 for 10 min at RT to label surface $GABA_B$ receptors and imaged over 0 – 60 min at RT. *B*, The rate of internalisation of BTX-AF555 tagged $R1b^{BBS}R2$ heteromers (□), and $R1b^{BBS-ASA}$ (●) and $R1b^{BBS-ASA-AA}$ (▲) homomers at RT (n = 8-9). *C*, Exponential decay time constants for the rate of decay of membrane fluorescence for $R1b^{BBS}R2$, $R1a^{BBS-ASA}$ and $R1a^{BBS-ASA-AA}$. *D*, Extent of internalisation for $R1b^{BBS}R2$ receptors, and $R1b^{BBS-ASA}$ or $R1b^{BBS-ASA-AA}$ homomers. NS – Not significant, *P<0.05, One-way ANOVA. Scale bar = 5 µm.

5.2.3 R1aR2 internalise slower than R1bR2 from the surface of hippocampal neurons

To determine if R1aR2 receptors internalise slower from the surface of hippocampal neurons than R1bR2 receptors, the constitutive internalisation of $R1a^{BBS}R2$ and $R1b^{BBS}R2$ was studied in the soma of cultured hippocampal neurons (14-21 DIV) transfected with cDNAs encoding for $R1a^{BBS}$ or $R1b^{BBS}$, R2, and eGFP were studied at PT.

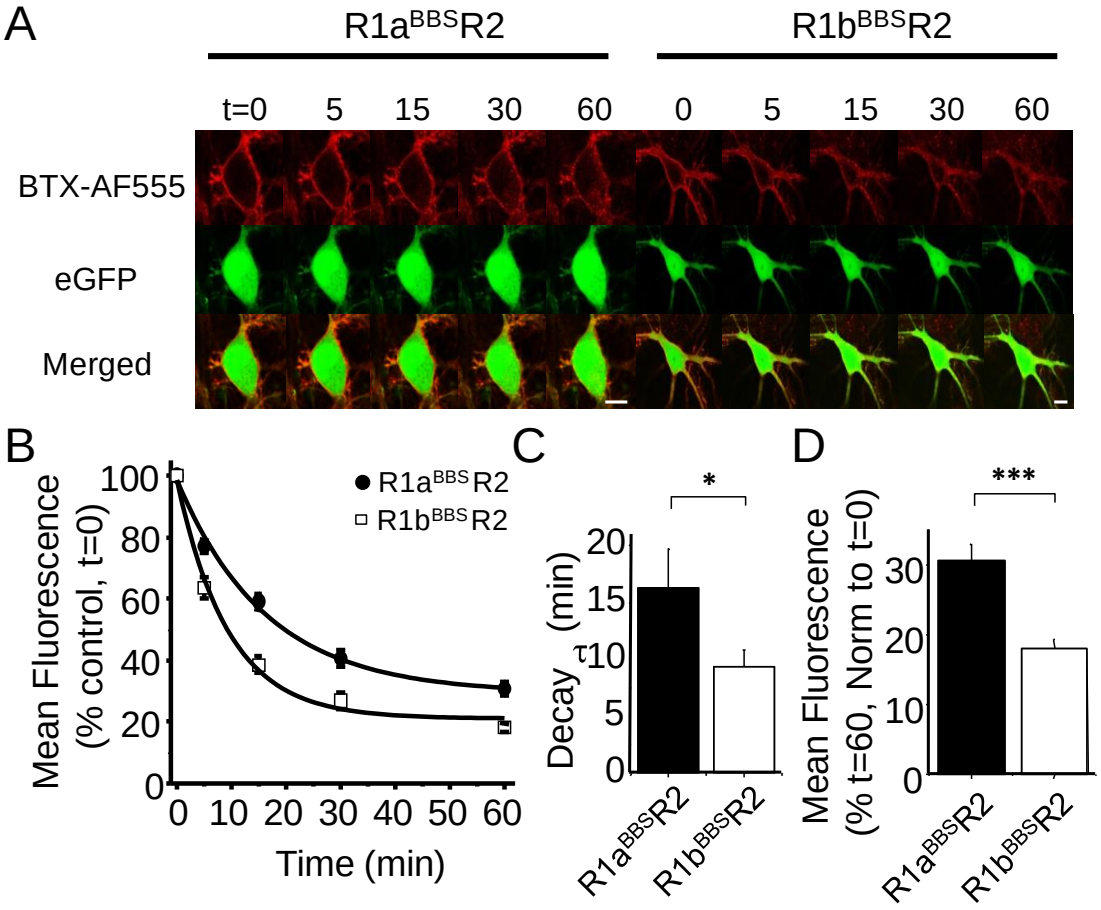

Figure 5.3 - R1bR2 receptors constitutively internalise at a faster rate and to a greater extent compared to R1aR2.

A, Hippocampal neurons at 14-21 DIV, expressing $R1a^{BBS}$ or $R1b^{BBS}$ with R2 and eGFP were incubated in 1 mM d-TC followed by 3 µg/ml BTX-AF555 at RT and imaged at different time points at 30-32°C. *B,* Rates of constitutive internalisation of BTX-AF555 tagged $R1a^{BBS}R2$ (●) and $R1b^{BBS}R2$ (□) receptors (n = 7-12). *C,* Exponential decay time constants for the rate of decay of membrane fluorescence of $R1a^{BBS}R2$ and $R1b^{BBS}R2$

receptors. *D,* Extent of constitutive internalisation of $R1a^{BBS}R2$ and $R1b^{BBS}R2$ receptors. * P<0.05, ***P<0.001. Scale bar 10 μm.

The cells were incubated with d-TC (1 mM) for 5 min followed by BTX-AF555 (3 μg/ml, 10 min) and imaged at different time points to construct surface fluorescence decay curves for internalisation (Fig. 5.3*A, B*). Constitutive internalisation resulted in a rapid decrease of surface fluorescence for each receptor isoform (Fig. 5.3*B*) with endocytic compartments filled with BTX-AF555. The extent of internalisation for $R1b^{BBS}R2$ receptors was greater (18.1 ± 1.2 %; n = 12) compared to $R1a^{BBS}R2$ (30.7 ± 2.2; n = 7, P<0.0001; Fig 5.3*D*). The rate of internalisation for $R1b^{BBS}R2$ (9.4 ±1.5 min; n = 12) was also significantly faster compared to $R1a^{BBS}R2$ (16.3 ± 2.5 min; n = 7; P < 0.05; Fig. 5.3*B, C*). This implies that the R1aR2 subtype of the $GABA_B$ receptor internalises at a slower rate and lesser extent than the R1bR2 subtype in the soma of hippocampal neurons in culture. Given the differential roles attributed to these two subtypes of the $GABA_B$ receptor in neuronal physiology, it is therefore of interest whether the subtype-specific internalisation profiles observed could explain some of the differences observed in signalling and will be studied in the future. The differences in internalisation observed could reflect an influence of the SDs on R1aR2 by modulating not only the extent but also the rate of receptor internalisation.

5.2.4 Membrane insertion is faster for R1bR2 compared to R1aR2 receptors

Whether the difference in the rates of internalisation could be extended to surface membrane insertion of $R1b^{BBS}R2$ and $R1a^{BBS}R2$ receptors was studied in transfected GIRK cells. UL-BTX (20 μg/ml) was applied at RT for 10 min to label all cell surface $GABA_B$ receptors. After washing to remove UL-BTX, BTX-AF555 (3 μg/ml) was applied at 37°C for different periods prior to imaging (Fig. 5.4*A*). Consistent with the internalisation assay, by measuring increased membrane fluorescence, a significant difference was observed in the rates of surface membrane insertion, with $R1b^{BBS}R2$ inserted at a faster rate (τ = 12.4 ± 2.9 min; n = 9) compared to $R1a^{BBS}R2$ (τ = 26.5 ± 2.4 min, n = 9; $P < 0.01$; Fig. 5.4*B, C*) receptors. The apparent staining observed at t = 0 (Fig. 5.4A) in the absence of BTX-AF555 is possibly due to auto-fluorescence of fixed cells. The plateau observed in the graphs (Fig. 5.4B) is due to the saturation of all the cell surface receptors in the presence of a high dose of BTX-AF555 in the extracellular medium and at the time points around the plateau phase the fluorescence is likely to represent equilibrium between internalisation, insertion of newly-synthesized receptors, and recycling receptors. In addition, degradation of $GABA_B$ receptors is also likely to occur during the course of the treatment with BTX-AF555. The kinetics of this equilibrium is of interest and could be studied in the future.

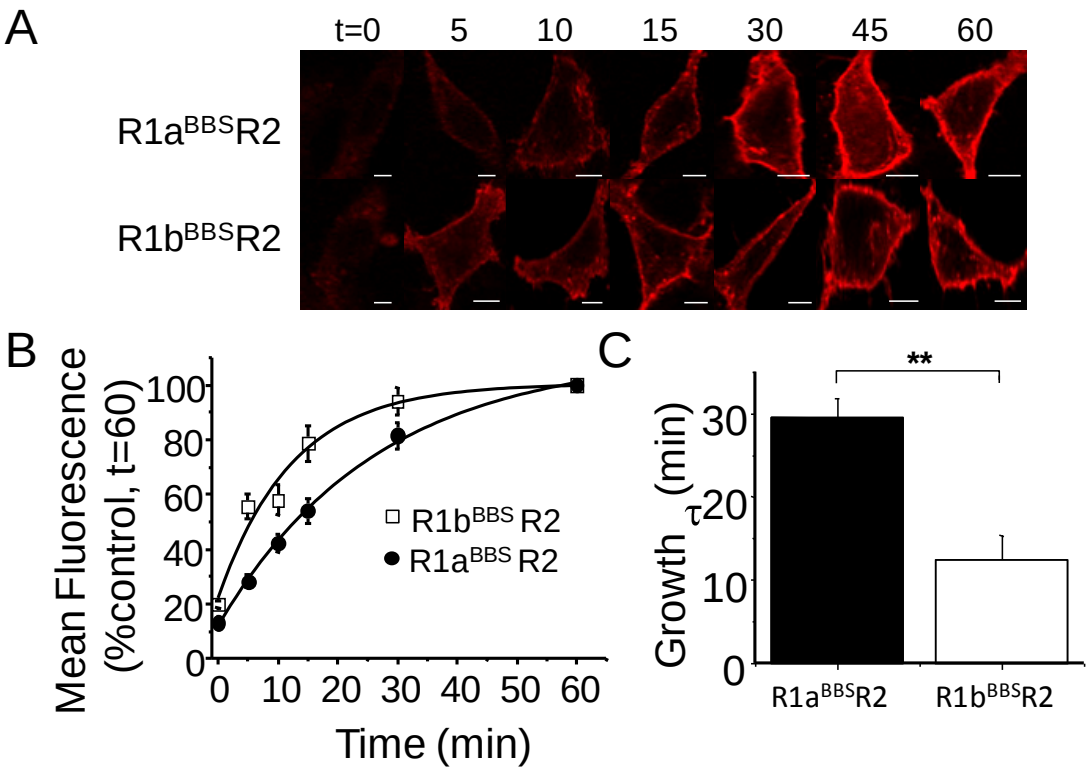

Figure 5.4 - R1b^{BBS}R2 receptors are constitutively inserted into the membrane at a faster rate than R1a^{BBS}R2 receptors.
A, GIRK cells transfected with cDNAs encoding for R1a^{BBS} or R1b^{BBS} with R2 and eGFP were incubated in 20 µg/ml UL-BTX for 10 mins at RT and incubated at 37°C for different times in 3 µg/ml BTX-AF555. *B,* Rates of constitutive insertion of R1a^{BBS}R2 (●) and R1b^{BBS}R2 (□) receptors (n = 9). C, Exponential growth time constants for the rate of increase in surface fluorescence of R1a^{BBS}R2 and R1b^{BBS}R2 receptors. ** P<0.01. Scale bar 5 µm.

Together these results indicate that the two subtypes of $GABA_B$ receptors have distinct dynamics on the cell surface with R1bR2 constitutively inserted into the cell surface at a faster rate than R1aR2 receptors. This difference in the insertion rates could also reflect the presence of the SDs on R1a serving to slow down insertion and internalisation profiles of R1aR2 compared to R1bR2 receptors.

5.2.5 SDs increase the stability of R1aR2 receptors

NMR interpreted structures of the SDs have revealed that SD1 is less compact than SD2 (Blein et al., 2004) implying that the two SDs could play differential roles in cellular physiology. In addition, the only known interaction partner of the SDs, to our knowledge, is fibulin-2, which interacts with SD1. To investigate how R1aR2 cell surface stability can be differentially regulated by the SDs compared to R1bR2, either the N-terminal ($R1a^{BBS}\Delta SD1$) or the C-terminal ($R1a^{BBS}\Delta SD2$) SDs were deleted in $R1a^{BBS}$ and constitutive internalisation of $R1a^{BBS}\Delta SD1R2$ and $R1a^{BBS}\Delta SD2R2$ studied. Hippocampal neuronal images expressing either $R1a^{BBS}\Delta SD1$ or $R1a^{BBS}\Delta SD2$, with R2 and eGFP, were analysed at 14-21 DIV. After blocking native nicotinic AChRs with d-TC (1 mM), BTX-AF555 was applied to monitor the surface fluorescence at different time points to follow receptor internalisation (Fig. 5.5*A, B*). Both $R1a^{BBS}\Delta SD1R2$ (τ = 6.5 ± 1.8 min; n = 9) and $R1a^{BBS}\Delta SD2R2$ (τ = 7.9 ± 1.3 min; n = 12; Fig 5.5*C*) constitutively internalised at similar rates that are indistinguishable from $R1b^{BBS}R2$ ($P>0.05$). However, when compared to $R1a^{BBS}R2$, both $R1a^{BBS}\Delta SD1R2$ ($P<0.01$) and $R1a^{BBS}\Delta SD2R2$ ($P<0.05$) internalised at faster rates. Moreover, the extent of internalisation for $R1a^{BBS}\Delta SD1R2$ (19.2 ± 2 %; n = 9) and $R1a^{BBS}\Delta SD2R2$ (19.4 ± 2.3 %; n = 12; Fig 5.5*D*) were similar to $R1b^{BBS}R2$ and significantly greater compared to $R1a^{BBS}R2$ ($P<0.01$). These results suggest that the slower internalisation profiles conferred by the SDs on R1aR2 require both SD1 and SD2. SDs are known to interact with a wide range of proteins in the extracellular matrix (Kirkitadze and Barlow, 2001) and specific protein-protein or protein-lipid interactions involving the SDs in R1a could anchor the R1aR2 receptors on the cell surface enabling them to reside on the cell surface for longer than the R1bR2 receptors.

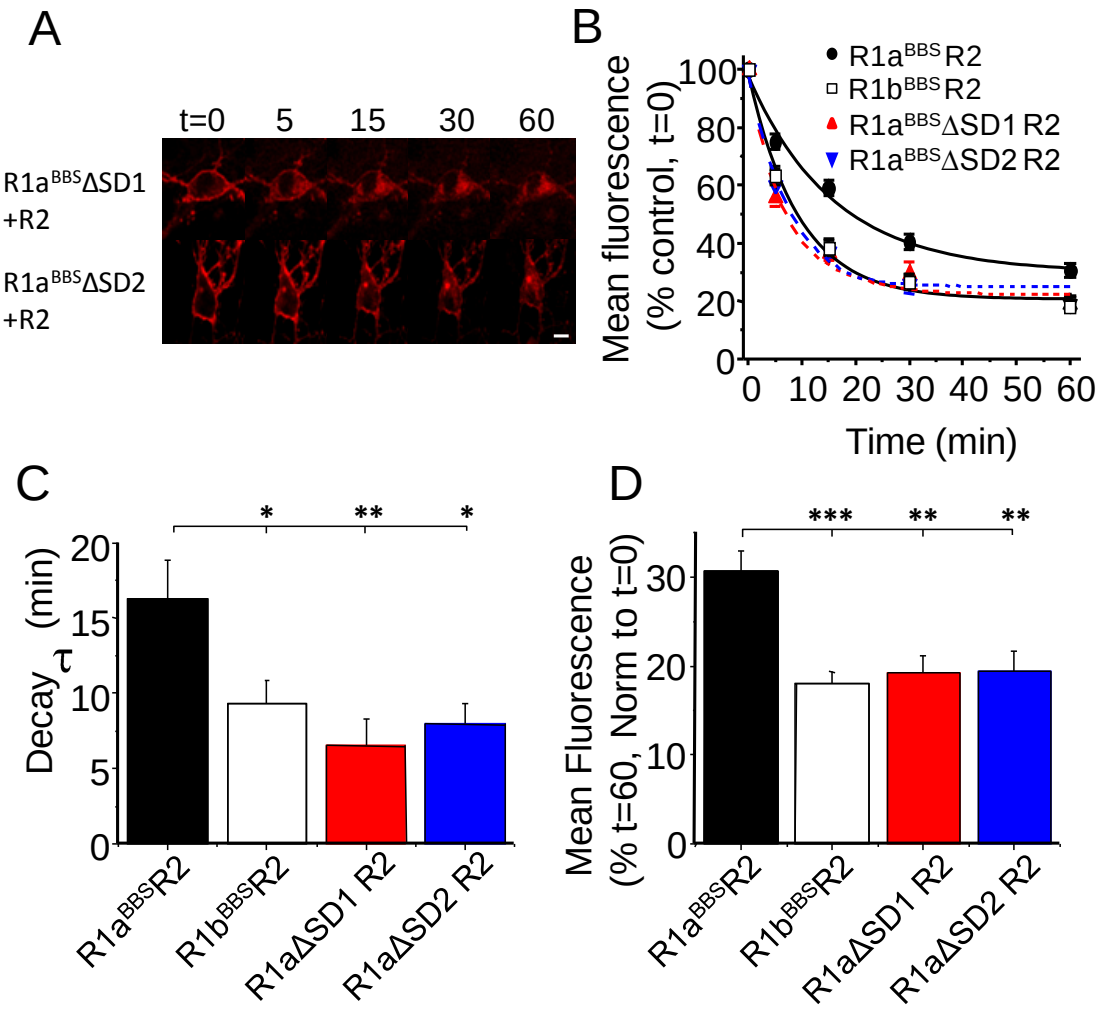

Figure 5.5 - Both SDs in R1a are important for imparting increased stability to R1aR2 receptors.

A, Hippocampal neurons at 14-21 DIV, expressing either R1a^{BBS}ΔSD1 or R1a^{BBS}ΔSD2 with R2 and eGFP were incubated in 1 mM d-TC for followed by 3 µg/ml BTX-AF555 for 10 min at RT and imaged at different time points at 30-32°C. *B,* Rates of constitutive internalisation of BTX-AF555 tagged R1a^{BBS}R2 (●), R1b^{BBS}R2 (□), R1a^{BBS}ΔSD1 R2 (▲), and R1a^{BBS}ΔSD2 R2 (▼) receptors (n = 7-12). *C,* Exponential decay time constants for the rate of decay of membrane fluorescence of R1a^{BBS}R2, R1b^{BBS}R2, R1a^{BBS}ΔSD1R2, and R1a^{BBS}ΔSD2R2 receptors. *D,* Extent of constitutive internalisation of R1a^{BBS}R2, R1b^{BBS}R2, R1a^{BBS}ΔSD1R2, and R1a^{BBS}ΔSD2R2 receptors. *** P<0.001, **P<0.01, *P<0.05, One way ANOVA. Scale bar 10 µm.

5.2.6 SDs stabilise R1aR2 receptors at dendrites and spines

R1aR2 and R1bR2 receptors are located postsynaptically near glutamatergic terminals which can be found opposite dendritic spines. Therefore, the internalisation profiles of R1aR2 and R1bR2 were studied in dendritic spines of unstimulated transfected hippocampal neurons in culture. The spines in these neurons would have basal levels of spontaneous neurotransmitter release and the sodium channel blocker tetrodotoxin was not added as it is unable to block miniature release of neurotransmitters and therefore the unstimulated and unevoked spine activity was considered as basal. In order to study the internalisation of receptors from the spines, dendritic projections with clearly visible spines were isolated and imaged at specific time-points for an hour. A region of interest was drawn around each individual spine from the eGFP image and the mean fluorescence in this region for the BTX-AF555 image was measured. In this way, individual spines fluorescences were monitored for an hour at specific time points. In addition, internalisation from the membrane of dendrites that lack spines was also studied by drawing a region of interest around the dendritic membrane given that here other presynaptic inputs releasing different neurotransmitters are present, eg GABA.

The rate of internalisation for $R1a^{BBS}R2$ (τ = 11.4 ± 3.1 min; n = 78 spines; Fig. 5.6*A, C*) was slower compared to $R1b^{BBS}R2$ (τ = 6.6 ± 1 min; n = 75 spines; P<0.0001; Fig. 5.6*A, C, E*), but interestingly, no differences were observed in the extent of internalisation between $R1a^{BBS}R2$ (32.8 ± 1 %; Fig. 5.6*A, C*) and $R1b^{BBS}R2$ (30.6 ± 1 %; P>0.05; Fig 5.6*A, C, F*) in dendritic spines.

Similar to our results on hippocampal somatic membranes and spines, internalisation of $R1a^{BBS}R2$ was again slower in dendrites than (19.8 ± 1.8 min; n = 13; Fig. 5.6*B, D*) than $R1b^{BBS}R2$ (9.2 ± 0.9 min; n=10; P<0.0001; Fig. 5.6*B, D, E*), but the extent of internalisation was greater for $R1b^{BBS}R2$ (22.8 ± 2.5 %; Fig. 5.*6B, D*) compared to $R1a^{BBS}R2$ (33.4 ± 1.7 %; P< 0.01 Fig 5.6*B, D, F*). This indicates the existence of different trafficking properties for the two $GABA_B$ receptor isoforms in hippocampal postsynaptic membranes.

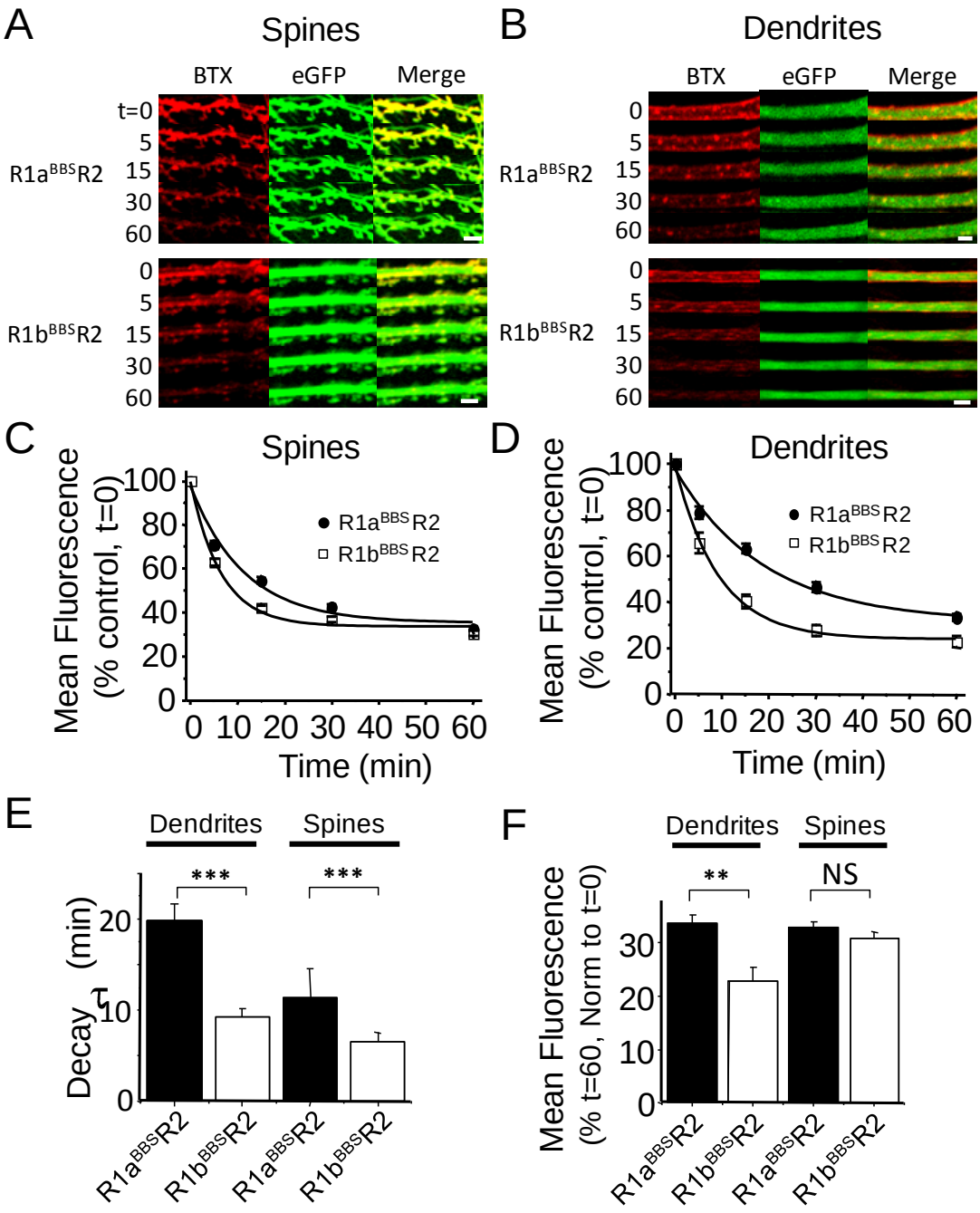

Figure 5.6 – SDs confer increased stability to R1aR2 receptors on dendritic membranes and spines.

A and B, Hippocampal neurons at 14-21 DIV, expressing either $R1a^{BBS}$ or $R1b^{BBS}$ with R2 and eGFP were incubated in 1 mM d-TC followed by 3 µg/ml BTX-AF555 for 10 min at RT and spines (A) or dendrites (B) imaged at different time points at 30-32°C. *C,* Rates of constitutive internalisation of $R1a^{BBS}R2$ (●) and $R1b^{BBS}R2$ (□) on dendritic membranes (n = 10-13). *D,* Rates of constitutive internalisation of $R1a^{BBS}R2$ (●) and $R1b^{BBS}R2$ (□) in spines (n = 75-78). *E,* Exponential decay time constants for the rate of decay of membrane fluorescence of $R1a^{BBS}R2$ and $R1b^{BBS}R2$ receptors in dendrites *(left)* and spines *(right)*. (F) Extent of constitutive internalisation of $R1a^{BBS}R2$ and $R1b^{BBS}R2$ receptors in dendrites *(left)* and spines *(right)*. NS- Not significant, *** P<0.001, ** P<0.01. Scale bar 2 µm.

5.2.7 BBS tag on mGluR2 receptors

To further establish the role of the SDs on receptor trafficking, we inserted these domains into another GPCR, mGluR2, which lacks SDs. mGluR2 was chosen as it is a class-C GPCR and is similar in structure to the $GABA_B$ receptors. In addition, like the $GABA_B$ receptor, it couples to Gαi/o. We first inserted the BBS site 6 amino acids from the N-terminus of mGluR2 ($mGluR2^{BBS}$; Fig 5.7*A*) and then created an $mGluR2^{BBS}$ receptor-SDs chimera ($mGluR2^{BBS}$-SD) in which amino acids G16 to N159 comprising the two SDs of $GABA_B$ receptors were inserted adjacent to the BBS.

Neurons transfected with $mGluR2^{BBS}$ or $mGluR2^{BBS}$-SD bound BTX-AF555 with high specificity (Fig. 5.7B). Live cell imaging of BTX-AF555 tagged $mGluR2^{BBS}$ and $mGluR2^{BBS}$-SD was performed in hippocampal neurons at PT. Compared with both R1aR2 ($P<0.001$) and R1bR2 ($P<0.001$), the $mGluR2^{BBS}$ receptors exhibited increased stability at the cell surface (Fig. 5.7*B, C*), with slower rates (29.8 ± 4.5 min; n = 8, Fig. 5.7*D*) and lower extents (41.2 ± 3; n = 8; Fig 5.7*E*) of internalisation. Over a 1 hr imaging period, only a small amount of fluorescence containing BTX-AF555 was observed to accumulate internally, in comparison to that observed for $GABA_B$ receptors. Significantly, the presence of the two SDs in the chimera, $mGluR2^{BBS}$-SD, increased receptor stability at the surface, reducing the rate of internalisation further (42.3 ± 8 min; n = 7; $P<0.001$; Fig. 5.7 *B-D*) and lowering the extent of internalisation (64.5 ± 2.2 %; n = 7; $P<0.0001$; Fig. 5.7*E*) compared to that for $mGluR2^{BBS}$. These data confirm that the SDs confer increased stability on the $GABA_B$ R1aR2 receptors compared to R1bR2.

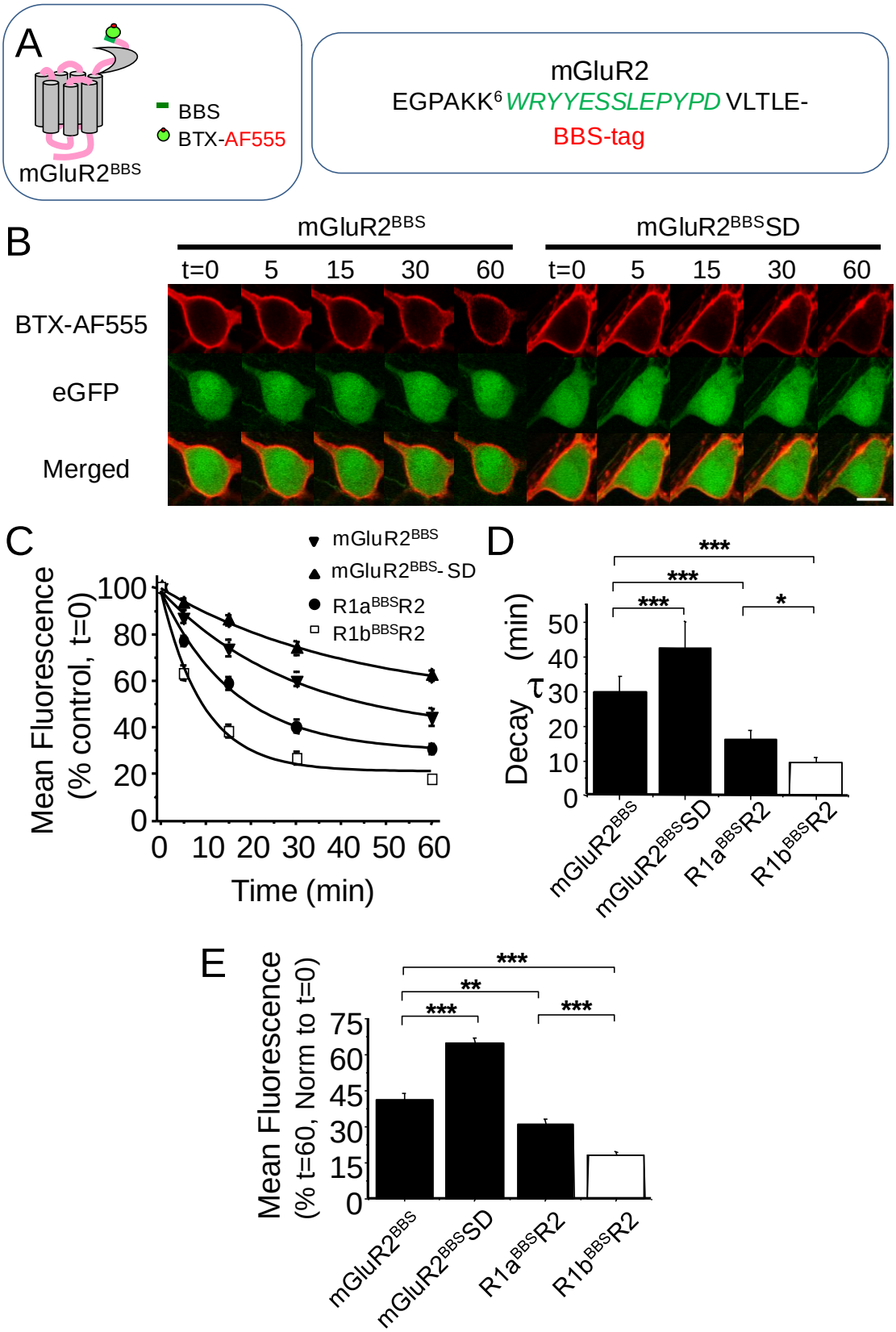

Figure 5.7 –SDs stabilise mGluR2 receptors.
A, Schematic diagram showing the location for the BBS epitope in mGluR2 receptor. The BBS was inserted between Lys6 and Val7. *B,* Hippocampal neurons at 14-21 DIV, expressing either $mGluR2^{BBS}$ or $mGluR2^{BBS}$-SD were incubated in 1 mM d-TC followed by 3 µg/ml BTX-AF555 for 10 min at RT and imaged at different time points at 30-32°C. *C,* Rates of constitutive internalisation of BTX-AF555 tagged $mGluR2^{BBS}$ (▼),

$mGluR2^{BBS}$-SD (▲), $R1a^{BBS}R2$ (●), and $R1b^{BBS}R2$ (□) receptors (n = 7-12). *D,* Exponential decay time constants for the rate of decay of membrane fluorescence of $mGluR2^{BBS}$, $mGluR2^{BBS}$-SD, $R1a^{BBS}R2$, and $R1b^{BBS}R2$ receptors. *E,* Extents of constitutive internalisation of $mGluR2^{BBS}$, $mGluR2^{BBS}$-SD, $R1a^{BBS}R2$, and $R1b^{BBS}R2$ receptors. *** P<0.001, ** P<0.01, * P<0.05. One way ANOVA. Scale bar 10 μm.

5.3 Discussion

By using a BTX-tagging method, distinct trafficking itineraries of the two major subtypes of $GABA_B$ receptors found in the CNS, R1aR2 and R1bR2 has been dissected here. Placing the BBS in the N-terminus of R1b allowed heteromers containing this subunit to be followed in real time in a similar fashion to that previously described for $R1a^{BBS}$ using fluorescently-labelled BTX. While recent studies have focused on the internalisation properties of R1aR2 receptors (Wilkins et al., 2008; Vargas et al., 2008; Grampp et al., 2008; Grampp et al., 2007), R1bR2 receptors have been less characterised. Clearly, the BBS did not alter the functional properties of recombinant $R1b^{BBS}R2$ receptors, assessed using whole-cell patch-clamp electrophysiology. Furthermore, the BTX binding to $R1b^{BBS}$ was of sufficient high affinity to allow the monitoring of the cell surface stability of R1bR2 receptors in hippocampal somatic and dendritic membranes, and also in dendritic spines.

5.3.1 R2 and stabilisation of $GABA_B$ receptors

$GABA_B$ receptors are obligate heterodimers with R1 and R2 subunits playing distinct parts in signalling and trafficking. Recently a new role for R2 in stabilising R1a subunits upon formation of the heterodimer has been reported (Hannan et al., 2011). R2

confers stability by an interaction between its C-terminal tail with a di-leucine motif in the C-terminal coiled-coil domain of R1a. In the present study, R2 clearly performs a similar role for the R1b subunit. This was demonstrated by replacing the ER retention motif, RSR on R1b, for ASA. These $R1b^{BBS\text{-}ASA}$ receptors were expressed on the cell surface and constitutively internalised at a faster rate than $R1b^{BBS}R2$ highlighting the importance of R2 in regulating surface R1bR2. The significance of the di-leucine motif on the R1 coiled-coil domain interacting with the R2 C-terminal tail was emphasised by mutating the di-leucines on $R1b^{BBS\text{-}ASA\text{-}LL}$ to alanines ($R1b^{BBS\text{-}ASA\text{-}AA}$), which slowed the rate of internalisation matching that of $R1b^{BBS}R2$. However, there is an important distinction in the trafficking behaviour between R1a and R1b - the extent of internalisation of $R1b^{BBS\text{-}ASA}$ was similar to $R1b^{BBS}R2$, differing from $R1a^{BBS\text{-}ASA}$, which internalised to a greater extent than $R1a^{BBS}R2$. Given that the major structural difference between R1a and R1b are the two SDs in R1a, this implied that these domains impart additional stability upon R1aR2 receptors compared to Rb1R2.

5.3.2 SDs regulate $GABA_B$ receptor trafficking

The different cell surface stabilities of R1aR2 and R1bR2 receptors in hippocampal neurons required the presence of both SDs in the R1a subunit as deletions of either SD promoted internalisation profiles indistinguishable from R1bR2 receptors.

The importance of the SDs for receptor trafficking extends beyond $GABA_B$ receptors. This was revealed by inserting a BBS into the N-terminus of another class C GPCR, the mGluR2 receptor, which does not contain innate SDs, but otherwise closely resembles

$GABA_B$ receptors (Pin et al., 2003; Pin et al., 2009). Notably, $mGluR2^{BBS}$ receptors internalised slower from the cell surface compared to either subtype of $GABA_B$ receptor, both in terms of rates and extents of internalisation, suggesting the existence of diverse trafficking mechanisms within the class C GPCR family. The insertion of the two SDs rendered increased stability to $mGluR2^{BBS-SD}$ confirming their role in stabilising surface $GABA_B$ R1aR2 receptors.

The mechanism by which SDs stabilise R1aR2 and the chimeric mGluR2 is unknown. Given the N-terminal location of the SDs, it is likely that protein-protein or protein-lipid interactions in the extracellular matrix are important.

The SDs in R1a have been previously noted for their importance in differential subcellular targeting of R1aR2 compared to R1bR2 receptors (Vigot et al., 2006). The SDs form an axonal targeting signal for the preferential transport of R1aR2 receptors, although R1aR2 and R1bR2 receptors can also be found in the soma and dendrites (Biermann et al., 2010). The interacting partners that are important for axonal targeting have not been identified. However, similar to their stabilising role for R1a, the presence of both SDs are an absolute requirement. It is possible that the SDs may interact across the subunits in the R1aR2 heteromer enabling SD1-SD2 to stabilise the larger oligomeric complex on the cell surface.

Generally, SDs are well known to engage in specific protein-protein interactions and their role in the immune system has been relatively well characterised (Kirkitadze and Barlow, 2001). The two SDs in R1a are atypical in structure to the rest of the SD family and the SD1 of R1a is less compact in structure than SD2 (Blein et al., 2004). SD1 interacts with the extracellular matrix protein fibulin-2 in vitro. In addition to this, a

soluble excreted isoform of part of the R1a subunit, R1j, is mostly comprised of the two SDs. This protein inhibits the function of $GABA_B$ heteroreceptors and recognises binding partners on neuronal membranes although the sites of attachment have not been identified (Tiao et al., 2008). The mechanism by which internalisation is slowed could involve specific protein-protein or protein-lipid interactions involving the SDs in R1a that anchor the R1aR2 receptors on the cell surface and enable them to reside on the plasma membrane longer compared to the R1bR2 receptors. In addition, the interaction between the SDs of R1aR2 heteromers could also alter the oligomeric states of the R1aR2 receptors and therefore make them more resistant to internalisation. The mechanism by which the SDs would decrease the rate of internalisation and increase the extent of internalisation in R1aR2 is of interest and could be studied further in the future.

It is therefore likely that the SDs interact with other proteins that could modulate the signalling and trafficking of $GABA_B$ R1aR2 receptors. To this end, R1j has recently been reported in humans (Lee et al., 2010).

5.3.3 Physiological consequences

Presynaptic $GABA_B$ receptors are classified into autoreceptors- or heteroreceptors depending on whether they inhibit the release of GABA or glutamate respectively. This is achieved by inhibition of VGCCs (Bettler and Tiao, 2006; Bettler et al., 2004). Due to preferential targeting, R1aR2 receptors are considered more abundant at axon terminals, specifically glutamatergic terminals, where the effectively inhibit Ca^{2+} influx

(Guetg et al., 2009; Vigot et al., 2006). By contrast, at postsynaptic sites, both R1aR2 and R1bR2 appear similarly effective at activating GIRK currents (Guetg et al., 2009). Significantly, R1aR2 presynaptic heteroreceptors are selectively activated by low concentrations of baclofen to reduce glutamate release (Guetg et al., 2009). The role of the SDs in stabilising the R1aR2 subtype at the cell surface would ensure this population of presynaptic $GABA_B$ receptors are not easily internalised acting as a brake against uncontrolled release of glutamate during excitotoxicity. Indeed, presynaptic $GABA_B$ receptors reduce multivesicular glutamate release (Chalifoux and Carter, 2010) specifically reducing synaptic levels of glutamate that will affect the amplitude of excitatory postsynaptic potentials (EPSPs).

By contrast, at postsynaptic sites, the R1bR2 subtype, at least in layer 5 neocortical neurons, is mostly responsible for Ca^{2+} spike inhibition (Perez-Garci et al., 2006). Given the propensity for the R1bR2 subtype to internalise to a greater extent compared to R1aR2 receptors, this would allow the development of postsynaptic NMDA-receptor mediated synaptic plasticity (Terunuma et al., 2010; Guetg et al., 2010) under physiological conditions. However, under extreme pathophysiological conditions, the increased internalisation of R1bR2 may contribute to neurotoxicity.

Clearly R1aR2 receptors will also be present at postsynaptic (extrasynaptic) sites, and these will be capable of ameliorating excessive glutamate-mediated excitation. However, in the neck of the dendritic spines, very near the crucial locus of glutamatergic afferents, R1aR2 receptors are not more stable at the cell surface compared to R1bR2 receptors. This surprising difference, compared with R1aR2 receptors elsewhere, would also facilitate glutamate-mediated synaptic plasticity. It

would also increase Ca^{2+} influx via NMDA channels by limiting the $GABA_B$ receptor-mediated inhibition of PKA, presumably promoting phosphorylation of NMDA receptors (Chalifoux and Carter, 2010; Chalifoux and Carter, 2011) and resulting plasticity. This important caveat in terms of R1a stability also implies that whatever proteins the R1a subunit SDs are interacting with at the cell surface, these must be absent in or closely-around dendritic spines.

Thus by exercising fine control over $GABA_B$ receptor trafficking through the R1a subunit and its associated SDs, fine tuning of local glutamate-mediated synaptic plasticity is enabled without the need to alter the trafficking dynamics of $GABA_B$ receptors all over the cell surface.

5.4 Summary

- The BBS approach can be used to study the trafficking of R1b subunits
- R2 subunits stabilse R1b subunits on the cell surface by interacting with a di-leucine motif in the C-terminal coiled-coil domain
- R1aR2 receptors are more stable than R1bR2 receptors in hippocampal neurons
- SDs confer increased stability to R1aR2 receptors
- Both SDs are required for R1aR2 receptors to be more stable on the cells surface
- mGluR2 receptors are more stable on the cell surface than $GABA_B$ receptors
- SDs can impart increased stability to mGluR2 receptors

Chapter VI

Lateral mobility of single $GABA_B$ receptors

6.1 Introduction

In addition to endocytosis and insertion of newly synthesized or recycling receptors, movement of receptors in the plane of the cell membrane by lateral diffusion provides an important means of regulating signalling efficacy during synaptic transmission (Triller and Choquet, 2008; Triller and Choquet, 2005; Triller and Choquet, 2003). The lateral mobility of neuronal $GABA_B$ receptors so far has received little attention, particularly around synaptic compartments. The only known report of $GABA_B$ receptor lateral mobility, based on FRAP, demonstrated that $GABA_B$ R1bR2 receptors move very slowly on the surface of COS-7 cells and hippocampal neurons in culture, and that a stretch of 24 amino acids from 862 to 886 on the C-terminal tail of R2 acts controls lateral mobility in COS-7 cells (Pooler and McIlhinney, 2007). Chronic (1 hr) treatment with 100 µM baclofen was reported to increase the lateral mobility of R1bR2 receptors on COS-7 cells although the effect of baclofen on R1aR2 receptors, and more importantly the effect of baclofen on $GABA_B$ receptors in neurons, has not been reported thus far. Disruption of the cytoskeleton with the actin polymerisation blocker latrunculin and tubulin polymerisation blocker colchicine has been reported to have no effect on the lateral mobility of $GABA_B$ R2 subunits in COS-7 cells. However, the effect

of disrupting the cytoskeleton on the lateral mobility of $GABA_B$ heteromers has not been studied (Pooler and McIlhinney, 2007).

SPT of receptors using QD nano-particles allows the lateral mobility of single receptors on the cell surface to be studied. To date, this has not been applied to single $GABA_B$ receptors. Receptor numbers, in and around synaptic compartments is especially important for signalling efficacy. Recently a BTX based approach was used to study SPT of α7 (Burli et al., 2010; Fernandes et al., 2010) and α3 (Fernandes et al., 2010) nicotinic AChRs. Here, the BBS tagging strategy was extended to study the mobility of single $GABA_B$ R1aR2 and R1bR2 receptors in hippocampal neurons in culture using QDs to identify factors that influenced the lateral mobility of $GABA_B$ receptors.

6.2 Results

6.2.1 Specificity of QDs labelling of $GABA_B$ receptors

$GABA_B$ ($R1a^{BBS}R2$/ $R1b^{BBS}R2$) receptors containing the BBS site were labelled with QD655-streptavidin (QD655) via biotinylated BTX (BTX-B) (Fig. 6.1A) and the specificity of labelling studied in hippocampal neurons in culture at 14-16 DIV. Neurons transfected with $R1a^{BBS}$ or $R1b^{BBS}$ with R2 and eGFP pre-incubated in 1 mM d-TC for 5 min were incubated in 2 µg/ml BTX-B for 2 min followed by 10 pM QD655 for 1 min at 37°C. After washing off the excess QD655 the cells were fixed and imaged (Fig. 6.1B). At 10 pM QD655 (Fig 6.1B), QD staining was only observed for both $R1a^{BBS}R2$ and $R1b^{BBS}R2$ in neurons that also contained eGFP although some small amounts of non-specific labelling was observed at higher concentrations of QD655 (data not shown). Such non-specific interactions of QDs are quite possibly due to interactions of the polyethylene glycol linkers and the nanoparticles with living tissue and have been observed by other groups (personal communication - Antoine Triller). Therefore, all subsequent experiments were carried out at a QD655 concentration of 10 pM. In order to further verify that the QD labelling to the BBS containing receptors was specific, cells transfected with $R1a^{BBS}R2$ and eGFP were pre-incubated in 1 mM d-TC for 5 min and incubated in 2 µg/ml unlabelled BTX for 2 min at 37°C followed by 10 pM QD655 for 1 min at 37°C, washed, fixed and imaged (Fig. 6.1B). These cells were not treated with BTX-B that links the QD655s to BBS and therefore as expected no QD655 staining was observed (Fig. 6.1B). In addition, eGFP transfected cells were pre-incubated in 1 mM d-TC for 5 min and incubated in 2 µg/ml unlabelled BTX for 2 min at 37°C followed by 10 pM QD655 for 1 min at 37°C, washed, fixed and imaged (Fig. 6.1B). These cells

also did not label with QD655 as the cells did not express a BBS tagged receptor (Fig. 6.1B) thereby validating the suitability of the BBS approach for tagging $GABA_B$ receptors with QDs.

The variations in the images of dendrites observed in Fig. 6.1B is possibly due to the wide variation that exists in neuronal morphology within cells of the same culture and in addition cells from different cultures. While utmost efforts were made to standardise the conditions of cultures including the media, maintenance of cultures and transfections such variations are difficult to avoid and are likely to be due to differences in the specific microenvironments to which individual neurons are exposed to on a coverslip during their development. However, such variations in conditions are unlikely to effect the interpretation of the specificity of binding as at low concentrations of QD655, very little non-specific binding was observed.

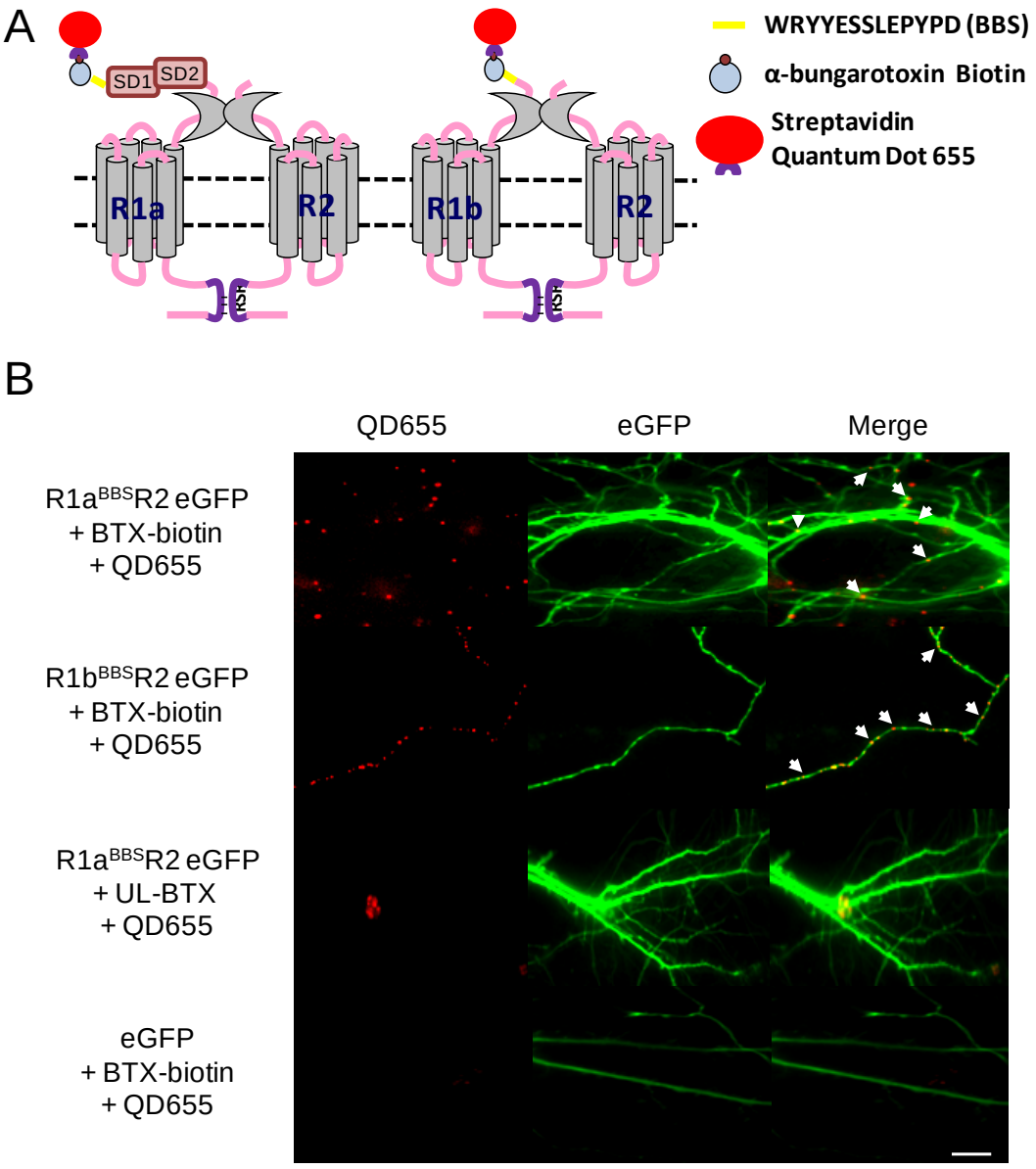

Figure 6.1 – Specific labelling of $GABA_B$ receptors with QDs.

A, Schematic diagram showing the QD labelling technique of BBS containing $GABA_B$ $R1a^{BBS}R2$ and $R1b^{BBS}R2$ receptors. *B*, Images of hippocampal neurons in culture expressing eGFP with or without $R1a^{BBS}R2$/ $R1b^{BBS}R2$ pre-incubated with 1 mM d-TC for 5 min followed by 2 µg/ml of either biotinylated BTX (BTX-B) or unlabelled BTX (UL-BTX) at 37°C for 2 min and 10 pM Quantum Dot 655- streptavidin (QD655) for 1 min at 37°C. QDs have been shown with arrows

6.2.2 Lateral mobility of $GABA_B$ receptors on hippocampal neurons

Having established, that the BBS containing $GABA_B$ receptors could be specifically labelled using QD655 and BTX-B, the lateral mobility of $GABA_B$ R1a^{BBS}R2 and R1b^{BBS}R2 receptors was studied in cultured hippocampal neurons. Cells expressing R1a^{BBS}/ R1b^{BBS}, R2 and eGFP pre-incubated in 1 mM d-TC for 5 min, were incubated in 2 µg/ml BTX-B for 2 min followed by 10 pM QD655 for 1 min at 37°C. After washing off the excess QD655 the cells were mounted on an environmental chamber at 37°C and an image series obtained at 33 Hz.

R1a^{BBS}R2 receptors were more mobile with longer and less confined trajectories and compared to R1b^{BBS}R2 receptors (Fig. 6.2A-B). R1a^{BBS}R2 receptors had a higher median diffusion coefficient, *D*, (0.12 $\mu m^2 s^{-1}$, n = 1529; Fig. 6.2*A, C, D*) compared to R1b^{BBS}R2 receptors (0.07 $\mu m^2 s^{-1}$, n = 804; P<0.001 Mann-Whitney test (MW), Fig. 6.2*B, C, D*). In addition R1a^{BBS}R2 receptors were less confined than R1b^{BBS}R2 receptors as suggested from the plateau phases of the MSD plot (Fig. 6.2E).

Together these results suggest a dominant role for the SDs in determining the lateral mobility of $GABA_B$ R1aR2 receptors as these are the major structural differences between R1a and R1b.

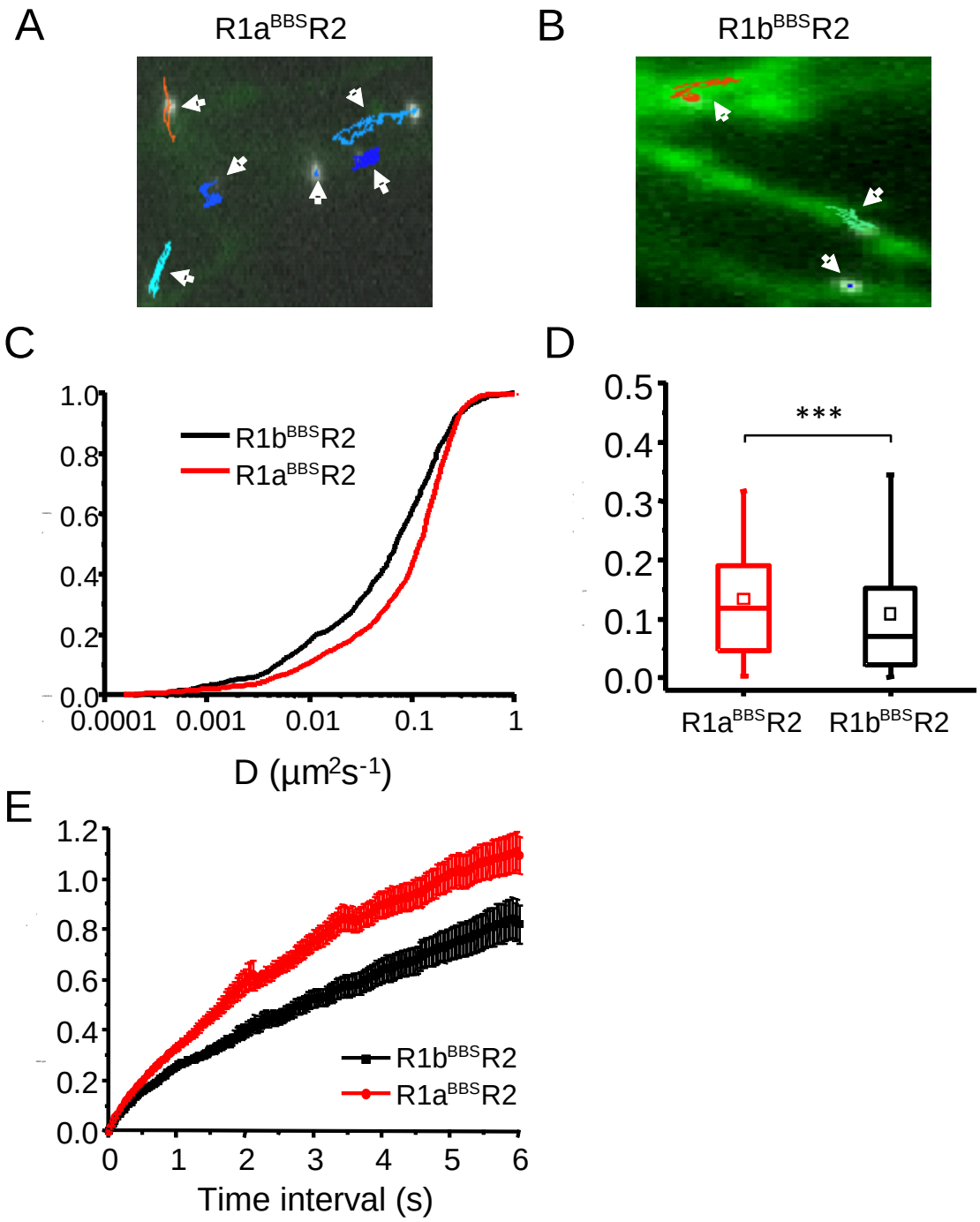

Figure 6.2 – SPT of $GABA_B$ receptor on hippocampal neurons.

A and B, Hippocampal neurons expressing eGFP and R1a^{BBS}R2 (A) or R1b^{BBS}R2 (B) receptors were incubated with d-TC for 5 min , followed by 2 µg/ml BTX-B at 37°C for 2 min and 10 pM QD655 for 1 min at 37°C and imaged. Single QD655 particles were tracked and their trajectories have been shown with different colours on an eGFP background which are the dendrites. *C,* Cumulative probability distribution of Diffusion coefficients, D, R1a^{BBS}R2 (red) and R1b^{BBS}R2 (black). *D,* Distribution of D values (Median, 25-75% interquartile range, mean (square), whiskers = 5 and 95% confidence intervals) for R1a^{BBS}R2 (red) and R1b^{BBS}R2 (red) receptors. *** P<0.001 MW test. *E,*

Averaged MSD plot (mean ± SEM) of the same trajectories analyzed in *C.* Trajectories have been shown with arrows

6.2.3 Agonist induced lateral mobility of $GABA_B$ receptors

Chronic stimulation of $GABA_B$ R1bR2 receptors with baclofen (100 µM for 1 hr) has been reported to increase the lateral mobility of these receptors in COS-7 cells (Pooler and McIlhinney, 2007). Since, $GABA_B$ receptors in physiological conditions are unlikely to encounter such high levels of agonist over a such a prolonged period of time, SPT was used to study the lateral mobility of $GABA_B$ R1a^{BBS}R2 and R1b^{BBS}R2 receptors in hippocampal neurons in response to agonist activation during imaging. Cells expressing R1a^{BBS} or R1b^{BBS} with R2 and eGFP were pre-incubated in 1 mM d-TC for 5 min, then incubated in 2 µg/ml BTX-B for 2 min followed by 10 pM QD655 for 1 min at 37°C. After washing off the excess QD655 the cells were mounted on an environmental chamber in 100 µM baclofen at 37°C and imaged.

In response to stimulation with 100 µM baclofen, R1a^{BBS}R2 receptors explored the cell surface of hippocampal neurons with a lower median *D*, (0.103 $\mu m^2 s^{-1}$, n = 3262; P<0.001 MW; Fig. 6.3*A, D*) compared to untreated R1a^{BBS}R2 controls. In contrast, R1b^{BBS}R2 receptors explored the cell surface of hippocampal neurons with a higher median *D*, (0.09 $\mu m^2 s^{-1}$, n=3061, P<0.001 MW; Fig. 6.2*B, D)* in response to stimulation with 100 µM baclofen compared to untreated R1b^{BBS}R2. Statistical significance in this part and the rest of this chapter was calculated by first running a Kolmogorov-Smirnov test for normal distribution. In all the cases, the data did not fit to normal distribution profiles and therefore the Mann-Whitney U tests for non parametric data was applied

to the distribution of D values. This test compares the median D values between datasets for look statistical significance of the differences observed between the values. The data has been presented in the form of box-plots with the open squares representing the means of the datasets.

Even though, 100 µM baclofen slowed down $R1a^{BBS}R2$ receptors and speeded up $R1b^{BBS}R2$ receptors, the median D of $R1a^{BBS}R2$ in the presence of 100 µM baclofen was still higher than the median D of $R1b^{BBS}R2$ in the presence of 100 µM baclofen ($P<0.01$ MW; Fig. 6.2*C, D*) suggesting that these two types of receptors have very distinct lateral mobility profiles both in the presence and absence of agonist activation.

100 µM baclofen did not alter the confinement of $R1a^{BBS}R2$ receptors (Fig. 6.3E) or $R1b^{BBS}R2$ receptors (Fig. 6.3F) compared to untreated control, and in the presence of the agonist $R1a^{BBS}R2$ receptors remained less confined than $R1b^{BBS}R2$ receptors (Fig. 6.2G).

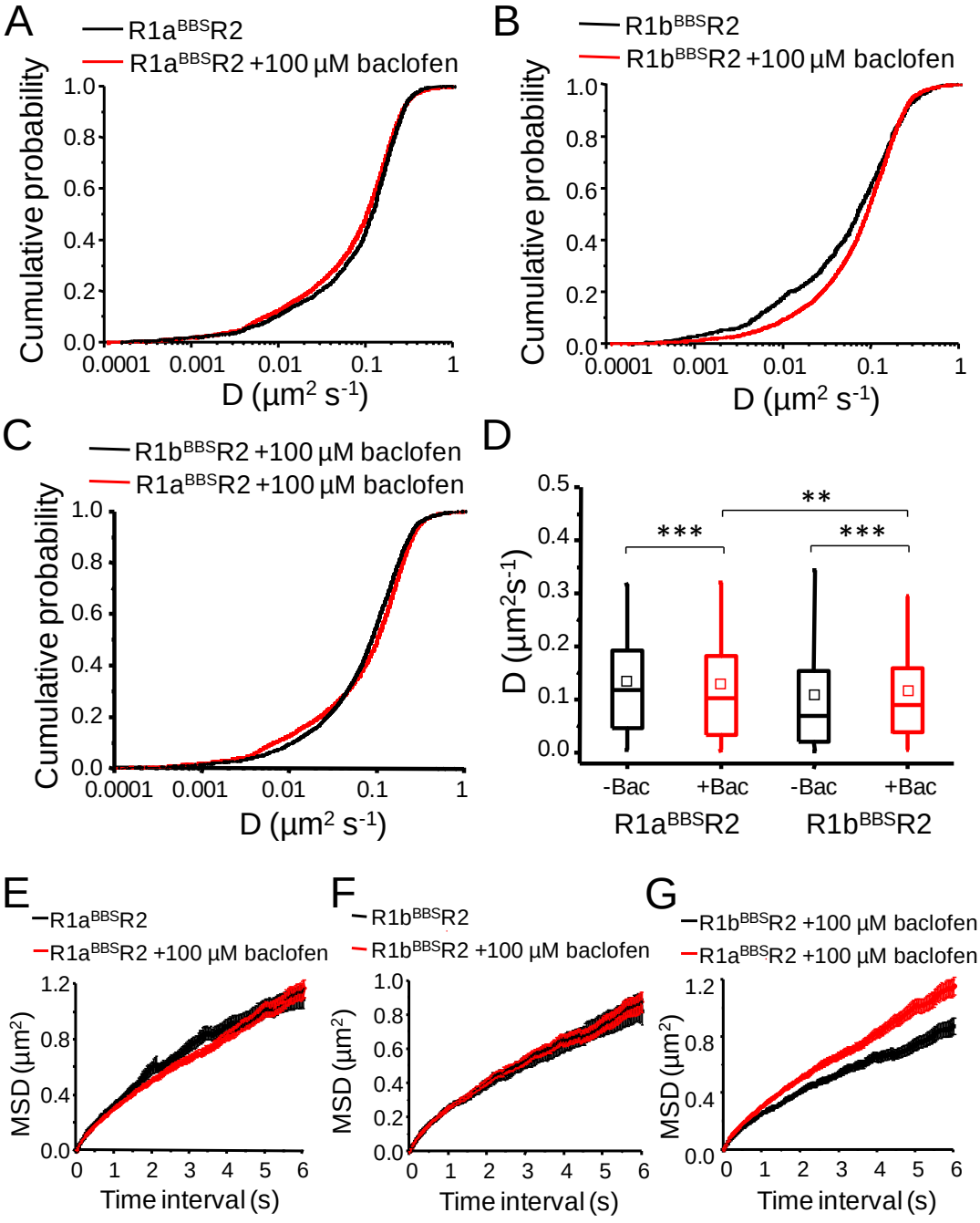

Figure 6.3 – Agonist induced lateral mobility of $GABA_B$ receptors.

A and B, Cumulative probability distribution of diffusion coefficients, D, of hippocampal neurons expressing eGFP and R1a^{BBS}R2 (A) or R1b^{BBS}R2, (B) receptors incubated with d-TC for 5 min, followed by 2 µg/ml BTX-B at 37°C for 2 min and 10 pM QD655 for 1 min at 37°C and imaged in 100 µM baclofen (red) or in Krebs (black). *C*, Cumulative probability distribution of D of R1a^{BBS}R2 (red) and R1b^{BBS}R2 (black) imaged in 100 µM baclofen. *D*, Distribution of D values (Median, 25-75% interquartile range, mean (square), whisker = 5 and 95% confidence intervals) for R1a^{BBS}R2 and R1b^{BBS}R2 receptors imaged in 100 µM baclofen (+bac/ red) or in control Krebs (-bac/ black). *** P<0.001, **P<0.01 MW test. *E,* Averaged MSD plot (mean ± SEM) of R1a^{BBS}R2 receptors in 100 µM baclofen (red) or in Krebs (black). *F*, Averaged MSD plot (mean ± SEM) of R1b^{BBS}R2 receptors in 100 µM baclofen (red) or in Krebs (black). *G*, Averaged

MSD plot (mean ± SEM) of $R1a^{BBS}R2$ receptors (red) and $R1b^{BBS}R2$ receptors (black) in 100 µM baclofen.

6.2.3 Lateral mobility of $GABA_B$ receptors at presynaptic terminals

Having studied the lateral mobility of ensembles of $GABA_B$ receptors on hippocampal neurons, the SPT technique was extended to study the lateral mobility of these receptors in and around presynaptic terminals containing labelled synaptophysin (Tarsa and Goda, 2002) in order to study the lateral mobility of this particular population of $GABA_B$ receptors. R1aR2 receptors have been described to be abundant in presynaptic glutamatergic terminals in addition to being targeted preferentially to axons compared to R1bR2 receptors (Biermann et al., 2010). Although the SDs mediate this preferential targeting, R1bR2 receptors traffic to the axons in smaller quantities (Biermann et al., 2010). Cells expressing $R1a^{BBS}$ or $R1b^{BBS}$ with R2 and synaptophysin-eGFP, pre-incubated in 1 mM d-TC for 5 min, were incubated in 2 µg/ml BTX-B for 2 min followed by 10 pM QD655 for 1 min at 37°C. After washing off the excess QD655 the cells were mounted on an environmental chamber at 37°C and imaged.

$R1a^{BBS}R2$ receptors were found mainly in extrasynaptic areas (defined as extrasynaptic; Fig. 6.4A) around synaptophysin terminals with 74% (1702/2301) of the receptors only found in extrasynaptic areas, whereas 12% (284/2301) of the QDs colocalised with synaptophysin and remained confined within clusters (classed as presynaptic; Fig. 6.4A) and the remaining 14% (315/2301) of the receptors moved between extra- and presynaptic areas (defined as exchanging; Fig. 6.4A). This suggests that a proportion of $R1a^{BBS}R2$ receptors are recruited to synaptophysin containing presynaptic terminals.

Extrasynaptic $R1a^{BBS}R2$ receptors were more mobile with a higher median D (0.124 $\mu m^2 s^{-1}$, n = 1834) than presynaptic $R1a^{BBS}R2$ receptors (0.078 $\mu m^2 s^{-1}$, n = 445, P<0.001 MW; Fig. 6.4B). Of the receptors that exchanged between presynaptic and extrasynaptic compartments, the average transition from presynaptic-to-extrasynaptic areas was 51% (160/315) and from extrasynaptic-to-presynaptic areas was 43% (135/315). In addition to being less mobile, the presynaptic $R1a^{BBS}R2$ receptors were more confined than extrasynaptic $R1a^{BBS}R2$ receptors (Fig. 6.4E). Such large variations from Brownian motion, observed with synaptic $R1a^{BBS}R2$ receptors, is either due to high apparent viscosity of the presynaptic terminal or due to an interaction of $R1a^{BBS}R2$ receptors with proteins that cause them to slow down at synapses or a combination of the two.

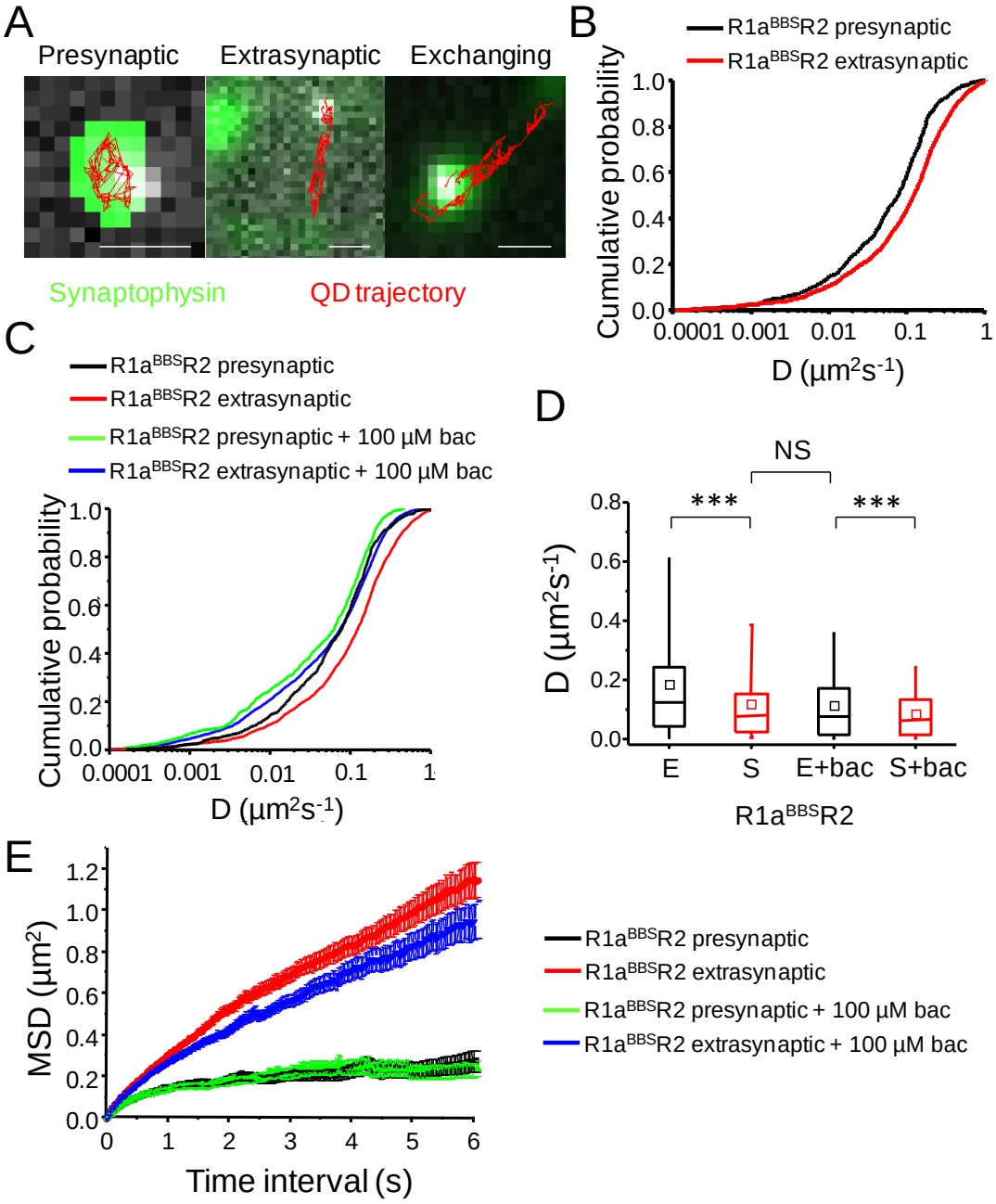

Figure 6.4 – Lateral mobility of R1a^{BBS}R2 at presynaptic terminals.
A, Examples of presynaptic, extrasynaptic and exchanging trajectories (red) around presynaptic terminals (green) of hippocampal neurons expressing R1a^{BBS}R2 and synaptophysin-eGFP incubated with 1 mM d-TC for 5 min , followed by 2 µg/ml BTX-B for 2 min and 10 pM QD655 for 1 min at 37°C and imaged. Scale bars 1 µm. *B*, Cumulative probability distribution of diffusion coefficients for R1a^{BBS}R2 receptors in synaptic (black) and extrasynaptic (red) areas. *C*, Cumulative probability distribution of diffusion coefficients (D) of synaptic (black) and extrasynaptic (red) R1a^{BBS}R2 receptors in Krebs, and synaptic (green) and extrasynaptic (blue) R1a^{BBS}R2 receptors in the presence of 100 µM baclofen. *D*, Distribution of D values (Median, 25-75% interquartile range, mean (square), whisker = 5 and 95% confidence intervals) for synaptic (S/ red) and extrasynaptic (E/ black) R1a^{BBS}R2 receptors in the presence of 100 µM baclofen (+bac) or in Krebs. *** P<0.001, NS – not significant MW test. *E,* Averaged MSD plot (mean ± SEM) of synaptic (black) and extrasynaptic (red) R1a^{BBS}R2 receptors

in control Krebs and synaptic (green) and extrasynaptic (blue) $R1a^{BBS}R2$ receptors in the presence of 100 µM baclofen

The effect of agonist treatment on the lateral mobility of $R1a^{BBS}R2$ receptors was studied in the presence of 100 µM baclofen and compared to untreated controls. Baclofen did not alter the relative localisation of $R1a^{BBS}R2$ receptors with 79% (2658/3381) found in extrasynaptic areas, 12% (415/3381) colocalised with synaptophysin, and 9% (308/3381) of the receptors exchanged fractions between extra- and presynaptic clusters. As observed with the untreated controls, extrasynaptic $R1a^{BBS}R2$ receptors were more mobile with a higher median D (0.075 $\mu m^2 s^{-1}$, n = 2741) than presynaptic $R1a^{BBS}R2$ receptors (0.063 $\mu m^2 s^{-1}$, n = 516; Fig. 6.3C, D; $P<0.001$ MW) in the presence of baclofen. However, baclofen decreased the mobility of extrasynaptic ($P<0.001$ MW) as well as presynaptic receptors ($P<0.001$ MW) compared to controls in Krebs with the extrasynaptic receptors showing a more pronounced retardation in mobility. There was no difference ($P>0.05$ MW test) between the diffusion coefficients of presynaptic $R1a^{BBS}R2$ receptors in control Krebs and extrasynaptic $R1a^{BBS}R2$ receptors treated in baclofen. In addition, fewer transitions between presynaptic and extrasynaptic compartments were observed in response to baclofen treatment compared to untreated controls. In presence of baclofen, the average transition from presynaptic-to- extrasynaptic areas was 34% (104/308) and extrasynaptic-to-presynaptic areas was 33% (101/308). Baclofen did not alter the confinement of $R1a^{BBS}R2$ receptors compared to untreated controls in Krebs (Fig. 6.4E).

Next, the lateral mobility of $R1b^{BBS}R2$ receptors was studied around synaptophysin containing presynaptic terminals. Similar to $R1a^{BBS}R2$ receptors, $R1b^{BBS}R2$ receptors were found mainly in extrasynaptic areas around synaptophysin terminals with 71% (1109/1553) of the QDs found only in extrasynaptic areas whereas 11% (174/1553) colocalised with synaptophysin and remained confined within clusters, and 23% (270/ 1153) of the receptors exchanged fractions between extra- and presynaptic clusters. This suggests that a proportion of $GABA_B$ $R1b^{BBS}R2$ receptors are also recruited to presynaptic terminals. Similar to $R1a^{BBS}R2$ receptors, extrasynaptic $R1b^{BBS}R2$ receptors were more mobile with higher median D (0.129 $\mu m^2 s^{-1}$, n = 1206) than presynaptic $R1b^{BBS}R2$ receptors (0.108 $\mu m^2 s^{-1}$, n=278, $P<0.01$ MW; Fig. 6.5A, B). The average transition between synaptic and extrasynaptic areas was 39% (104/270) and extrasynaptic and presynaptic areas were 37% (100/270). In addition to being less mobile, presynaptic $R1b^{BBS}R2$ receptors were more confined than extrasynaptic $R1b^{BBS}R2$ receptors (Fig. 6.5C).

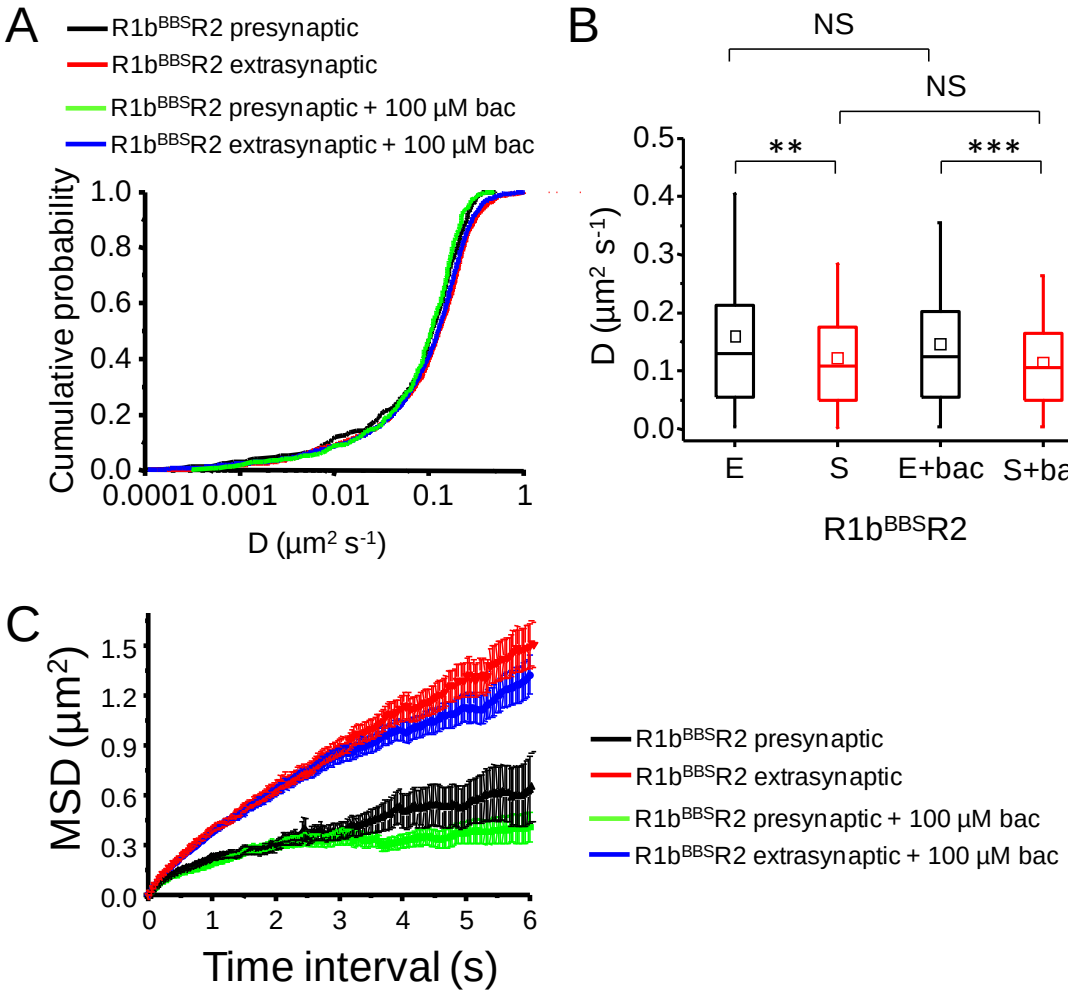

Figure 6.5 – Lateral mobility of R1b^{BBS}R2 at presynaptic terminals.
A, Cumulative probability distribution of diffusion coefficients (D) of presynaptic (black) and extrasynaptic (red) R1b^{BBS}R2 receptors in Krebs and synaptic (green) and extrasynaptic (blue) R1b^{BBS}R2 receptors in the presence of 100 µM baclofen. Hippocampal neurons expressing R1b^{BBS}R2 and synaptophysin-eGFP were incubated with 1 mM d-TC for 5 min , followed by 2 µg/ml BTX-B for 2 min and 10 pM QD655 for 1 min at 37°C and imaged in the presence of 100 µM baclofen or control Krebs. *B*, Distribution of D values (Median, 25-75% interquartile range, mean (square), whisker = 5 and 95% confidence intervals) for synaptic (S/ red) and extrasynaptic (E/ black) R1a^{BBS}R2 receptors in the presence of 100 µM baclofen (+bac) or in Krebs. ** P<0.01, *** P<0.001, NS – not significant MW. *C,* Averaged MSD plot (mean ± SEM) of synaptic (black) and extrasynaptic (red) R1b^{BBS}R2 receptors in control Krebs and synaptic (green) and extrasynaptic (blue) R1b^{BBS}R2 receptors in the presence of 100 µM baclofen

The effect of agonist on the lateral mobility of $R1b^{BBS}R2$ receptors was studied in the presence of 100 µM baclofen and baclofen did not alter the localisations of $R1b^{BBS}R2$ receptors with 75% (1714/2284) of the receptors present in extrasynaptic areas, 12% (278/ 2284) present in synaptophysin clusters, and 13% (292/ 2284) exchanging fractions between presynaptic and extrasynaptic compartments. As observed for untreated controls, extrasynaptic $R1b^{BBS}R2$ receptors were more mobile with higher median D (0.125 $\mu m^2 s^{-1}$, n = 1815) than presynaptic $R1b^{BBS}R2$ receptors (0.106 $\mu m^2 s^{-1}$, n = 398, P<0.001 MW; Fig. 6.5A, B) in the presence of baclofen. However, baclofen had no effect on diffusion coefficients of extrasynaptic (P>0.05; Fig. 6.5B) or presynaptic (P>0.05; 6.5B) $R1b^{BBS}R2$ receptors around synaptophysin clusters compared to untreated controls. In addition, there was no difference between the transitions between receptors that exchanged between presynaptic and extrasynaptic portions. The average transition from synaptic-to-extrasynaptic areas was 41% (121/292) and extrasynaptic-to-presynaptic areas was 35% (102/292). The confinement of receptors was also unchanged in response to baclofen treatment (Fig. 6.5C).

6.3 Discussion

Here, the BBS strategy has been extended once more to study the lateral mobility of single $GABA_B$ receptors on hippocampal neurons. The specificity of $GABA_B$ receptor-QD reaction was demonstrated in neurons where no labelling of BBS containing receptors was observed in the presence of UL-BTX and in the absence of BTX-B. The

ability to specifically label single $GABA_B$ receptors allowed SPT of receptors in real time in order to discriminate factors that affect the lateral mobility of $GABA_B$ receptors.

One issue that has been controversial is whether the 10-30 nm QDs can access the active zones membranes of synapses. The synaptic cleft has been estimated to be around 30 nm (Landis et al., 1988) and it is likely that the smaller QDs could access this space when attached to the extracellular portion of receptors. One study has used transmission electron microscopy to report the localisation of QDs within the synaptic cleft (Dahan et al., 2003) whereas another study has found a difference between synaptic diffusion coefficients of glycine receptors calculated using QDs and the organic dye Cy3 (Groc et al., 2004). The diffusion coefficients predicted using QDs were slower than those calculated using Cy3 suggesting that the QDs are under size constraints when they enter the synapse. Given that $GABA_B$ receptors are predominantly perisynaptic and are rarely found in the active zone, the issue of whether QDs can go within an active zone for this receptor is unlikely to make a difference. However, experiments using an organic dye like Cy3 for the $GABA_B$ receptor will be useful to compare with the diffusion coefficients observed here in this study.

6.3.1 SDs as mediators of lateral diffusion

Previous reports of $GABA_B$ receptor lateral mobility have only studied the R1bR2 receptor (Pooler and McIlhinney, 2007) and therefore any subtype specific lateral mobility of the $GABA_B$ receptor has not been addressed. Using SPT, the mobility of the two subtypes of the $GABA_B$ receptor has been studied and R1aR2 receptors are

laterally more mobile with higher diffusion coefficients than R1bR2 receptors on hippocampal neurons in culture. R1aR2 and R1bR2 have been demonstrated to have distinct internalisation kinetics because of the presence of the SDs in R1a (chapter V). The role of the SDs in lateral mobility is therefore interesting as the two subtypes of the $GABA_B$ receptor have distinct lateral mobility profiles conferred on R1a by the SDs. To this end, it will be of interest to determine if one of the SDs imparts this differential lateral mobility profile on R1aR2 receptors or whether both SDs are necessary.

Extrasynaptic R1aR2 receptors around synaptophysin containing compartments do not differ in terms of their median diffusion coefficients compared to extrasynaptic R1bR2 receptors in the same areas ($P>0.05$ MW). This implies that once in the axon surface, both R1aR2 and R1bR2 receptors explore the axonal membrane with similar rates. However, the median diffusion coefficient of presynaptic R1bR2 receptors is greater than the median diffusion coefficient of R1aR2 receptors ($P<0.001$ MW) suggesting that once recruited in a presynaptic terminal from extrasynaptic areas, R1aR2 receptors are anchored by a yet unknown protein that causes it to slow down more than R1bR2 receptors within the presynaptic compartment. R1aR2 receptors have been described to form presynaptic heteroreceptors at glutamatergic terminals (Vigot et al., 2006) and in addition to preferential targeting to axons via the SDs in R1a (Biermann et al., 2010), increased anchoring of these receptors in the presynaptic terminal compared to R1bR2 receptors could explain why R1aR2 receptors contribute significantly to presynaptic signalling via $GABA_B$ receptors whereas R1bR2 receptors do not.

6.3.2 Agonist induced changes in lateral mobility of $GABA_B$ receptors

R1bR2 has been described to diffuse more rapidly on the cell surface in response to chronic (1 hr) baclofen treatment (Pooler and McIlhinney, 2007). Although the baclofen treatment that has been used here is much briefer, it does appear to increase the mobility of R1bR2 receptors and this complements results obtained using FRAP studies (Pooler and McIlhinney, 2007). However, in the synaptophysin containing presynaptic terminals treatment with baclofen did not result in any change of mobility of either extrasynaptic or presynaptic R1bR2 receptors. This implies that the increase of mobility that has been observed for ensemble R1bR2 receptors in the presence of baclofen is being manifest through other synaptic compartments that do not contain synaptophysin. These could possibly involve postsynaptic clusters containing PSD95 or gephyrin with important physiological implications.

In contrast, ensemble R1aR2 receptors displayed reduced mobility in response to baclofen. This further suggests that in addition to demonstrating differential properties in terms of internalisation, the R1aR2 and R1bR2 subtypes have different lateral mobility profiles in the presence of baclofen and quite possibly GABA. In synaptophysin containing presynaptic terminals the effect of baclofen on R1aR2 receptors was more pronounced than on R1bR2 and R1aR2 receptors' lateral mobility was decreased. This could be important for signalling regulation as fewer extrasynaptic receptors will be recruited to synapses from extrasynaptic areas and the synaptic receptors that have been activated will remain within the synapses in desensitised states.

$GABA_B$ R1aR2 and R1bR2 receptors display reduced mobility upon entering synaptophysin containing presynaptic terminals from extrasynaptic areas which could

be due to the increase of the apparent viscosity of the cell surface within the synaptic compartment (Renner et al., 2009; Renner et al., 2008). Although this may account partly for the slow-down of the receptors, the effect of baclofen in slowing down synaptic as well as extrasynaptic receptors in a subtype-specific manner suggests the involvement of protein-protein interactions that stabilise the R1aR2 receptors possibly involving the SDs. The SDs could be interacting with proteins would could potentially anchor R1aR2 receptors in the synaptic compartments and slow their mobility in the extrasynaptic compartments in response to activation by GABA but have no effect on R1bR2 receptors. Several other receptors demonstrate slower mobilities in synapses compared to extrasynaptic compartments due to interaction with scaffolding proteins or the cytoskeleton. The AMPA receptor binds actin (Shen et al., 2000) and the $GABA_A$ receptor interacts with the anchoring protein gephyrin (Meier et al., 2001). To this end, the effect of disruption of the cytoskeleton on the $GABA_B$ receptors lateral mobility will be of interest in identifying interacting partners of SDs.

6.4 Summary

- BBS strategy can be used to study the lateral mobility of $GABA_B$ receptors
- R1aR2 receptors are more laterally mobile on hippocampal neurons than R1bR2 receptors
- Agonist activation increases the ensemble lateral mobility of R1bR2 receptors but slows down R1aR2 receptors
- $GABA_B$ receptors are more mobile in presynaptic synaptophysin containing extrasynaptic compartments than synaptic ones
- Agonist activation slows down both presynaptic and extrasynaptic R1aR2 receptors but has no effect on R1bR2 receptors in these compartments

Chapter VII

General Discussion

7.1 Using the BBS tag approach for studying receptor mobility

Several biochemical and imaging strategies have been used to probe receptor trafficking in live cells. In this study, the BBS tagging approach was extended to tag $GABA_B$ R1b, $GABA_B$ R2, and mGluR2 receptors with fluorescently labelled or biotinylated BTX. The BBS containing receptors bound to BTX with high affinities and the functioning of $GABA_B$ receptors remained unaltered by the insertion of the BBS. In addition, fluorescent BTX did not bleach significantly under the experimental conditions and this allowed the study of real-time internalisation kinetics in live GIRK cells and hippocampal neurons and membrane insertion kinetics in fixed cells.

The BBS strategy was used to report, for the first time in live cells, clathrin- and dynamin- dependence of $GABA_B$ R1aR2 receptor internalisation. In addition to clathrin-dependent internalisation, a significant amount of non-clathrin- and non-dynamin-dependent internalisation was observed suggesting that a proportion of $GABA_B$ receptors internalise via such pathways. These pathways are likely to be important as they represent a major route for the internalisation of $GABA_B$ receptors. Provided the rates of recycling, degradation and insertion of newly synthesised receptors do not change, blocking these pathways will impart increased stability to $GABA_B$ receptors as

a greater number of them will accumulate on the cell surface and this will have physiological significance given the importance of cell surface numbers of $GABA_B$ receptors for slow synaptic inhibition in the CNS.

Even though several studies, including this one, have reported the clathrin- and dynamin-dependence of $GABA_B$ receptor internalisation, the structural motif that mediates the recruitment of $GABA_B$ receptors into clathrin-coated pits remains unknown. Tyrosine motifs (YxxΦ; where x can be any amino acid and Φ is a bulky hydrophobic residue) (Bonifacino and Traub, 2003) have been well characterised as internalisation motifs and although the C-terminal tail of R1 does not contain such a motif, the C-terminal tail of R2 contains a classical tyrosine motif with the sequence $Y^{830}QEL^{833.}$ The critical tyrosine along with the hydrophobic leucine residues were mutated to alanines to investigate whether this motif was involved in clathrin-dependent internalisation, but no change in the rate or extent was observed when the mutated R2 was co-expressed with R1a in live GIRK cells.

In addition, C-terminal truncations of R1a or R2 were also not observed to alter the rates or extents of internalisation in live GIRK cells and therefore it is conceivable that the clathrin recruitment interaction motif is located in the intracellular loops or in other parts of the receptor. To study the role of ubiquitination in internalisation of R1aΔCT, all the lysines on the intracellular loops of R1a were substituted to arginines; however no alteration to the rate or extent of internalisation was observed compared to R1aΔCT discounting a role for ubiquitination. A role for SUMOylation in the internalisation of $GABA_B$ receptors additionally can be discounted on this basis, since this also requires a lysine residue buried in a consensus sequence of Ψ-K-X-D/E (where

Ψ is a hydrophobic residue, K is a lysine residue, X is any amino acid and D or E is an acidic residue) (Wilkinson and Henley, 2010; Kantamneni et al., 2011; Wilkinson et al., 2010; Wilkinson et al., 2008).

The use of a combination of fluorescently labelled intracellular endosomal markers allowed the study of the trafficking itineraries of $GABA_B$ R1aR2 receptors in the endosomal compartments. These receptors are internalised into early endosomes from where they can be recruited to late endosomes for lysosomal degradation or recycling endosomes for recycling back to the cell surface. This technique could be extended in future to study the effect of drugs in the intracellular trafficking of $GABA_B$ receptors by using advanced co-localisation algorithms.

The use of the novel modified BBS approach allowed simultaneous labelling and monitoring of each $GABA_B$ receptor subunit with two different fluorophores in live cells in real-time demonstrating that these two subunits are internalised together. Although the fluorescence intensity achieved using this approach was lower using the modified BBS compared to the unmodified BBS, this method could be used to study the association of two different proteins in which the BBS tag can be engineered and differentially labelled. One particular step where modification of the labelling method can be improved is the reduction step of MTSES by DTT bound to the modified BBS. A stronger reducing agent, for which the treatment time will be shorter, will enhance this technique. To this end, the use of a photosensitive oxidising agent to block the interaction of BTX with modified BBS could be used to achieve better labelling speeds.

There are several advantages of using the BBS strategy to study receptor internalisation compared to conventional antibody based approaches. The size of BTX

is almost half of a F(ab)' fragment and less than a sixth of an antibody molecule. This would allow the BBS to access areas that an antibody complex will not be able to within the plasma membrane. In addition to this, BTX is smaller in size than other proteins used for studying trafficking for instance snap tags and the clip tags are more than double the size of a BTX molecule, an eGFP molecule is about one and a half times the size of BTX, and streptavidin tetramers are more than three times the size of BTX. Another advantage of the BBS strategy is that as BTX is cell impermeable, cell surface receptors can be selectively labelled. pH sensitive versions of GFP are capable of discriminating cell surface receptors from intracellular receptors although internalised receptors cannot be monitored in real-time using this strategy and the signal-to –noise achieved with these fluorophores is often quite low.

The disadvantage of the BBS strategy is that only recombinant receptors can be studied and the BBS has to be engineered to a suitable location in a receptor from where it will not effect functionality. While the BTX is smaller than antibodies and other molecules it is still seventy-four amino acids and this is large compared to organic dyes such as fluorescent maleamide compounds that are used for cysteine labelling.

7.2 Structural motifs for internalisation

This study has highlighted the importance of heterodimerisation in the cell surface stability of $GABA_B$ receptors. A di-leucine motif in the coiled-coil domain of R1a and R1b is masked by the C-terminal tail of R2 and this slows internalisation of the R1

subunits. This is ultimately important for $GABA_B$ receptors to deliver slow and prolonged inhibition in the CNS. Proteins or drugs that could alter this interaction will destabilise $GABA_B$ heteromers reducing the efficacy of inhibition with physiological consequences. In addition to the di-leucine motif, the SDs of R1a have been identified as an important determinant of membrane stability for the R1aR2 subtype of the $GABA_B$ receptor and allows the receptor to internalise at a slower rate and to a lesser extent in the soma and dendrites, and at a slower rate but unchanged extent in the spines, compared to the R1bR2 subtype. In order for the R1aR2 receptors to be more stable than the R1bR2 receptors, the presence of both SDs is required. In addition, the two SDs together increased the surface stability to mGluR2 receptors demonstrating the importance of these domains in determining receptor stability at the cell surface.

Given the important roles played by the SDs in $GABA_B$ receptors, the identification of interactions of SDs with proteins has been an important area of research. Fibulin-2 has been reported to interact with SD1 (Blein et al., 2004) although at this point of time the importance of this interaction is not clear and has to be investigated further. CHOP provides another interesting interaction partner as this protein can interact with the N-terminus of R1a but not R1b and the co-expression of CHOP with $GABA_B$ receptors in HEK-293 cells reduces the cell surface expression of R1aR2 receptors, but has no effect on R1bR2 receptors. The levels of CHOP are elevated during ER stress (Oyadomari et al., 2002) and CHOP knockout mice are less prone to neuronal cell death during ischemia suggesting an important role for CHOP in apoptosis during ischemia (Tajiri et al., 2004). Moreover, oxygen-glucose deprivation to induce ischemia in organotypic brain slices has been reported to alter the total level of R2 subunits while having no effect on the expression of R1 subunits (Cimarosti et al., 2009). Such means of

regulating the cell surface of $GABA_B$ receptors in a subtype-specific manner during ischemia and ER stress could therefore have potentially important implications in neuronal survival and plasticity.

7.3 Functional implications for stability and lateral mobility

The number of $GABA_B$ receptors available in the pre- and postsynaptic compartments is an important determinant of synaptic inhibition. Three mechanisms exist that recruit and remove receptors from specific signalling domains on the cell surface. These include internalisation of surface receptors from the signalling domain into intracellular compartments, insertion of newly-synthesised or recycling receptors, into the domain on the cell surface, and lateral movement of the receptors on the plane of the cell membrane into or out of the signalling domain (Triller and Choquet, 2008; Carroll et al., 2001). In addition to this, synapses themselves are macromolecular assemblies that are in a dynamic equilibrium as the postsynaptic scaffold proteins undergo redistribution in terms of spine plasticity and activity dependent changes. In this study, R1aR2 receptors have been demonstrated to have different trafficking properties compared to R1bR2 receptors. Importantly, the lateral mobility of R1aR2 but not R1bR2 receptors was reduced in response to baclofen treatment in both synaptophysin containing pre- and extrasynaptic terminals which could explain why R1aR2 and not R1bR2 presynaptic heteroreceptors are activated by low concentrations of baclofen to reduce glutamate release (Guetg et al., 2009). In addition, due to the presence of SDs, R1aR2 receptors will be more stable on the cell surface in terms of internalisation compared to R1bR2 receptors ensuring a higher signalling efficacy of

presynaptic $GABA_B$ R1aR2 receptors which will inhibit the release of glutamate during excitotoxicity.

SPT has been used for the first time to demonstrate continuous random Brownian diffusion of $GABA_B$ receptors on the neuronal plasma membrane. The changes in mobility observed in response to baclofen imply that these receptors exhibit directed motion in addition to random motion. Indeed, the multiple alpha helices and RNA-linker protein 1 (Marlin 1) interacts with the C-terminal tail of R1 and links $GABA_B$ receptors to microtubules (Couve et al., 2004). In addition to this, Marlin 1 was immunoprecipitated with the molecular microtubule motor protein, Kinesin-I, from adult mice brain lysates and $GABA_B$R1 was immunoprecipitated with Kinesin-I in COS-7 cells further validating that $GABA_B$ receptors interact with microtubules (Vidal et al., 2007). Moreover, the PDZ domain containing protein, Mupp1, has been reported to interact with $GABA_B$ R2 in an interaction requiring Leu941. Mutating this residue reduces expression of $GABA_B$ receptors in COS-7 cells (Balasubramanian et al., 2007). Interestingly, Mupp1 is enriched in the postsynaptic density and acts as a scaffold for a number of proteins (Estevez et al., 2008; Krapivinsky et al., 2004). Thus, microtubules and Mupp1 could play a role in the lateral mobility of $GABA_B$ receptors.

In this study, the main focus of lateral mobility of $GABA_B$ receptors has been around presynaptic terminals, and in addition, internalisation of $GABA_B$ receptors has been studied at spines and dendrites that are likely to contain postsynaptic sites. In layer 5 neocortical neurons, R1bR2 inhibits Ca^{2+} spikes (Perez-Garci et al., 2006) and as the R1bR2 is less stable on the cell surface compared to R1aR2 this would likely facilitate the development of postsynaptic NMDA-receptor mediated synaptic plasticity

(Terunuma et al., 2010; Guetg et al., 2010) due to lower efficacy of inhibition. On the other hand R1aR2 receptors are also present at postsynaptic sites and these will be capable of inhibiting excessive glutamate-mediated excitation due to their lower rate of turnover from the cell surface compared to R1bR2 receptors. However, there is no difference in the extents of internalisation between the two subtypes in the spines with potentially important consequences, as the neck of the spines are close to glutamatergic inputs, and due to the high turnover of both the subtypes of the $GABA_B$ receptors in the spines, glutamate-mediated synaptic plasticity could also be facilitated. Therefore subtype-specific $GABA_B$ receptor trafficking, dependent on the SDs, could fine tune local glutamate-mediated synaptic plasticity. To investigate further, future work on $GABA_B$ signalling will need to focus on the effect of agonists on the lateral mobility of the two $GABA_B$ receptor subtypes around excitatory synapses containing PSD95 and around inhibitory synapses containing gephyrin.

References

Addolorato G, Caputo F, Capristo E, Domenicali M, Bernardi M, Janiri L, Agabio R, Colombo G, Gessa GL, Gasbarrini G (2002a) Baclofen efficacy in reducing alcohol craving and intake: a preliminary double-blind randomized controlled study. Alcohol Alcohol 37:504-508.

Addolorato G, Caputo F, Capristo E, Janiri L, Bernardi M, Agabio R, Colombo G, Gessa GL, Gasbarrini G (2002b) Rapid suppression of alcohol withdrawal syndrome by baclofen. Am J Med 112:226-229.

Alcor D, Gouzer G, Triller A (2009) Single-particle tracking methods for the study of membrane receptors dynamics. Eur J Neurosci 30:987-997.

Arancibia-Carcamo IL, Yuen EY, Muir J, Lumb MJ, Michels G, Saliba RS, Smart TG, Yan Z, Kittler JT, Moss SJ (2009) Ubiquitin-dependent lysosomal targeting of $GABA_A$ receptors regulates neuronal inhibition. Proc Natl Acad Sci U S A 106:17552-17557.

Ashby MC, Ibaraki K, Henley JM (2004) It's green outside: tracking cell surface proteins with pH-sensitive GFP. Trends Neurosci 27:257-261.

Ashery U, Koch H, Scheuss V, Brose N, Rettig J (1999) A presynaptic role for the ADP ribosylation factor (ARF)-specific GDP/GTP exchange factor msec7-1. Proc Natl Acad Sci U S A 96:1094-1099.

Awapara J, LANDUA AJ, FUERST R, SEALE B (1950) Free γ-aminobutyric acid in brain. J Biol Chem 187:35-39.

Baker KA, Taylor JW, Lilly GE (1985) Treatment of trigeminal neuralgia: use of baclofen in combination with carbamazepine. Clin Pharm 4:93-96.

Balasubramanian S, Fam SR, Hall RA (2007) $GABA_B$ receptor association with the PDZ scaffold Mupp1 alters receptor stability and function. J Biol Chem 282:4162-4171.

Balasubramanian S, Teissere JA, Raju DV, Hall RA (2004) Hetero-oligomerization between $GABA_A$ and $GABA_B$ receptors regulates $GABA_B$ receptor trafficking. J Biol Chem 279:18840-18850.

Bannai H, Levi S, Schweizer C, Inoue T, Launey T, Racine V, Sibarita JB, Mikoshiba K, Triller A (2009) Activity-dependent tuning of inhibitory neurotransmission based on $GABA_AR$ diffusion dynamics. Neuron 62:670-682.

Bartoi T, Rigbolt KTG, Du D, K+¦hr G, Blagoev B, Kornau HC (2010) $GABA_B$ Receptor Constituents Revealed by Tandem Affinity Purification from Transgenic Mice. Journal of Biological Chemistry 285:20625-20633.

Becher A, Green A, Ige AO, Wise A, White JH, McIlhinney RA (2004) Ectopically expressed γ-aminobutyric acid receptor B is functionally down-regulated in isolated lipid raft-enriched membranes. Biochem Biophys Res Commun 321:981-987.

Becher A, White JH, McIlhinney RA (2001) The γ -aminobutyric acid receptor B, but not the metabotropic glutamate receptor type-1, associates with lipid rafts in the rat cerebellum. J Neurochem 79:787-795.

Becker R, Alberti O, Bauer BL (1997) Continuous intrathecal baclofen infusion in severe spasticity after traumatic or hypoxic brain injury. J Neurol 244:160-166.

Beleboni RO, Carolino RO, Pizzo AB, Castellan-Baldan L, Coutinho-Netto J, Dos Santos WF, Coimbra NC (2004) Pharmacological and biochemical aspects of GABAergic neurotransmission: pathological and neuropsychobiological relationships. Cell Mol Neurobiol 24:707-728.

Bettler B, Kaupmann K, Mosbacher J, Gassmann M (2004) Molecular structure and physiological functions of $GABA_B$ receptors. Physiol Rev 84:835-867.

Bettler B, Tiao JY (2006) Molecular diversity, trafficking and subcellular localization of $GABA_B$ receptors. Pharmacol Ther 110:533-543.

Biermann B, Ivankova-Susankova K, Bradaia A, Abdel AS, Besseyrias V, Kapfhammer JP, Missler M, Gassmann M, Bettler B (2010) The Sushi domains of $GABA_B$ receptors function as axonal targeting signals. J Neurosci 30:1385-1394.

Bist R, Bhatt DK (2009) The evaluation of effect of alpha-lipoic acid and vitamin E on the lipid peroxidation, γ -amino butyric acid and serotonin level in the brain of mice (Mus musculus) acutely intoxicated with lindane. J Neurol Sci 276:99-102.

Blein S, Ginham R, Uhrin D, Smith BO, Soares DC, Veltel S, McIlhinney RA, White JH, Barlow PN (2004) Structural analysis of the complement control protein (CCP) modules of $GABA_B$ receptor 1a: only one of the two CCP modules is compactly folded. J Biol Chem 279:48292-48306.

Bogdanov Y, Michels G, Armstrong-Gold C, Haydon PG, Lindstrom J, Pangalos M, Moss SJ (2006) Synaptic $GABA_A$ receptors are directly recruited from their extrasynaptic counterparts. EMBO J 25:4381-4389.

Bohlen P, Huot S, Palfreyman MG (1979) The relationship between GABA concentrations in brain and cerebrospinal fluid. Brain Res 167:297-305.

Bonifacino JS, Traub LM (2003) Signals for sorting of transmembrane proteins to endosomes and lysosomes. Annu Rev Biochem 72:395-447.

Bowery NG, Bettler B, Froestl W, Gallagher JP, Marshall F, Raiteri M, Bonner TI, Enna SJ (2002) International Union of Pharmacology. XXXIII. Mammalian γ-Aminobutyric $Acid_B$ Receptors: Structure and Function. Pharmacol Rev 54:247-264.

Bowery NG, Doble A, Hill DR, Hudson AL, Shaw JS, Turnbull MJ, Warrington R (1981) Bicuculline-insensitive GABA receptors on peripheral autonomic nerve terminals. Eur J Pharmacol 71:53-70.

Bowery NG, Enna SJ (2000) γ-aminobutyric acid$_B$ receptors: first of the functional metabotropic heterodimers. J Pharmacol Exp Ther 292:2-7.

Bowery NG, Hill DR, Hudson AL, Doble A, Middlemiss DN, Shaw J, Turnbull M (1980) (-)Baclofen decreases neurotransmitter release in the mammalian CNS by an action at a novel GABA receptor. Nature 283:92-94.

Bowery NG, Hudson AL (1979) γ-Aminobutyric acid reduces the evoked release of [^{3}H]-noradrenaline from sympathetic nerve terminals [proceedings]. Br J Pharmacol 66:108P.

Bowery NG, Smart TG (2006) GABA and glycine as neurotransmitters: a brief history. Br J Pharmacol 147 Suppl 1:S109-S119.

Brar SP, Smith MB, Nelson LM, Franklin GM, Cobble ND (1991) Evaluation of treatment protocols on minimal to moderate spasticity in multiple sclerosis. Arch Phys Med Rehabil 72:186-189.

Brock C, Boudier L, Maurel D, Blahos J, Pin JP (2005) Assembly-dependent surface targeting of the heterodimeric GABA$_B$ Receptor is controlled by COPI but not 14-3-3. Mol Biol Cell 16:5572-5578.

Bucci C, Thomsen P, Nicoziani P, McCarthy J, van Deurs B (2000) Rab7: a key to lysosome biogenesis. Mol Biol Cell 11:467-480.

Burli T, Baer K, Ewers H, Sidler C, Fuhrer C, Fritschy JM (2010) Single particle tracking of α7 nicotinic AChR in hippocampal neurons reveals regulated confinement at glutamatergic and GABAergic perisynaptic sites. PLoS One 5:e11507.

Burt DR, Kamatchi GL (1991) GABA$_A$ receptor subtypes: From pharmacology to molecular biology. FASEB Journal 5:2916-2923.

Calver AR, Robbins MJ, Cosio C, Rice SQ, Babbs AJ, Hirst WD, Boyfield I, Wood MD, Russell RB, Price GW, Couve A, Moss SJ, Pangalos MN (2001) The C-Terminal Domains of the GABA$_B$ Receptor Subunits Mediate Intracellular Trafficking But Are Not Required for Receptor Signaling. J Neurosci 21:1203-1210.

Carroll RC, Beattie EC, von ZM, Malenka RC (2001) Role of AMPA receptor endocytosis in synaptic plasticity. Nat Rev Neurosci 2:315-324.

Casanova JE (2007) Regulation of Arf activation: the Sec7 family of guanine nucleotide exchange factors. Traffic 8:1476-1485.

Cates LA, Li VS, Yakshe CC, Fadeyi MO, Andree TH, Karbon EW, Enna SJ (1984) Phosphorus analogues of γ-aminobutyric acid, a new class of anticonvulsants. J Med Chem 27:654-659.

Chalifoux JR, Carter AG (2010) GABA$_B$ receptors modulate NMDA receptor calcium signals in dendritic spines. Neuron 66:101-113.

Chalifoux JR, Carter AG (2011) $GABA_B$ receptor modulation of voltage-sensitive calcium channels in spines and dendrites. J Neurosci 31:4221-4232.

Chang CC (1999) Looking back on the discovery of α-bungarotoxin. J Biomed Sci 6:368-375.

Cherezov V, Rosenbaum DM, Hanson MA, Rasmussen SG, Thian FS, Kobilka TS, Choi HJ, Kuhn P, Weis WI, Kobilka BK, Stevens RC (2007) High-resolution crystal structure of an engineered human β2-adrenergic G protein-coupled receptor. Science 318:1258-1265.

Cimarosti H, Kantamneni S, Henley JM (2009) Ischaemia differentially regulates $GABA_B$ receptor subunits in organotypic hippocampal slice cultures. Neuropharmacology 56:1088-1096.

Comps-Agrar L, Kniazeff J, Norskov-Lauritsen L, Maurel D, Gassmann M, Gregor N, Prezeau L, Bettler B, Durroux T, Trinquet E, Pin JP (2011) The oligomeric state sets $GABA_B$ receptor signalling efficacy. EMBO J 30:2336-2349.

Conner SD, Schmid SL (2003) Regulated portals of entry into the cell. Nature 422:37-44.

Connolly CN, Kittler JT, Thomas P, Uren JM, Brandon NJ, Smart TG, Moss SJ (1999) Cell surface stability of γ-aminobutyric acid type A receptors. Dependence on protein kinase C activity and subunit composition. J Biol Chem 274:36565-36572.

Corringer PJ, Le Novere N, Changeux JP (2000) Nicotinic receptors at the amino acid level. Annu Rev Pharmacol Toxicol 40:431-458.

Couve A, Filippov AK, Connolly CN, Bettler B, Brown DA, Moss SJ (1998) Intracellular retention of recombinant $GABA_B$ receptors. J Biol Chem 273:26361-26367.

Couve A, Kittler JT, Uren JM, Calver AR, Pangalos MN, Walsh FS, Moss SJ (2001) Association of $GABA_B$ receptors and members of the 14-3-3 family of signaling proteins. Mol Cell Neurosci 17:317-328.

Couve A, Restituito S, Brandon JM, Charles KJ, Bawagan H, Freeman KB, Pangalos MN, Calver AR, Moss SJ (2004) Marlin-1, a novel RNA-binding protein associates with $GABA_B$ receptors. J Biol Chem 279:13934-13943.

Couve A, Thomas P, Calver AR, Hirst WD, Pangalos MN, Walsh FS, Smart TG, Moss SJ (2002) Cyclic AMP-dependent protein kinase phosphorylation facilitates $GABA_B$ receptor-effector coupling. Nat Neurosci 5:415-424.

Couvineau A, Laburthe M (2011) The Family B1 GPCR: Structural Aspects and Interaction with Accessory Proteins. Curr Drug Targets.

Cryan JF, Kaupmann K (2005) Don't worry 'B' happy!: a role for $GABA_B$ receptors in anxiety and depression. Trends Pharmacol Sci 26:36-43.

Dahan M, Levi S, Luccardini C, Rostaing P, Riveau B, Triller A (2003) Diffusion dynamics of glycine receptors revealed by single-quantum dot tracking. Science 302:442-445.

de Hoop MJ, Huber LA, Stenmark H, Williamson E, Zerial M, Parton RG, Dotti CG (1994) The involvement of the small GTP-binding protein Rab5a in neuronal endocytosis. Neuron 13:11-22.

Delaney KA, Murph MM, Brown LM, Radhakrishna H (2002) Transfer of M2 muscarinic acetylcholine receptors to clathrin-derived early endosomes following clathrin-independent endocytosis. J Biol Chem 277:33439-33446.

Donnelly SR, Hawkins TE, Moss SE (1999) A conserved nuclear element with a role in mammalian gene regulation. Hum Mol Genet 8:1723-1728.

Dunlap K, Fischbach GD (1981) Neurotransmitters decrease the calcium conductance activated by depolarization of embryonic chick sensory neurones. J Physiol 317:519-535.

Durkin MM, Gunwaldsen CA, Borowsky B, Jones KA, Branchek TA (1999) An in situ hybridization study of the distribution of the $GABA_{B2}$ protein mRNA in the rat CNS. Brain Res Mol Brain Res 71:185-200.

Dutar P, NIcoll RA (1988) A physiological role for $GABA_B$ receptors in the central nervous system. Nature 332:156-158.

Duthey B, Caudron S, Perroy J, Bettler B, Fagni L, Pin JP, Prezeau L (2002) A single subunit (GB2) is required for G-protein activation by the heterodimeric $GABA_B$ receptor. J Biol Chem 277:3236-3241.

Eisele JL, Bertrand S, Galzi JL, Devillers-Thiery A, Changeux JP, Bertrand D (1993) Chimaeric nicotinic-serotonergic receptor combines distinct ligand binding and channel specificities. Nature 366:479-483.

Estevez MA, Henderson JA, Ahn D, Zhu XR, Poschmann G, Lubbert H, Marx R, Baraban JM (2008) The neuronal RhoA GEF, Tech, interacts with the synaptic multi-PDZ-domain-containing protein, MUPP1. J Neurochem 106:1287-1297.

Fairfax BP, Pitcher JA, Scott MG, Calver AR, Pangalos MN, Moss SJ, Couve A (2004) Phosphorylation and chronic agonist treatment atypically modulate $GABA_B$ receptor cell surface stability. J Biol Chem 279:12565-12573.

Felder CB, Graul RC, Lee AY, Merkle HP, Sadee W (1999) The Venus flytrap of periplasmic binding proteins: an ancient protein module present in multiple drug receptors. AAPS PharmSci 1:E2.

Fernandes CC, Berg DK, Gomez-Varela D (2010) Lateral mobility of nicotinic acetylcholine receptors on neurons is determined by receptor composition, local domain, and cell type. J Neurosci 30:8841-8851.

Filippov AK, Couve A, Pangalos MN, Walsh FS, Brown DA, Moss SJ (2000) Heteromeric assembly of $GABA_BR1$ and $GABA_BR2$ receptor subunits inhibits Ca^{2+} current in sympathetic neurons. J Neurosci 20:2867-2874.

Foord SM, Bonner TI, Neubig RR, Rosser EM, Pin JP, Davenport AP, Spedding M, Harmar AJ (2005) International Union of Pharmacology. XLVI. G protein-coupled receptor list. Pharmacol Rev 57:279-288.

Franklin TR, Harper D, Kampman K, Kildea-McCrea S, Jens W, Lynch KG, O'Brien CP, Childress AR (2009) The $GABA_B$ agonist baclofen reduces cigarette consumption in a preliminary double-blind placebo-controlled smoking reduction study. Drug Alcohol Depend 103:30-36.

Fredriksson R, Schioth HB (2005) The repertoire of G-protein-coupled receptors in fully sequenced genomes. Mol Pharmacol 67:1414-1425.

Froestl W, Mickel SJ, Hall RG, von SG, Strub D, Baumann PA, Brugger F, Gentsch C, Jaekel J, Olpe HR, . (1995a) Phosphinic acid analogues of GABA. 1. New potent and selective $GABA_B$ agonists. J Med Chem 38:3297-3312.

Froestl W, Mickel SJ, von SG, Diel PJ, Hall RG, Maier L, Strub D, Melillo V, Baumann PA, Bernasconi R, . (1995b) Phosphinic acid analogues of GABA. 2. Selective, orally active $GABA_B$ antagonists. J Med Chem 38:3313-3331.

Fromm GH (1994) Baclofen as an adjuvant analgesic. J Pain Symptom Manage 9:500-509.

Galvez T, Duthey B, Kniazeff J, Blahos J, Rovelli G, Bettler B, Prezeau L, Pin JP (2001) Allosteric interactions between GB1 and GB2 subunits are required for optimal $GABA_B$ receptor function. EMBO J 20:2152-2159.

Galvez T, Parmentier ML, Joly C, Malitschek B, Kaupmann K, Kuhn R, Bittiger H, Froestl W, Bettler B, Pin JP (1999) Mutagenesis and modeling of the $GABA_B$ receptor extracellular domain support a venus flytrap mechanism for ligand binding. J Biol Chem 274:13362-13369.

Galvez T, Prezeau L, Milioti G, Franek M, Joly C, Froestl W, Bettler B, Bertrand HO, Blahos J, Pin JP (2000) Mapping the agonist-binding site of $GABA_B$ type 1 subunit sheds light on the activation process of $GABA_B$ receptors. J Biol Chem 275:41166-41174.

Gassmann M, et al. (2004) Redistribution of $GABA_{B(1)}$ protein and atypical $GABA_B$ responses in $GABA_{B(2)}$-deficient mice. J Neurosci 24:6086-6097.

George SR, Fan T, Xie Z, Tse R, Tam V, Varghese G, O'Dowd BF (2000) Oligomerization of μ- and δ-opioid receptors. Generation of novel functional properties. J Biol Chem 275:26128-26135.

Gether U, Asmar F, Meinild AK, Rasmussen SG (2002) Structural basis for activation of G-protein-coupled receptors. Pharmacol Toxicol 91:304-312.

Getova D, Bowery NG (1998) The modulatory effects of high affinity $GABA_B$ receptor antagonists in an active avoidance learning paradigm in rats. Psychopharmacology (Berl) 137:369-373.

Gjoni T, Urwyler S (2009) Changes in the properties of allosteric and orthosteric $GABA_B$ receptor ligands after a continuous, desensitizing agonist pretreatment. Eur J Pharmacol 603:37-41.

Goei VL, Choi J, Ahn J, Bowlus CL, Raha-Chowdhury R, Gruen JR (1998) Human γ-aminobutyric acid B receptor gene: complementary DNA cloning, expression, chromosomal location, and genomic organization. Biol Psychiatry 44:659-666.

Gonzalez-Maeso J, Wise A, Green A, Koenig JA (2003) Agonist-induced desensitization and endocytosis of heterodimeric $GABA_B$ receptors in CHO-K1 cells. Eur J Pharmacol 481:15-23.

Grampp T, Notz V, Broll I, Fischer N, Benke D (2008) Constitutive, agonist-accelerated, recycling and lysosomal degradation of $GABA_B$ receptors in cortical neurons. Mol Cell Neurosci 39:628-637.

Grampp T, Sauter K, Markovic B, Benke D (2007) γ-aminobutyric acid type B receptors are constitutively internalized via the clathrin-dependent pathway and targeted to lysosomes for degradation. J Biol Chem 282:24157-24165.

Groc L, Choquet D, Stephenson FA, Verrier D, Manzoni OJ, Chavis P (2007a) NMDA receptor surface trafficking and synaptic subunit composition are developmentally regulated by the extracellular matrix protein Reelin. J Neurosci 27:10165-10175.

Groc L, Heine M, Cognet L, Brickley K, Stephenson FA, Lounis B, Choquet D (2004) Differential activity-dependent regulation of the lateral mobilities of AMPA and NMDA receptors. Nat Neurosci 7:695-696.

Groc L, Lafourcade M, Heine M, Renner M, Racine V, Sibarita JB, Lounis B, Choquet D, Cognet L (2007b) Surface trafficking of neurotransmitter receptor: comparison between single-molecule/quantum dot strategies. J Neurosci 27:12433-12437.

Guetg N, Abdel AS, Holbro N, Turecek R, Rose T, Seddik R, Gassmann M, Moes S, Jenoe P, Oertner TG, Casanova E, Bettler B (2010) NMDA receptor-dependent $GABA_B$ receptor internalization via CaMKII phosphorylation of serine 867 in $GABA_{B1}$. Proc Natl Acad Sci U S A 107:13924-13929.

Guetg N, Seddik R, Vigot R, Turecek R, Gassmann M, Vogt KE, Brauner-Osborne H, Shigemoto R, Kretz O, Frotscher M, Kulik A, Bettler B (2009) The $GABA_{B1a}$ isoform mediates heterosynaptic depression at hippocampal mossy fiber synapses. J Neurosci 29:1414-1423.

Guyon A, Leresche N (1995) Modulation by different $GABA_B$ receptor types of voltage-activated calcium currents in rat thalamocortical neurones. J Physiol 485 (Pt 1):29-42.

Haney M, Hart CL, Foltin RW (2006) Effects of baclofen on cocaine self-administration: opioid- and nonopioid-dependent volunteers. Neuropsychopharmacology 31:1814-1821.

Hanley JG, Khatri L, Hanson PI, Ziff EB (2002) NSF ATPase and α-/β-SNAPs disassemble the AMPA receptor-PICK1 complex. Neuron 34:53-67.

Hannan S, Wilkins ME, Dehghani-Tafti E, Thomas P, Baddeley SM, Smart TG (2011) γ-Aminobutyric Acid Type B ($GABA_B$) Receptor Internalization Is Regulated by the R2 Subunit. J Biol Chem 286:24324-24335.

Harayama N, Shibuya I, Tanaka K, Kabashima N, Ueta Y, Yamashita H (1998) Inhibition of N- and P/Q-type calcium channels by postsynaptic $GABA_B$ receptor activation in rat supraoptic neurones. J Physiol 509 (Pt 2):371-383.

Harel M, Kasher R, Nicolas A, Guss JM, Balass M, Fridkin M, Smit AB, Brejc K, Sixma TK, Katchalski-Katzir E, Sussman JL, Fuchs S (2001) The binding site of acetylcholine receptor as visualized in the X-Ray structure of a complex between α-bungarotoxin and a mimotope peptide. Neuron 32:265-275.

Havlickova M, Prezeau L, Duthey B, Bettler B, Pin JP, Blahos J (2002) The intracellular loops of the GB2 subunit are crucial for G-protein coupling of the heteromeric γ-aminobutyrate B receptor. Mol Pharmacol 62:343-350.

Hayashi T (1956) Chemical Physiology of Excitation in Nerve and Muscle.

Hein P, Frank M, Hoffmann C, Lohse MJ, Bunemann M (2005) Dynamics of receptor/G protein coupling in living cells. EMBO J 24:4106-4114.

Hendry SH, Schwark HD, Jones EG, Yan J (1987) Numbers and proportions of GABA-immunoreactive neurons in different areas of monkey cerebral cortex. J Neurosci 7:1503-1519.

Hering-Hanit R (1999) Baclofen for prevention of migraine. Cephalalgia 19:589-591.

Hering-Hanit R, Gadoth N (2000) Baclofen in cluster headache. Headache 40:48-51.

Hooke R (1965) Micrographia:or some physiological descriptions of minute bodies made by magnifying glasses with observations and inquiries thereupon. Royal Soiety, London, UK. J. Martyn and J. Allestry.

Howarth M, Liu W, Puthenveetil S, Zheng Y, Marshall LF, Schmidt MM, Wittrup KD, Bawendi MG, Ting AY (2008) Monovalent, reduced-size quantum dots for imaging receptors on living cells. Nat Methods 5:397-399.

Huston E, Cullen GP, Burley JR, Dolphin AC (1995) The involvement of multiple calcium channel sub-types in glutamate release from cerebellar granule cells and its modulation by $GABA_B$ receptor activation. Neuroscience 68:465-478.

Inoue M, Matsuo T, Ogata N (1985a) Baclofen activates voltage-dependent and 4-aminopyridine sensitive K^+ conductance in guinea-pig hippocampal pyramidal cells maintained in vitro. Br J Pharmacol 84:833-841.

Inoue M, Matsuo T, Ogata N (1985b) Characterization of pre- and postsynaptic actions of (-)-baclofen in the guinea-pig hippocampus in vitro. Br J Pharmacol 84:843-851.

Isomoto S, Kaibara M, Sakurai-Yamashita Y, Nagayama Y, Uezono Y, Yano K, Taniyama K (1998) Cloning and tissue distribution of novel splice variants of the rat $GABA_B$ receptor. Biochem Biophys Res Commun 253:10-15.

Ivanov AI (2008) Pharmacological inhibition of endocytic pathways: is it specific enough to be useful? Methods Mol Biol 440:15-33.

Jackson TR, Kearns BG, Theibert AB (2000) Cytohesins and centaurins: mediators of PI 3-kinase-regulated Arf signaling. Trends Biochem Sci 25:489-495.

Jacob TC, Moss SJ, Jurd R (2008) $GABA_A$ receptor trafficking and its role in the dynamic modulation of neuronal inhibition. Nat Rev Neurosci 9:331-343.

Jaskolski F, Henley JM (2009) Synaptic receptor trafficking: the lateral point of view. Neuroscience 158:19-24.

Jones KA, Borowsky B, Tamm JA, Craig DA, Durkin MM, Dai M, Yao WJ, Johnson M, Gunwaldsen C, Huang LY, Tang C, Shen QR, Salon JA, Morse K, Laz T, Smith KE, Nagarathnam D, Noble SA, Branchek TA, Gerald C (1998) $GABA_B$ receptors function as a heteromeric assembly of the subunits $GABA_BR1$ and $GABA_BR2$. Nature 396:674-679.

Kammerer RA, Frank S, Schulthess T, Landwehr R, Lustig A, Engel J (1999) Heterodimerization of a functional $GABA_B$ receptor is mediated by parallel coiled-coil alpha-helices. Biochemistry 38:13263-13269.

Kantamneni S, Correa SA, Hodgkinson GK, Meyer G, Vinh NN, Henley JM, Nishimune A (2007) GISP: a novel brain-specific protein that promotes surface expression and function of $GABA_B$ receptors. J Neurochem 100:1003-1017.

Kantamneni S, Holman D, Wilkinson KA, Correa SA, Feligioni M, Ogden S, Fraser W, Nishimune A, Henley JM (2008) GISP binding to TSG101 increases GABA receptor stability by down-regulating ESCRT-mediated lysosomal degradation. J Neurochem 107:86-95.

Kantamneni S, Holman D, Wilkinson KA, Nishimune A, Henley JM (2009) GISP increases neurotransmitter receptor stability by down-regulating ESCRT-mediated lysosomal degradation. Neurosci Lett 452:106-110.

Kantamneni S, Wilkinson KA, Jaafari N, Ashikaga E, Rocca D, Rubin P, Jacobs SC, Nishimune A, Henley JM (2011) Activity-dependent SUMOylation of the brain-specific scaffolding protein GISP. Biochemical and Biophysical Research Communications 409:657-662.

Karlin A, Akabas MH (1998) Substituted-cysteine accessibility method. Methods Enzymol 293:123-145.

Kasher R, Balass M, Scherf T, Fridkin M, Fuchs S, Katchalski-Katzir E (2001) Design and synthesis of peptides that bind alpha-bungarotoxin with high affinity. Chem Biol 8:147-155.

Kaupmann K, Huggel K, Heid J, Flor PJ, Bischoff S, Mickel SJ, McMaster G, Angst C, Bittiger H, Froestl W, Bettler B (1997) Expression cloning of $GABA_B$ receptors uncovers similarity to metabotropic glutamate receptors. Nature 386:239-246.

Kaupmann K, Malitschek B, Schuler V, Heid J, Froest W, Beck P, Mosbacher J, Bischoff S, Kulik A, Shigemoto R, Karschin A, Bettler B (1998) $GABA_B$-receptor subtypes assemble into functional heteromeric complexes. Nature 396:683-687.

Kelly BT, McCoy AJ, Spate K, Miller SE, Evans PR, Honing S, Owen DJ (2008) A structural explanation for the binding of endocytic dileucine motifs by the AP2 complex. Nature 456:976-979.

Kerr DI, Ong J, Johnston GA, Abbenante J, Prager RH (1988) 2-Hydroxy-saclofen: an improved antagonist at central and peripheral $GABA_B$ receptors. Neurosci Lett 92:92-96.

Kerr DI, Ong J, Prager RH, Gynther BD, Curtis DR (1987) Phaclofen: a peripheral and central baclofen antagonist. Brain Res 405:150-154.

Kirkitadze MD, Barlow PN (2001) Structure and flexibility of the multiple domain proteins that regulate complement activation. Immunol Rev 180:146-161.

Kniazeff J, Galvez T, Labesse G, Pin JP (2002) No ligand binding in the GB2 subunit of the $GABA_B$ receptor is required for activation and allosteric interaction between the subunits. J Neurosci 22:7352-7361.

Krach LE (2009) Intrathecal baclofen use in adults with cerebral palsy. Dev Med Child Neurol 51 Suppl 4:106-112.

Krapivinsky G, Medina I, Krapivinsky L, Gapon S, Clapham DE (2004) SynGAP-MUPP1-CaMKII synaptic complexes regulate p38 MAP kinase activity and NMDA receptor-dependent synaptic AMPA receptor potentiation. Neuron 43:563-574.

Kuner R, Kohr G, Grunewald S, Eisenhardt G, Bach A, Kornau HC (1999) Role of heteromer formation in $GABA_B$ receptor function. Science 283:74-77.

Kunishima N, Shimada Y, Tsuji Y, Sato T, Yamamoto M, Kumasaka T, Nakanishi S, Jingami H, Morikawa K (2000) Structural basis of glutamate recognition by a dimeric metabotropic glutamate receptor. Nature 407:971-977.

Kuramoto N, Wilkins ME, Fairfax BP, Revilla-Sanchez R, Terunuma M, Tamaki K, Iemata M, Warren N, Couve A, Calver A, Horvath Z, Freeman K, Carling D, Huang L, Gonzales C, Cooper E, Smart TG, Pangalos MN, Moss SJ (2007) Phospho-Dependent Functional

Modulation of $GABA_B$ Receptors by the Metabolic Sensor AMP-Dependent Protein Kinase. Neuron 53:233-247.

Laffray S, Tan K, Dulluc J, Bouali-Benazzouz R, Calver AR, Nagy F, Landry M (2007) Dissociation and trafficking of rat $GABA_B$ receptor heterodimer upon chronic capsaicin stimulation. Eur J Neurosci 25:1402-1416.

Lal R, et al. (2009) Arbaclofen placarbil, a novel R-baclofen prodrug: improved absorption, distribution, metabolism, and elimination properties compared with R-baclofen. J Pharmacol Exp Ther 330:911-921.

Landis DM, Hall AK, Weinstein LA, Reese TS (1988) The organisation of cytoplasm at the presynaptic active zone of a central nervous system synapse. Neuron 1: 201–209.

Lasarge CL, Banuelos C, Mayse JD, Bizon JL (2009) Blockade of $GABA_B$ receptors completely reverses age-related learning impairment. Neuroscience 164:941-947.

Leaney JL, Tinker A (2000) The role of members of the pertussis toxin-sensitive family of G proteins in coupling receptors to the activation of the G protein-gated inwardly rectifying potassium channel. Proc Natl Acad Sci U S A 97:5651-5656.

Lee C, Mayfield RD, Harris RA (2010) Intron 4 containing novel $GABA_{B1}$ isoforms impair $GABA_B$ receptor function. PLoS One 5:e14044.

Lee SP, So CH, Rashid AJ, Varghese G, Cheng R, Lanca AJ, O'Dowd BF, George SR (2004) Dopamine D1 and D2 receptor Co-activation generates a novel phospholipase C-mediated calcium signal. J Biol Chem 279:35671-35678.

Levi S, Dahan M, Triller A (2011) Labeling neuronal membrane receptors with quantum dots. Cold Spring Harb Protoc 2011:rot5580.

Li Y, Stern JE (2004) Activation of postsynaptic $GABA_B$ receptors modulate the firing activity of supraoptic oxytocin and vasopressin neurones: role of calcium channels. J Neuroendocrinol 16:119-130.

Ling W, Shoptaw S, Majewska D (1998) Baclofen as a cocaine anti-craving medication: a preliminary clinical study. Neuropsychopharmacology 18:403-404.

Liu J, Maurel D, Etzol S, Brabet I, Ansanay H, Pin JP, Rondard P (2004) Molecular determinants involved in the allosteric control of agonist affinity in the $GABA_B$ receptor by the $GABA_{B2}$ subunit. J Biol Chem 279:15824-15830.

Liu J, Zheng Q, Deng Y, Cheng CS, Kallenbach NR, Lu M (2006) A seven-helix coiled coil. Proc Natl Acad Sci U S A 103:15457-15462.

Macia E, Ehrlich M, Massol R, Boucrot E, Brunner C, Kirchhausen T (2006) Dynasore, a cell-permeable inhibitor of dynamin. Dev Cell 10:839-850.

Maier PJ, Marin I, Grampp T, Sommer A, Benke D (2010) Sustained glutamate receptor activation down-regulates $GABA_B$ receptors by shifting the balance from recycling to lysosomal degradation. J Biol Chem 285:35606-35614.

Malenka RC (2003) Synaptic plasticity and AMPA receptor trafficking. Ann N Y Acad Sci 1003:1-11.

Malinow R, Malenka RC (2002) AMPA receptor trafficking and synaptic plasticity. Annu Rev Neurosci 25:103-126.

Malitschek B, Schweizer C, Keir M, Heid J, Froestl W, Mosbacher J, Kuhn R, Henley J, Joly C, Pin JP, Kaupmann K, Bettler B (1999) The N-terminal domain of γ-aminobutyric $Acid_B$ receptors is sufficient to specify agonist and antagonist binding. Mol Pharmacol 56:448-454.

Marchese A, Paing MM, Temple BR, Trejo J (2008) G Protein-Coupled Receptor Sorting to Endosomes and Lysosomes. Annu Rev Pharmacol Toxicol 48:601-629.

Margeta-Mitrovic M, Jan YN, Jan LY (2000) A trafficking checkpoint controls $GABA_B$ receptor heterodimerization. Neuron 27:97-106.

Margeta-Mitrovic M, Jan YN, Jan LY (2001a) Function of GB1 and GB2 subunits in G protein coupling of $GABA_B$ receptors. Proc Natl Acad Sci U S A 98:14649-14654.

Margeta-Mitrovic M, Jan YN, Jan LY (2001b) Ligand-induced signal transduction within heterodimeric $GABA_B$ receptor. Proc Natl Acad Sci U S A 98:14643-14648.

Marshall FH, Jones KA, Kaupmann K, Bettler B (1999) $GABA_B$ receptors - the first 7TM heterodimers. Trends Pharmacol Sci 20:396-399.

Martin SC, Russek SJ, Farb DH (1999) Molecular identification of the human $GABA_BR2$: cell surface expression and coupling to adenylyl cyclase in the absence of $GABA_BR1$. Mol Cell Neurosci 13:180-191.

Martin SC, Russek SJ, Farb DH (2001) Human $GABA_BR$ genomic structure: evidence for splice variants in $GABA_BR1$ but not $GABA_BR2$. Gene 278:63-79.

Matsushita S, Nakata H, Kubo Y, Tateyama M (2010) Ligand-induced rearrangements of the $GABA_B$ receptor revealed by fluorescence resonance energy transfer. J Biol Chem 285:10291-10299.

Maurel D, Comps-Agrar L, Brock C, Rives ML, Bourrier E, Ayoub MA, Bazin H, Tinel N, Durroux T, Prezeau L, Trinquet E, Pin JP (2008) Cell-surface protein-protein interaction analysis with time-resolved FRET and snap-tag technologies: application to GPCR oligomerization. Nat Methods 5:561-567.

Maurel D, Kniazeff J, Mathis G, Trinquet E, Pin JP, Ansanay H (2004) Cell surface detection of membrane protein interaction with homogeneous time-resolved fluorescence resonance energy transfer technology. Anal Biochem 329:253-262.

McCormick DA (1989) GABA as an inhibitory neurotransmitter in human cerebral cortex. J Neurophysiol 62:1018-1027.

McCudden CR, Hains MD, Kimple RJ, Siderovski DP, Willard FS (2005) G-protein signaling: back to the future. Cell Mol Life Sci 62:551-577.

McDonald NA, Henstridge CM, Connolly CN, Irving AJ (2007a) An essential role for constitutive endocytosis, but not activity, in the axonal targeting of the CB1 cannabinoid receptor. Mol Pharmacol 71:976-984.

McDonald NA, Henstridge CM, Connolly CN, Irving AJ (2007b) Generation and functional characterization of fluorescent, N-terminally tagged CB1 receptor chimeras for live-cell imaging. Mol Cell Neurosci 35:237-248.

Meier J, Vannier C, Serge A, Triller A, Choquet D (2001) Fast and reversible trapping of surface glycine receptors by gephyrin. Nat Neurosci 4:253-260.

Mercer AJ, Chen M, Thoreson WB (2011) Lateral mobility of presynaptic L-type calcium channels at photoreceptor ribbon synapses. J Neurosci 31:4397-4406.

Meresse S, Gorvel JP, Chavrier P (1995) The rab7 GTPase resides on a vesicular compartment connected to lysosomes. J Cell Sci 108 (Pt 11):3349-3358.

Mikasova L, Groc L, Choquet D, Manzoni OJ (2008) Altered surface trafficking of presynaptic cannabinoid type 1 receptor in and out synaptic terminals parallels receptor desensitization. Proc Natl Acad Sci U S A 105:18596-18601.

Mintz IM, Bean BP (1993) $GABA_B$ receptor inhibition of P-type Ca^{2+} channels in central neurons. Neuron 10:889-898.

Mirzadegan T, Benko G, Filipek S, Palczewski K (2003) Sequence analyses of G-protein-coupled receptors: similarities to rhodopsin. Biochemistry 42:2759-2767.

Misgeld U, Bijak M, Jarolimek W (1995) A physiological role for $GABA_B$ receptors and the effects of baclofen in the mammalian central nervous system. Prog Neurobiol 46:423-462.

Mohammad S, Baldini G, Granell S, Narducci P, Martelli AM, Baldini G (2007) Constitutive traffic of melanocortin-4 receptor in Neuro2A cells and immortalized hypothalamic neurons. J Biol Chem 282:4963-4974.

Mohrmann K, van der SP (1999) Regulation of membrane transport through the endocytic pathway by rabGTPases. Mol Membr Biol 16:81-87.

Moise L, Liu J, Pryazhnikov E, Khiroug L, Jeromin A, Hawrot E (2010) $K_{(V)}$4.2 channels tagged in the S1-S2 loop for α-bungarotoxin binding provide a new tool for studies of channel expression and localization. Channels (Austin) 4:115-123.

Monnier C, Tu H, Bourrier E, Vol C, Lamarque L, Trinquet E, Pin JP, Rondard P (2011) Trans-activation between 7TM domains: implication in heterodimeric $GABA_B$ receptor activation. EMBO J 30:32-42.

Morishita R, Kato K, Asano T (1990) $GABA_B$ receptors couple to G proteins G_o, G_{o*} and G_{i1} but not to G_{i2}. FEBS Lett 271:231-235.

Moss SJ, Smart TG (2001) Constructing inhibitory synapses. Nat Rev Neurosci 2:240-250.

Muller H, Borner U, Zierski J, Hempelmann G (1987) Intrathecal baclofen for treatment of tetanus-induced spasticity. Anesthesiology 66:76-79.

Mutneja M, Berton F, Suen KF, Luscher C, Slesinger PA (2005) Endogenous RGS proteins enhance acute desensitization of $GABA_B$ receptor-activated GIRK currents in HEK-293T cells. Pflugers Arch 450:61-73.

Nakamura Y, Hinoi E, Takarada T, Takahata Y, Yamamoto T, Fujita H, Takada S, Hashizume S, Yoneda Y (2011) Positive Regulation by $GABA_BR1$ Subunit of Leptin Expression through Gene Transactivation in Adipocytes. PLoS One 6:e20167.

Naslavsky N, Weigert R, Donaldson JG (2003) Convergence of non-clathrin- and clathrin-derived endosomes involves Arf6 inactivation and changes in phosphoinositides. Mol Biol Cell 14:417-431.

Nehring RB, Horikawa HP, El Far O, Kneussel M, Brandstatter JH, Stamm S, Wischmeyer E, Betz H, Karschin A (2000) The metabotropic $GABA_B$ receptor directly interacts with the activating transcription factor 4. J Biol Chem 275:35185-35191.

Neubig RR, Gantzos RD, Thomsen WJ (1988) Mechanism of agonist and antagonist binding to α2 adrenergic receptors: evidence for a precoupled receptor-guanine nucleotide protein complex. Biochemistry 27:2374-2384.

NIcoll RA (2004) My close encounter with $GABA_B$ receptors. Biochem Pharmacol 68:1667-1674.

Nishikawa M, Hirouchi M, Kuriyama K (1997) Functional coupling of G_i subtype with $GABA_B$ receptor/adenylyl cyclase system: analysis using a reconstituted system with purified GTP-binding protein from bovine cerebral cortex. Neurochem Int 31:21-25.

Nomura R, Suzuki Y, Kakizuka A, Jingami H (2008) Direct detection of the interaction between recombinant soluble extracellular regions in the heterodimeric metabotropic γ-aminobutyric acid receptor. J Biol Chem 283:4665-4673.

Nygaard R, Frimurer TM, Holst B, Rosenkilde MM, Schwartz TW (2009) Ligand binding and micro-switches in 7TM receptor structures. Trends Pharmacol Sci 30:249-259.

O'Brien CF, Seeberger LC, Smith DB (1996) Spasticity after stroke. Epidemiology and optimal treatment. Drugs Aging 9:332-340.

Olsen RW (2002) GABA. American College of Neuropsychopharmacology.

Ong J, Kerr DI, Doolette DJ, Duke RK, Mewett KN, Allen RD, Johnston GA (1993) R-(-)-β-phenyl-GABA is a full agonist at $GABA_B$ receptors in brain slices but a partial agonist in the ileum. Eur J Pharmacol 233:169-172.

Overington JP, Al Lazikani B, Hopkins AL (2006) How many drug targets are there? Nat Rev Drug Discov 5:993-996.

Oyadomari S, Araki E, Mori M (2002) Endoplasmic reticulum stress-mediated apoptosis in pancreatic β-cells. Apoptosis 7:335-345.

Paing MM, Johnston CA, Siderovski DP, Trejo J (2006) Clathrin adaptor AP2 regulates thrombin receptor constitutive internalisation and endothelial cell resensitization. Mol Cell Biol 26:3231-3242.

Palczewski K (2006) G protein-coupled receptor rhodopsin. Annu Rev Biochem 75:743-767.

Palczewski K, Kumasaka T, Hori T, Behnke CA, Motoshima H, Fox BA, Le T, I, Teller DC, Okada T, Stenkamp RE, Yamamoto M, Miyano M (2000) Crystal structure of rhodopsin: A G protein-coupled receptor. Science 289:739-745.

Pandey KN (2009) Functional roles of short sequence motifs in the endocytosis of membrane receptors. Front Biosci 14:5339-5360.

Paredes DA, Cartford MC, Catlow BJ, Samec A, Avilas M, George A, Schlunck A, Small B, Bickford PC (2009) Neurotransmitter release during delay eyeblink classical conditioning: role of norepinephrine in consolidation and effect of age. Neurobiol Learn Mem 92:267-282.

Penn RD, Kroin JS (1984) Intrathecal baclofen alleviates spinal cord spasticity. Lancet 1:1078.

Penn RD, Kroin JS (1985) Continuous intrathecal baclofen for severe spasticity. Lancet 2:125-127.

Perez-Garci E, Gassmann M, Bettler B, Larkum ME (2006) The $GABA_{B1b}$ isoform mediates long-lasting inhibition of dendritic Ca^{2+} spikes in layer 5 somatosensory pyramidal neurons. Neuron 50:603-616.

Perroy J, Adam L, Qanbar R, Chenier S, Bouvier M (2003) Phosphorylation-independent desensitization of $GABA_B$ receptor by GRK4. EMBO J 22:3816-3824.

Pfaff T, Malitschek B, Kaupmann K, Prezeau L, Pin JP, Bettler B, Karschin A (1999) Alternative splicing generates a novel isoform of the rat metabotropic $GABA_BR1$ receptor. Eur J Neurosci 11:2874-2882.

Pin JP, Comps-Agrar L, Maurel D, Monnier C, Rives ML, Trinquet E, Kniazeff J, Rondard P, Pr+¬zeau L (2009) G-protein-coupled receptor oligomers: two or more for what? Lessons from mGlu and $GABA_B$ receptors. The Journal of Physiology 587:5337-5344.

Pin JP, Galvez T, Prezeau L (2003) Evolution, structure, and activation mechanism of family 3/C G-protein-coupled receptors. Pharmacol Ther 98:325-354.

Pin JP, Kniazeff J, Goudet C, Bessis AS, Liu J, Galvez T, Acher F, Rondard P, Prezeau L (2004) The activation mechanism of class-C G-protein coupled receptors. Biol Cell 96:335-342.

Pin JP, Kniazeff J, Liu J, Binet V, Goudet C, Rondard P, Prezeau L (2005) Allosteric functioning of dimeric class C G-protein-coupled receptors. FEBS J 272:2947-2955.

Pin JP, Parmentier ML, Prezeau L (2001) Positive allosteric modulators for gamma-aminobutyric acid(B) receptors open new routes for the development of drugs targeting family 3 G- protein-coupled receptors. Mol Pharmacol 60:881-884.

Pin JP, Prezeau L (2007) Allosteric modulators of $GABA_B$ receptors: mechanism of action and therapeutic perspective. Curr Neuropharmacol 5:195-201.

Pontier SM, Lahaie N, Ginham R, St Gelais F, Bonin H, Bell DJ, Flynn H, Trudeau LE, McIlhinney J, White JH, Bouvier M (2006) Coordinated action of NSF and PKC regulates $GABA_B$ receptor signaling efficacy. EMBO J 25:2698-2709.

Pooler AM, Gray AG, McIlhinney RA (2009) Identification of a novel region of the $GABA_{B2}$ C-terminus that regulates surface expression and neuronal targeting of the $GABA_B$ receptor. Eur J Neurosci 29:869-878.

Pooler AM, McIlhinney RA (2007) Lateral diffusion of the $GABA_B$ receptor is regulated by the $GABA_{B2}$ C terminus. J Biol Chem 282:25349-25356.

Pozza MF, Manuel NA, Steinmann M, Froestl W, Davies CH (1999) Comparison of antagonist potencies at pre- and post-synaptic $GABA_B$ receptors at inhibitory synapses in the CA1 region of the rat hippocampus. Br J Pharmacol 127:211-219.

Racine V, Sachse M, Salamero J, Fraisier V, Trubuil A, Sibarita JB (2007) Visualization and quantification of vesicle trafficking on a three-dimensional cytoskeleton network in living cells. J Microsc 225:214-228.

Ramoino P, Gallus L, Beltrame F, Diaspro A, Fato M, Rubini P, Stigliani S, Bonanno G, Usai C (2006) Endocytosis of $GABA_B$ receptors modulates membrane excitability in the single-celled organism Paramecium. J Cell Sci 119:2056-2064.

Ramoino P, Usai C, Beltrame F, Fato M, Gallus L, Tagliafierro G, Magrassi R, Diaspro A (2005) $GABA_B$ receptor intracellular trafficking after internalisation in Paramecium. Microsc Res Tech 68:290-295.

Renner M, Choquet D, Triller A (2009) Control of the postsynaptic membrane viscosity. J Neurosci 29:2926-2937.

Renner M, Specht CG, Triller A (2008) Molecular dynamics of postsynaptic receptors and scaffold proteins. Curr Opin Neurobiol 18:532-540.

Restituito S, Couve A, Bawagan H, Jourdain S, Pangalos MN, Calver AR, Freeman KB, Moss SJ (2005) Multiple motifs regulate the trafficking of $GABA_B$ receptors at distinct checkpoints within the secretory pathway. Mol Cell Neurosci 28:747-756.

Rhee SG, Bae YS (1997) Regulation of phosphoinositide-specific phospholipase C isozymes. J Biol Chem 272:15045-15048.

Richer M, David M, Villeneuve LR, Trieu P, Ethier N, Petrin D, Mamarbachi AM, Hebert TE (2009) $GABA_{B1}$ receptors are coupled to the ERK1/2 MAP kinase pathway in the absence of $GABA_{B2}$ subunits. J Mol Neurosci 38:67-79.

Robbins MJ, Calver AR, Filippov AK, Hirst WD, Russell RB, Wood MD, Nasir S, Couve A, Brown DA, Moss SJ, Pangalos MN (2001) $GABA_{B2}$ is essential for g-protein coupling of the $GABA_B$ receptor heterodimer. J Neurosci 21:8043-8052.

Roberts E (1986) GABA: The road to neurotransmitter status. pp 1-39. New York.

Roberts E, Frankel S (1950) γ-Aminobutyric acid in brain: its formation from glutamic acid. J Biol Chem 187:55-63.

Robichon A, Tinette S, Courtial C, Pelletier F (2004) Simultaneous stimulation of GABA and β-adrenergic receptors stabilizes isotypes of activated adenylyl cyclase heterocomplex. BMC Cell Biol 5:25.

Rondard P, Huang S, Monnier C, Tu H, Blanchard B, Oueslati N, Malhaire F, Li Y, Trinquet E, Labesse G, Pin JP, Liu J (2008) Functioning of the dimeric $GABA_B$ receptor extracellular domain revealed by glycan wedge scanning. EMBO J 27:1321-1332.

Rozenfeld R, Devi LA (2010) Receptor heteromerization and drug discovery. Trends Pharmacol Sci 31:124-130.

Sauter K, Grampp T, Fritschy JM, Kaupmann K, Bettler B, Mohler H, Benke D (2005) Subtype-selective interaction with the transcription factor CCAAT/enhancer-binding protein (C/EBP) homologous protein (CHOP) regulates cell surface expression of $GABA_B$ receptors. J Biol Chem 280:33566-33572.

Scarselli M, Donaldson JG (2009) Constitutive internalization of G protein-coupled receptors and G proteins via clathrin-independent endocytosis. J Biol Chem 284:3577-3585.

Schwann T (1839) Microscopical researches into the accordance in the structure and growth of animals and plants. London: Printed for the Sydenham Society

Schwartz TW, Frimurer TM, Holst B, Rosenkilde MM, Elling CE (2006) Molecular mechanism of 7TM receptor activation--a global toggle switch model. Annu Rev Pharmacol Toxicol 46:481-519.

Schwarz DA, Barry G, Eliasof SD, Petroski RE, Conlon PJ, Maki RA (2000) Characterization of γ-aminobutyric acid receptor $GABA_{B(1e)}$, a $GABA_{B(1)}$ splice variant encoding a truncated receptor [In Process Citation]. J Biol Chem 275:32174-32181.

Schwenk J, Metz M, Zolles G, Turecek R, Fritzius T, Bildl W, Tarusawa E, Kulik A, Unger A, Ivankova K, Seddik R, Tiao JY, Rajalu M, Trojanova J, Rohde V, Gassmann M, Schulte U, Fakler B, Bettler B (2010) Native $GABA_B$ receptors are heteromultimers with a family of auxiliary subunits. Nature 465:231-235.

Sekine-Aizawa Y, Huganir RL (2004) Imaging of receptor trafficking by using α-bungarotoxin-binding-site-tagged receptors. Proc Natl Acad Sci U S A 101:17114-17119.

Shaban H, Humeau Y, Herry C, Cassasus G, Shigemoto R, Ciocchi S, Barbieri S, van der PH, Kaupmann K, Bettler B, Luthi A (2006) Generalization of amygdala LTP and conditioned fear in the absence of presynaptic inhibition. Nat Neurosci 9:1028-1035.

Shen L, Liang F, Walensky LD, Huganir RL (2000) Regulation of AMPA Receptor GluR1 Subunit Surface Expression by a 4.1N-Linked Actin Cytoskeletal Association. The Journal of Neuroscience 20:7932-7940.

Sherrington CS (1906) The integrative action of the nervous system. Charles Scribner's Sons: New York. 1906

Shoptaw S, Yang X, Rotheram-Fuller EJ, Hsieh YC, Kintaudi PC, Charuvastra VC, Ling W (2003) Randomized placebo-controlled trial of baclofen for cocaine dependence: preliminary effects for individuals with chronic patterns of cocaine use. J Clin Psychiatry 64:1440-1448.

Smith CR, LaRocca NG, Giesser BS, Scheinberg LC (1991) High-dose oral baclofen: experience in patients with multiple sclerosis. Neurology 41:1829-1831.

Smith MA, Yancey DL, Morgan D, Liu Y, Froestl W, Roberts DC (2004) Effects of positive allosteric modulators of the $GABA_B$ receptor on cocaine self-administration in rats. Psychopharmacology (Berl) 173:105-111.

Stanasila L, Abuin L, Dey J, Cotecchia S (2008) Different internalization properties of the α1a- and α1b-adrenergic receptor subtypes: the potential role of receptor interaction with β-arrestins and AP50. Mol Pharmacol 74:562-573.

Stayer C, Tronnier V, Dressnandt J, Mauch E, Marquardt G, Rieke K, Muller-Schwefe G, Schumm F, Meinck HM (1997) Intrathecal baclofen therapy for stiff-man syndrome and progressive encephalomyelopathy with rigidity and myoclonus. Neurology 49:1591-1597.

Stenmark H, Olkkonen VM (2001) The Rab GTPase family. Genome Biol 2: Reviews 3007.

Tajiri S, Oyadomari S, Yano S, Morioka M, Gotoh T, Hamada JI, Ushio Y, Mori M (2004) Ischemia-induced neuronal cell death is mediated by the endoplasmic reticulum stress pathway involving CHOP. Cell Death Differ 11:403-415.

Takeda S, Kadowaki S, Haga T, Takaesu H, Mitaku S (2002) Identification of G protein-coupled receptor genes from the human genome sequence. FEBS Lett 520:97-101.

Tarsa L, Goda Y (2002) Synaptophysin regulates activity-dependent synapse formation in cultured hippocampal neurons. PNAS 99:1012-1016.

Terunuma M, Vargas KJ, Wilkins ME, Ramirez OA, Jaureguiberry-Bravo M, Pangalos MN, Smart TG, Moss SJ, Couve A (2010) Prolonged activation of NMDA receptors promotes dephosphorylation and alters postendocytic sorting of $GABA_B$ receptors. Proc Natl Acad Sci U S A 107:13918-13923.

Thomas P, Mortensen M, Hosie AM, Smart TG (2005) Dynamic mobility of functional $GABA_A$ receptors at inhibitory synapses. Nat Neurosci 8:889-897.

Thuault SJ, Brown JT, Sheardown SA, Jourdain S, Fairfax B, Spencer JP, Restituito S, Nation JH, Topps S, Medhurst AD, Randall AD, Couve A, Moss SJ, Collingridge GL, Pangalos MN, Davies CH, Calver AR (2004) The GABA(B2) subunit is critical for the trafficking and function of native $GABA_B$ receptors. Biochem Pharmacol 68:1655-1666.

Tiao JY, Bradaia A, Biermann B, Kaupmann K, Metz M, Haller C, Rolink AG, Pless E, Barlow PN, Gassmann M, Bettler B (2008) The sushi domains of secreted $GABA_{B1}$ isoforms selectively impair $GABA_B$ heteroreceptor function. J Biol Chem 283:31005-31011.

Tran-Van-Minh A, Dolphin AC (2010) The alpha2delta ligand gabapentin inhibits the Rab11-dependent recycling of the calcium channel subunit α2δ-2. J Neurosci 30:12856-12867.

Triller A, Choquet D (2003) Synaptic structure and diffusion dynamics of synaptic receptors. Biol Cell 95:465-476.

Triller A, Choquet D (2005) Surface trafficking of receptors between synaptic and extrasynaptic membranes: and yet they do move! Trends Neurosci 28:133-139.

Triller A, Choquet D (2008) New concepts in synaptic biology derived from single-molecule imaging. Neuron 59:359-374.

Tuteja N (2009) Signaling through G protein coupled receptors. Plant Signal Behav 4:942-947.

Ulrich D, Bettler B (2007) $GABA_B$ receptors: synaptic functions and mechanisms of diversity. Curr Opin Neurobiol 17:298-303.

Urwyler S (2011) Allosteric modulation of family C G-protein-coupled receptors: from molecular insights to therapeutic perspectives. Pharmacol Rev 63:59-126.

Urwyler S, Mosbacher J, Lingenhoehl K, Heid J, Hofstetter K, Froestl W, Bettler B, Kaupmann K (2001) Positive allosteric modulation of native and recombinant γ-aminobutyric acid$_B$ receptors by 2,6-Di-tert-butyl-4-(3-hydroxy-2,2-dimethyl-propyl)-phenol (CGP7930) and its aldehyde analog CGP13501. Mol Pharmacol 60:963-971.

Urwyler S, Pozza MF, Lingenhoehl K, Mosbacher J, Lampert C, Froestl W, Koller M, Kaupmann K (2003) N,N'-Dicyclopentyl-2-methylsulfanyl-5-nitro-pyrimidine-4,6-diamine (GS39783) and structurally related compounds: novel allosteric enhancers of γ -aminobutyric acid$_B$ receptor function. J Pharmacol Exp Ther 307:322-330.

Vargas KJ, Terunuma M, Tello JA, Pangalos MN, Moss SJ, Couve A (2008) The availability of surface GABA$_B$ receptors is independent of γ-aminobutyric acid but controlled by glutamate in central neurons. J Biol Chem 283:24641-24648.

Vernon E, Meyer G, Pickard L, Dev K, Molnar E, Collingridge GL, Henley JM (2001) GABA$_B$ receptors couple directly to the transcription factor ATF4. Mol Cell Neurosci 17:637-645.

Vidal RL, Ramirez OA, Sandoval L, Koenig-Robert R, Hartel S, Couve A (2007) Marlin-1 and conventional kinesin link GABA$_B$ receptors to the cytoskeleton and regulate receptor transport. Mol Cell Neurosci 35:501-512.

Vigot R, Barbieri S, Brauner-Osborne H, Turecek R, Shigemoto R, Zhang YP, Lujan R, Jacobson LH, Biermann B, Fritschy JM, Vacher CM, Muller M, Sansig G, Guetg N, Cryan JF, Kaupmann K, Gassmann M, Oertner TG, Bettler B (2006) Differential compartmentalization and distinct functions of GABA$_B$ receptor variants. Neuron 50:589-601.

Villemure JF, Adam L, Bevan NJ, Gearing K, Chenier S, Bouvier M (2005) Subcellular distribution of GABA$_B$ receptor homo- and hetero-dimers. Biochem J 388:47-55.

Wang LH, Rothberg KG, Anderson RG (1993) Mis-assembly of clathrin lattices on endosomes reveals a regulatory switch for coated pit formation. J Cell Biol 123:1107-1117.

White JH, McIllhinney RA, Wise A, Ciruela F, Chan WY, Emson PC, Billinton A, Marshall FH (2000) The GABA$_B$ receptor interacts directly with the related transcription factors CREB2 and ATFx. Proc Natl Acad Sci U S A 97:13967-13972.

White JH, Wise A, Main MJ, Green A, Fraser NJ, Disney GH, Barnes AA, Emson P, Foord SM, Marshall FH (1998) Heterodimerization is required for the formation of a functional GABA$_B$ receptor. Nature 396:679-682.

Wilkins ME, Li X, Smart TG (2008) Tracking cell surface GABA$_B$ receptors using an a-bungarotoxin tag. J Biol Chem 283:34745-34752.

Wilkinson KA, Henley JM (2010) Mechanisms, regulation and consequences of protein SUMOylation. Biochemical Journal 428:133-145.

Wilkinson KA, Nakamura Y, Henley JM (2010) Targets and consequences of protein SUMOylation in neurons. Brain Research Reviews 64:195-212.

Wilkinson KA, Nishimune A, Henley JM (2008) Analysis of SUMO-1 modification of neuronal proteins containing consensus SUMOylation motifs. Neuroscience Letters 436:239-244.

Wolfe BL, Trejo J (2007) Clathrin-dependent mechanisms of G protein-coupled receptor endocytosis. Traffic 8:462-470.

Xia Z, Dudek H, Miranti CK, Greenberg ME (1996) Calcium influx via the NMDA receptor induces immediate early gene transcription by a MAP kinase/ERK-dependent mechanism. J Neurosci 16:5425-5436.

Xie X, Smart TG (1992a) γ-Hydroxybutyrate depresses monosynaptic excitatory and inhibitory postsynaptic potentials in rat hippocampal slices. Eur J Pharmacol 223:193-196.

Xie X, Smart TG (1992b) γ-hydroxybutyrate hyperpolarizes hippocampal neurones by activating $GABA_B$ receptors. Eur J Pharmacol 212:291-294.

Yuan H, Michelsen K, Schwappach B (2003) 14-3-3 dimers probe the assembly status of multimeric membrane proteins. Curr Biol 13:638-646.

Zerial M, McBride H (2001) Rab proteins as membrane organizers. Nat Rev Mol Cell Biol 2:107-117.

Zhang J, Ferguson SS, Barak LS, Menard L, Caron MG (1996) Dynamin and β-arrestin reveal distinct mechanisms for G protein-coupled receptor internalisation. J Biol Chem 271:18302-18305.